SEMMELWEIS EGYETEM

DOKTORI ISKOLA

Ph.D. értekezések

3032.

SZEGVÁRI GÁBOR ADRIÁN

Légzőszervi megbetegedések
című program

Programvezető: Dr. Müller Veronika, egyetemi tanár

Témavezető: Dr. Lohinai Zoltán, tudományos munkatárs

Exploring the translational potential of influencing macrophage polarization in the tumor microenvironment in small cell lung cancer with a Boolean control network model

PhD thesis

Gábor Szegvári

Semmelweis University Doctoral School

Károly Rácz Conservative Medicine Division

Supervisor: Zoltán Lohinai, MD, Ph.D.

Official reviewers: János Fekete, Ph.D
Tamás Korcsmáros, Ph.D

Head of the Complex Examination Committee: György Reusz, MD, D.Sc

Members of the Complex Examination Committee:
László Szabó, MD, Habil.
Tamás Micsik, MD, Ph.D

Budapest
2024

Table of Contents

Abbreviations

ADCC - Antibody-Dependent Cellular Cytotoxicity

ADCP - Antibody-Dependent Cellular Phagocytosis

ADMET - Absorption, Distribution, Metabolism, Excretion and Toxicity

AKT - RAC-alpha serine/threonine-protein kinase

ANXA1 - ANneXin A1

APC - Antigen Presenting Cell

API - Application Programming Interface

ASCL1 - Achaete-SCute family bHLH transcription factor 1

BCN - Boolean Control Network

BCG - Bacille Calmette-Guérin

B_{reg} - regulatory B lymphocyte

CCL - CC chemokine Ligand

CD - Cluster of Differentiation

CDH2 - CaDHerin 2

CHGA - CHromoGranin A

CHK1 - CHeckpoint Kinase 1

CIITA - Class II major histocompatibility complex TransActivator

CREBBP - cAMP Response Element-Binding protein Binding Protein

CRT - ChemoRadioTherapy

CTL - Cytotoxic T Lymphocyte (a.k.a. T_c)

CTLA-4 - Cytotoxic T Lymphocyte-Associated protein 4 (a.k.a. CD152)

CXCL - CXC chemokine Ligand

CXCR - CXC chemokine Receptor

DC - Dendritic Cell

dNLR - derived Neutrophil-to-Lymphocyte Ratio

ECM - ExtraCellular Matrix

EMA - European Medicines Agency

EMT - Epithelial-Mesenchymal Transition

EP300 - E1A binding Protein p300

ES-SCLC - Extensive Stage Small Cell Lung Cancer

FAERS - FDA Adverse Event Reporting System

FC - Fold Change

FCGR1A - Fc Gamma Receptor 1A

FDA - US Food and Drug Administration

FFPE - Formalin-Fixed, Paraffin-Embedded

FGF5 - Fibroblast Growth Factor 5

FoxP3 - Forkhead box P3

GM-CSF - Granulocyte-Macrophage Colony-Stimulating Factor (a.k.a. CSF2)

GO - Gene Ontology

GRN - Gene Regulatory Network

GRP - Gastrin Releasing Peptide

GZMA - GranZyMe A

H&E - Hematoxylin and Eosin

HCK - Hemopoietic Cell Kinase

HLA - Human Leukocyte Antigen

HPRD - Human Protein Reference Database

HUGO - Human Genome Organization

ICB - Immune Checkpoint Blockade

ICI - Immune Checkpoint Inhibition (or Inhibitor)

IDO - Indoleamine 2,3-DiOxygenase

IFI27 - InterFeron alpha Inducible protein 27

IFN - InterFeroN

IgG - Immunoglobulin G

IHC – ImmunoHistoChemistry

IKK - Inhibitor of nuclear factor Kappa B Kinase

IL - InterLeukin

iNOS - inducible Nitric Oxide Synthase

INS - INSulin

IRAK - Interleukin-1 Receptor-Associated Kinase

ISL1 - ISLet-1 (insulin gene enhancer protein)

ITGA - InTeGrin subunit Alpha

ITGB - InTeGrin subunit Beta

JAK - JAnus Kinase

KEGG - Kyoto Encyclopedia of Genes and Genomes

KRT5 - KeRaTin 5

LAG-3 - Lymphocyte-Activation Gene 3 (a.k.a. CD223)

LAP - Latency Associated Peptide

LDH - Lactate DeHydrogenase

LIPI - Lung Immune Prognostic Index

LN - Lymph Node

LS-SCLC - Limited Stage Small Cell Lung Cancer

MAD - Median Absolute Deviation

MAPK - Mitogen-Activated Protein Kinase

MDSC - Myeloid-Derived Suppressor Cell

MERTK – MER (Monocyte/Epithelium/Reproductive) proto-oncogene, Tyrosine Kinase

MHC - Major Histocompatibility Complex

MMP - Matrix MetalloProteinase

MoA - Mechanism of Action

MRC - Mannose Receptor C-type

MYC – MyeloCytomatosis

MyD88 - MYeloid Differentiation primary response 88

NCAM1 - Neural Cell Adhesion Molecule 1

NE - NeuroEndocrine

NES - Normalized Enrichment Score

NEUROD1 - NEUROgenic Differentiation 1

NFAT - Nuclear Factor of Activated T-cells

NFκB - Nuclear Factor kappa B

NK - Natural Killer

NKX2 - NK2 homeoboX

NO - Nitric Oxide

NSCLC - Non-Small Cell Lung Cancer

ORR - Objective Response Rate

OS - Overall Survival

PADC - Pancreatic ADenoCarcinoma

PAMP - Pathogen-Associated Molecular Pattern

PCI - Prophylactic Cranial Irradiation

PD-L1 - Programmed Death Ligand 1 (a.k.a. CD274)

PD-L2 - Programmed Death Ligand 2 (a.k.a. CD273)

PFS - Progression-Free Survival

pI - polarization index (see ch. 3.2.3.2.)

PI3K - PhosphatidylInositol-4,5-bisphosphate 3-Kinase

PIP_3 - PhosphatidylInositol (3,4,5)-trisPhosphate

PMID - PubMed IDentifier

POU2F3 - POU class 2 homeobox 3

pp - percentage point

PPI - Protein-Protein Interaction

RB1 - RetinoBlastoma protein 1

REST - REpresentational State Transfer (architectural style of API)

RNA – RiboNucleic Acid

RNAseq - RNA sequencing

ROI - Region Of Interest

ROS - Reactive Oxygen Species

RT - Radiation Therapy

SABR - Stereotactic ABlative Radiotherapy

SCLC - Small Cell Lung Cancer

SEER - Surveillance, Epidemiology, and End Results program

SIDER - Side Effect Resource

SOX3 - SRY-bOX transcription factor 3

Sp1 - Specificity Protein 1

STAT - Signal Transducer and Activator of Transcription

STK4 - Serine/Threonine-protein Kinase 4 (a.k.a. MST1)

STRING - Search Tool for Recurring Instances of Neighbouring Genes

synI - synergy index (see ch. 3.2.3.3.)

SYP - SYnaptoPhysin

TAM - Tumor-Associated Macrophage

TGF - Transforming Growth Factor

TF - Transcription Factor

T_h - helper T lymphocyte

TIL - Tumor Infiltrating Lymphocyte

TIME - Tumor Immune MicroEnvironment

TLR - Toll-Like Receptor

TMA - Tissue MicroArray

TMB - Tumor Mutation Burden

TME - Tumor MicroEnvironment

TNBC - Triple-Negative Breast Cancer

TNM - Tumor, lymph Nodes, Metastasis (classification system)

TNF - Tumor Necrosis Factor

TP - Tumor Protein (e.g., TP53)

TRAF - TNF Receptor Associated Factor

TRAIL - TNF-Related Apoptosis-Inducing Ligand

T_{reg} - regulatory T lymphocyte

TSV - Tab Separated Values

TTD - Therapeutic Target Database

Tyk2 - TYrosine Kinase 2 (JAK family member)

VEGF - Vascular Endothelial Growth Factor

YAP1 - Yes1 Associated transcriptional regulator

YBX3 - Y-BoX binding protein 3

yr - year

1. Introduction

1.1. Small Cell Lung Cancer

1.1.1. Epidemiology

While there has been remarkable progress in the treatment of many cancers, lung cancer, especially of the small cell type (SCLC), remains a very present and widespread problem, with over 2 million new cases worldwide expected yearly [1]. Even though a decrease in the number of smokers resulted in a slight decrease in incidence (1.1%/yr in men and 2.6%/yr in women) observable since 2006, in 2023, lung cancer is still estimated to become the second most common type of cancer in the US (over 12% of all cases) [2]. It also has local importance: the 2018 GLOBOCAN survey has shown that Hungary has one of the highest (age-standardized) incidence rates of lung cancer in both men and women, exceeding the world average by a factor of 2.46 and 2.81, respectively [1]. The most important risk factor is smoking, with over 80% of cases of lung cancer directly attributed to smoking [2], and 97-98% of SCLC sufferers being smokers [3,4].

In addition to its high prevalence, the progress of therapeutic options is slow, and the prognosis of patients remains disheartening. From the 80s, for three decades we saw no major improvement in clinical practice and survival rates stagnated [5]. According to the data collected in the US by the Surveillance, Epidemiology, and End Results Program (SEER), the 5-year survival rate for SCLC patients showed no significant change between 2004 and 2018, except for cases where it was diagnosed in the localized stage (and only a 0.8 pp/yr average increase there), but these account for only 6% of cases [6]. An analysis linking the SEER data with the registry of the National Death Index has concluded that any drop in mortality due to SCLC that could be observed between 2001 and 2016 is only a result of changes in incidence rates [7].

With classic chemotherapy (carboplatin + etoposide, see ch. 1.1.3.), median overall survival (OS) is only 10.3 months, with median progression-free survival (PFS) at 4.3 months in extensive-stage SCLC [8]. The advent of immunotherapy has brought considerable advancement in the case of many cancer types, but if it holds any breakthroughs for SCLC, we have yet to uncover them. The addition of atezolizumab, an immunotherapeutic that has just recently been made part of standard care (see ch. 1.2.3.), improves the previous numbers statistically significantly, but to an extent that is only slightly relevant clinically (to 12.3 and 5.2 months, respectively) [8].

1.1.2. Biomarkers

The mutations most often found in SCLC are those resulting in a loss of function of TP53 and RB1, two known tumor suppressor genes, directly or indirectly. These are present to the extent that some consider them obligatory. In addition, mutations in EP300, CREBBP, TP73, NOTCH1, -2 and -3 are nearly exclusive of each other and together cover approximately 60% of SCLC cases. Copy number amplification of MYC family genes is also frequent [9]. Unfortunately, loss of function mutations are hard to translate into a druggable target. Overexpression of cMYC has been associated with the effectiveness of CHK1 inhibition [10].

In addition to general markers, it was recognized as early as the 80s that there are subtypes of SCLC that show differential expression of several genes [11], among which the role of neuroendocrine (NE) genes has also been long since recognized [12]. However, this observation was mostly shelved for about 30 years, with only sporadic mention or usage in research, until with the advent of advanced sequencing techniques in the 2010s, the idea was finally revisited. There are two major approaches to subtype classification from this perspective. The first focuses on key transcription factors, mainly NEUROD1, ASCL1, POU2F3, and YAP1 [13–15]. The second utilizes a wider portion of the expression pattern and recognizes NE-high and NE-low clusters [16]. It has been shown that the two classifications are not independent, with NEUROD1 and ASCL1 associating with NE-high status [17]. We have followed a binary, NE-based classification in our studies.

The lung immune prognostic index (LIPI), calculated from serum lactate dehydrogenase (LDH) level and derived neutrophil-to-lymphocyte ratio (dNLR) has also been shown to have prognostic value regarding OS in all stages, and PFS in extensive SCLC [18]. A low NLR on its own also associates with longer OS [19]. The amount of necrosis in the tumor is associated with survival rate, with a high (10%+) ratio of necrosis providing a hazard ratio of 2.87 [20]. Tumor mutational burden (TMB) is also considered, mostly in relation to immunotherapies (see ch. 1.2.3.) but shows mixed results. A clinical trial of atezolizumab reported no predictive power [21]. A retrospective analysis of the KEYNOTE-158 study of pembrolizumab found an increase in objective response rate (ORR, 29% vs. 6%) in high-TMB patients [22].

1.1.3. Clinical practice

While there is progress in research, many new findings have yet to be translated into the field of patient care: neither the official classification of lung carcinomas [23], nor recognized treatment options [24] take into account the heterogeneity within SCLC. Currently, the 8th version of the TNM system (Tumor, lymph Nodes, Metastasis) is used for staging SCLC. In addition, the categories of limited or extensive stage are also used to inform clinical decisions [24]. Limited stage (LS) SCLC is defined as lesions that can be encompassed within a reasonable radiation field and overlaps with clinical stages I-IIA (up to T2, N0, M0), and possibly IIB-IIIC (N1-3, M0), depending on the position of the affected lymph nodes. Less than 5% of diagnoses are made in the limited stage. This is due to the fact that LS-SCLC is most often asymptomatic and therefore detected late. SCLC also progresses very rapidly, so that the patient has a LS malignancy for only a relatively short time. Thus, systematic screening would be the main way to improve early detection rates. At present, however, these do not show considerable benefits. Even after CT screening of patients selected on the basis of risk factors, only 14% of patients with SCLC were detected in the limited stage [25]. Extensive stage (ES) SCLC is defined as lesions that extend beyond a reasonable radiation field, and thus can correspond to clinical stages IIB-IV and is definitively the diagnosis if distant metastases are present (M1).

While in select cases of LS-SCLC, lobectomy is considered as a treatment option, surgical resection is not supported as a general option [26,27]. For most patients, systemic therapy with concurrent radiotherapy (chemoradiotherapy, or CRT) remains the recommended care. For this a regimen of cisplatin and etoposide is the foremost option in LS-SCLC and can be considered for ES-SCLC too, though carboplatin-etoposide with atezolizumab or durvalumab is preferred in that case [24]. The clinical use of the combination of cisplatin and etoposide dates back to 1985 [28]. Cisplatin and carboplatin are platinum complexes with an antimitotic effect, due to their ability to create DNA crosslinks, that differ mainly in their toxicity profile [29,30]. Etoposide is a topoisomerase II inhibitor that creates double-stranded DNA breaks [31,32]. Atezolizumab and durvalumab are immune checkpoint blockers (ICB) targeting PD-L1 and have only been part of standard care very recently (FDA approval came in 2019 and 2020, respectively [33]), supplementing platinum and etoposide combination chemotherapy (see ch. 1.2.3.). An early start of definitive thoracic radiotherapy (RT) is recommended, supported by

diagnostic and imaging techniques to better target the tumor and minimize the irradiation of other organs and thus the side effects. In inoperable cases a more focused and intense irradiation regimen (stereotactic ablative RT, a.k.a. SABR) can be utilized, targeting the primary tumor site or metastases [34]. Brain metastasis is a common complication and is frequently already present at the time of diagnosis. If it is not, prophylactic cranial irradiation (PCI) can be applied in LS-SCLC, with the aim of preventing brain metastases. Meta-analysis of data from the late 20th century has shown improvement in 3yr OS [35], but more recent studies have contested these conclusions [36], and alternatives are being explored due to the negative cognitive effects of brain irradiation. Official guidelines also call for caution in the application of PCI [24,37].

1.2. Tumor Immune Microenvironment

When cells undergo a cancerous transformation, its effects are not limited to those cells themselves and results in a complex process that markedly changes their surroundings. The change in phenotype, including cell surface and secreted molecules, brings about the development of the so-called tumor microenvironment (TME) in the adjoining tissue. The TME is divided into the tumor nest, directly between the neoplastic cells, and the stroma around it, composed of non-cancerous cells (e.g., fibroblasts, mesenchymal cells) and the extracellular matrix (ECM) maintained by them. As the situation progresses, various immune cells might also infiltrate either or both areas. The number and composition of these cells is crucial to the development of the tumor, and thus this aspect of the TME is often referred to as the tumor immune microenvironment (TIME).

The importance of the tumor (immune) microenvironment is becoming ever clearer. Beyond (and in some sense before) therapeutic approaches, this also has considerable impact on the experimental investigation of cancer. The adequacy of laboratory cell lines used out of context is being questioned, with some studies showing that the environment exerts more influence on the cells than their tissue of origin [38]. There are some attempts at preserving or recreating the TME, like patient-derived organoids [39], but *in vitro* studies are still challenging.

In the following subchapters I will first give a brief overview of the humoral and cellular components of the TIME to showcase both the individual elements and their interconnectedness, then explore its translational relevance.

1.2.1. Cytokines

Various small molecule transmitters are present in the TME, mediating the interaction between the tumor and the immune system. As such, some are secreted by the tumor cells themselves, others in reaction to those by surrounding cells, as the microenvironment takes shape.

Cytokines produced by the tumor can cause major alterations to the function of immune cells. Many tumors interfere with the maturation of monocytic cells, among others by producing VEGF, IL-6 and M-CSF, leading to the creation of improperly developed myeloid cells that lack proper MHCII expression and antigen presentation function (myeloid-derived suppressor cells, MDSC) [40,41]. The high levels of adenosine and hypoxic conditions can push macrophages toward an M2-like polarization (see ch. 1.3.3.) [42], and lead DCs to expressing VEGF, IL-6, IL-8, IL-10, COX-2, TGFβ and IDO [43]. DCs co-cultured with NSCLC also exhibit lower levels of TNFα and IL-12, which together with TGFβ and IDO lead to a lower number of IFNγ-producing Th1 cells, and an increase in immunosuppressive Treg cells in the TME [44,45].

In addition to the modulation of immune functions, cytokines can also affect tumor progression. In breast carcinoma, production of M-CSF has been shown to be necessary for metastasis, acting via the recruitment of macrophages [46]. In NSCLC, TGFβ is a major factor in triggering epithelial-mesenchymal transition (EMT), an early step in metastasis, with IL-6 enhancing its effects [47].

It is important to recognize that cytokine function is not necessarily absolute and can be heavily dependent on context [48]. CXCL10 has been shown to exhibit anti-angiogenic properties in melanoma [49], and to in addition inhibit metastasis in NSCLC [50], but has also been identified as a promoter of metastasis in colorectal cancer [51]. The role of TNFα in the TME is also not straightforward. As the name suggests, it was first described as a molecule capable of inducing tumor cell death [52], and it is still being explored as a potent co-factor in combination immunotherapy [53]. On the other hand, it can be secreted by tumor cells or induced by them in monocytes and has been shown to cause elevated PD-L1 expression in myeloid cells, hindering innate antitumor responses and immunotherapies [54]. It can also enhance TGFβ-mediated EMT [55], and $TNF\alpha^{-/-}$ mice were shown to be more resistant to skin tumors [56]. Even more concrete effects can be differentially modulated by the same cytokine. IL-10 has been shown to

both enhance $CD8^+$ T cell function [57], and to hinder it with the involvement of myeloid cells [58].

The above is only a fraction of all effects and connections established by cytokines in the TME, but even from this we can get a glimpse of the complexity of the system. Together with other clinical factors, like short half-life, narrow therapeutic window (i.e., timeframe in which application is effective), and adverse effects related to immunosuppression, this leads us to the conclusion that cytokine monotherapies in general are ineffective as a treatment option in (esp. advanced stage) cancer [59]. This is a trend in therapeutic intervention that our findings presented herein also reinforce (see ch. 4.3.2.).

1.2.2. Immune Cells

Proper characterization of the immune cell content of the TME is crucial. Indeed, this information has been found to be better at predicting clinical outcomes than clinical staging (TNM) in certain cases [60]. The overall level of immune infiltration is an important factor and can be referenced in multiple ways. A TME with low infiltration is sometimes called cold or immune-desert, with high infiltration referred to as hot or immune-oasis. Additional categories are also described sometimes, like ones with lymphoid-like structures attached to the tumor site [61]. These have a crucial impact on the effectiveness of immunotherapies (see ch. 1.2.3.).

In addition to the amount of immune cells, the presence of the various types and subtypes of lymphocytes and myeloid cells modulates tumor progression. As a rough outline, properly activated T_h1 cells, cytotoxic $CD8^+$ T cells (CTL), plasma cells and M1-like macrophages are able to target and eliminate tumor cells, while regulatory lymphocytes (T_{reg}, B_{reg}), MDSC and M2-like macrophage cells are immunosuppressive and thus can be tumorigenic. But as we will see in the following paragraphs, reality is more nuanced.

The helper subgroup of T lymphocytes (T_h) are coordinators of the immune response, mainly by modulating the cytokine milieu. Their various classes have markedly different profiles. T_h1 cells are induced by IFNγ and IL-12, and produce IFNγ, IL-2 and TNFβ [62]. T_h2 cells develop as a response to IL-4, and express IL-4, IL-13, and IL-6 [63]. T_h17 cells are induced by TGFβ and IL-6 [64], and secrete IL-17, GM-CSF, TNFα [65] and IL-22 [66].

$CD8^+$ T cells are often referred to as cytotoxic T lymphocytes (T_c, CTL), and treated as effector cells capable of attacking tumor cells, associated with better prognosis [67]. Generation of cytotoxic $CD8^+$ cells is induced by IL-12 and IL-2, and repressed by IL-4 [68,69]. As they express and are repressed through CTLA-4 and PD-1, they are one of the main targets of ICB therapies [70–72]. However, care must be taken when evaluating this population in the TME. There are multiple subtypes of this group, and not all of them are tumor suppressive [73]. In addition, even the presence of tumor antigen-spe cific, IFNγ-producing $CD8^+$ cells can be insufficient in preventing recurrence [74]. The ratio of CTLs specific to tumor antigens can also be as low as 10% [75,76].

Another subset of T lymphocytes is what is known as regulatory T cells (T_{reg}). These are $CD4^+CD25^+FoxP3^+$ cells, usually associated with immune tolerance and suppression [77,78]. They are a part of the physiologic T cell repertoire but can also be induced in specific environments (like the TME) and can acquire non-suppressive functionality too (producing IFNγ and IL-17) [79]. Induction involves TGFβ and IL-10 [80,81]. T_{reg}-s execute their inhibitory function via multiple pathways. They are able to suppress DC activity through surface expression of the MHCII receptor LAG-3 [82], hinder CTL function by modulating IL-2 [83], show cytotoxic activity against effector cells via granzyme and perforin [84], and express immunosuppressive molecules like CTLA-4, TGFβ and IL-10 [85,86].

Various types of B lymphocytes can also be found in the TME and associated lymphoid tissues, with their presence having a differing impact on prognosis [87]. Specific antibodies can mark tumor cells and trigger attacks from other immune cells: antibody-dependent cellular cytotoxicity (ADCC), mainly from NK cells [88–90], and antibody-dependent cellular phagocytosis (ADCP), mainly by macrophages [91]. B-cells also have antibody-independent functions. Certain subsets are able to produce IFNγ and IL-12, activating other immune cells, but also granzyme B and TRAIL, directly attacking tumor cells [92]. B lymphocytes can also stimulate T cells by acquiring a level of APC function [93], and via expression of the surface molecule CD27 [94]. On the other hand, a subset often termed regulatory B cells is present in multiple types of cancer and shows pro-tumorigenic functions, like promotion of T_{reg} formation [95], for which a direct interaction with tumor cells (via CD40/CD154) may be responsible by induction of IL-10 and TGFβ expression [96].

Dendritic cells (DC) are myeloid cells with APC function that can derive from both bone marrow precursors and circulating monocytes [97]. Mature DCs are often found in the peritumoral or stroma areas and in interaction with lymphocytes. However, in different cases this has both been reported as a factor associated with longer survival [98], and impeding cytotoxic T cell function [99]. This discrepancy might be explained by the existence of a $CD103^+$ subgroup induced by GM-CSF that is able to stimulate CTLs, while other DCs cannot [100].

There is also a category of myeloid cells that seems to be activated but immature. Myeloid derived suppressor cells (MDSC) are $CD33^+$ cells that can present with polymorphonuclear or monocytic morphology [101], and have been shown to correlate with tumor progression [102]. They are not a homogenous group, rather defined by their lack of differentiation into another myeloid effector type and immunosuppressive effect [103,104]. They hinder T lymphocytes via depletion of L-arginine [105–107], and secretion of nitric oxide (NO) [108]. Through production of IL-10, they are able to push TAMs towards an M2-like phenotype and lower their secretion of IL-12 [109]. MDSCs are also angiogenic, producing MMP9, and even able to take on endothelial properties [110].

Previous work in our group has investigated the immune infiltration of SCLC, with a focus on T lymphocytes ($CD3^+$, $CD8^+$) [111]. Here, we aim to expand on those findings by characterizing the myeloid cell population of the SCLC TME.

1.2.3. Immunotherapy

Historically, the treatment of cancers has largely focused on the direct targeting of tumor cells, even though there were some early therapies that aimed at the activation of the immune system. Like Coley's toxins, developed at the end of the 19th century, based on the observation of the effects of a Streptococcal infection on cancer patients [112]. In 1976, application of the BCG vaccine was reported to lower the recurrence of bladder cancer [113]. However, these failed to gain traction in the medical community until the 1990s, when the development of the first immune checkpoint blockers (ICB) spearheaded the current renaissance of tumor immunology, leading to the 2018 Nobel prize [114].

Most of ICB drugs to date are monoclonal antibodies (denoted with a -mab suffix in their name) that focus on one of two receptors and their interactions with ligands: programmed cell death protein 1 (PD-1 or CD279) with either programmed

death-ligand 1 (PD-L1 or CD274) or PD-L2 (CD273) or cytotoxic T lymphocyte associated protein 4 (CTLA4 or CD152) with either CD80 or CD86 (a.k.a. B7-1 and B7-2, respectively). Both receptors are expressed prominently (but not exclusively) on T lymphocytes [115].

The PD-1 pathway is critical for establishing immune tolerance, and defects lead to the development of autoimmune diseases [116,117]. Upregulated expression of the ligands on cancerous cells is able to trigger these defensive mechanisms and aid in immune escape. High expression of PD-L1 is common in hot TIMEs, and ICB targeted at the PD-1/PD-L1 interaction generally associates with better response [118]. Some of the more promising drugs inhibiting this pathway are nivolumab and pembrolizumab, targeting PD-1, and atezolizumab and durvalumab, targeting PD-L1. In the case of non-small cell lung cancer (NSCLC) the phase 3 trial of nivolumab has shown a 50% increase in progression-free survival [119], and there are studies reporting a remarkable increase in OS in 50%+ PD-L1^{+} tumors treated with pembrolizumab (14.2 to 30 months) and atezolizumab (13.1 to 20.2 months) [120], and a 44% increase in PFS (15.6 to 22.4 months) in 1%+ PD-L1^{+} tumors treated with durvalumab [121].

Interestingly, in contrast to NSCLC, in SCLC, PD-L1 expression as a predictive biomarker of responsiveness to immune checkpoint blockade is questionable, with conflicting and difficult to compare results. Joint analysis of two studies investigating pembrolizumab as a third-line treatment indicated a positive connection between marker expression and responsiveness [122]. But other clinical trials, of using atezolizumab [21], durvalumab [123], and pembrolizumab [124] as first-line treatment in ES-SCLC, reported no correlation between PD-L1 expression and benefit to patients. PD-L1 expression also shows no correlation with molecular subtypes of SCLC [125].

Atezolizumab and durvalumab have recently been introduced to the standard care of SCLC. While data from their use in a broader scope is yet unavailable, in clinical trials, the two show effects of a similar magnitude on median OS (10.3 to 12.3 and 10.4 to 12.9 months, respectively) and PFS rate (6.4% to 14.9% and 5.3% to 17.9% at 12 months, respectively) [8,126]. The indication of pembrolizumab and nivolumab for SCLC was withdrawn in 2021 and 2020, respectively, by their manufacturers after failing to meet primary endpoints of OS required to prolong their status after accelerated approval from the FDA [127,128].

The most likely mechanism of action for CTLA4 is by competing for ligands with the stimulatory receptor CD28 [129]. Either in NSCLC or SCLC, clinical trials of the CTLA-4 blockers tremelimumab and ipilimumab have not shown decisive results (NSCLC: [130,131], SCLC: [126,132,133]).

1.3. Macrophages

1.3.1. Development

Immune cells that perform phagocytosis as their main purpose are widespread throughout higher life forms: even in insects that have only three varieties of immune cells, one is a phagocyte [134], and mononuclear phagocytes can be found in all vertebrates [135]. In humans there are resident macrophages in nearly every type of tissue, derived from embryonic precursors, and bone marrow derived monocytes can also extravasate and differentiate into macrophages [136,137]. At first it was theorized that these circulating monocytes are the source of the tissue resident populations, but it has been shown that they are established prenatally and sustain themselves [138]. These local populations show differential gene expression based on their tissue of residence, showing the remarkable adaptive potential of macrophages [139].

1.3.2. Function

The main physiological functions of macrophages are:

- Phagocytosis
- Interfacing with the adaptive immune system, including antigen presentation
- Modulation of inflammation
- Aiding tissue remodeling, and wound healing

Phagocytosis itself can serve multiple purposes. This process aids in the cleanup of unnecessary structures during development and the remains of dead cells, as well as the removal of bacterial invaders. It also serves as the basis of the macrophages' function as antigen presenting cells (APCs). They are capable of expressing MHC class II molecules on their surface and interact with various lymphocytes to direct the adaptive response [140]. On the other hand, they are also capable of suppressing T cell proliferation, mostly via cytokine production [141]. This inherent duality is also present in their relation to inflammation. When presented with pathogen-associated molecular patterns (PAMP) through surface molecules, like various toll-like receptors (TLR), they release inflammatory cytokines (e.g., IL-1β) [142]. But they are also able to act in an

anti-inflammatory capacity, e.g., by secreting TGFβ [143]. During wound healing they take up and degrade collagen [144], modulate the development of stem cells [145], and induce the proliferation of epithelial cells via IL-10 [146].

This variety and variability makes them key components of the TME, and most of these functions should be considered when evaluating their role in cancer. They might work as effector cells as phagocytes, initiate adaptive responses via their APC function, and influence inflammation and angiogenesis [147]. They can affect not only the growth and status of primary tumors but can have a profound impact on the formation of metastases, with some considering macrophage involvement obligatory [148].

1.3.3. Polarization

Differentiation into a macrophage is not the last step in the development of these lines of mononuclear cells. As the cell senses its surroundings and adapts to its particular needs, another series of changes takes place, termed polarization. More than a simple response to a given stimulus, like cytotaxis, this reaction to the extracellular milieu involves considerable changes to gene expression and the overall function of the cell [149,150]. As it displays more plasticity, it is not classified as another step of differentiation, but it is nevertheless crucial in defining the role and effects of the cell.

It has been known for some time that different cytokines are able to induce monocyte to macrophage differentiation and that they have a differential effect. As far back as 1988, te Velde describes the effects of IL-4 in contrast to IFNγ [151]. That this effect can go beyond modulation of a single activation program was expressed by Stein and colleagues, who termed it “alternative activation” [152]. The idea started to mature in the mind of the scientific community, and we encounter the nomenclature of M1 and M2 macrophages, based on the T_h1- or T_h2-biased environment that produced them, first in 2000 [153]. The former is characterized by producing nitric oxide (NO) via expression of the inducible nitric oxide synthase (iNOS), and in general promotes an inflammatory response. The latter secretes ornithine, and in general serves a tissue regenerative function. Soon after, the concept was further refined with the identification of subtypes in the M2 group, with Mantovani and colleagues proposing the terms M2a, M2b and M2c [154]. With the rise of high-throughput techniques the process could be examined with even greater resolution, breaking up the discrete subgroups. Based on transcriptomic

analysis, Xue and colleagues have described the results of polarization as falling on a spectrum [155].

While it is not the most sophisticated level of description, even the distinction between M1 and M2 is important in the context of oncology. Studies that do not specify polarization status can associate macrophage infiltration with good or poor prognosis, but if it is taken into account, we can see that the presence of M1-like cells correlates with more positive outcomes, while M2-like cells are linked to poorer outcomes [156].

1.3.4. Therapeutic Repolarization

As research delved more into the different states of macrophages, it was also discovered that polarization is not terminal, but that a change in the molecular environment can result in adaptive alterations [157]. This also means that repolarization by therapeutic intervention can be a valid option in disease conditions supported by suboptimal macrophage populations, like chronic inflammation [158] or cancer [159].

However, this field of research is still young. Based on a search of available articles (on pubmed.ncbi.nlm.nih.gov, keywords: macrophage repolarization tumor), there are sporadic mentions before 2017 (5.4% of articles), but the intentional exploration of this approach has only picked up after 2019 (78% of articles).

A recent review of the field highlights the importance of the Jak/STAT, PI3K/Akt and NF-κB pathways, and reports some promising results concerning the CD47/SIRPα pathway as targets of repolarization therapy [160].

1.4. Computers in Medicine

1.4.1. Drug repositioning

The development of new drugs is costly, both in time and money. With the advancement of computer technology various options became available to streamline the process [161]. Based on chemical structure the ADMET (absorption, distribution, metabolism, excretion and toxicity) parameters of large libraries of small molecules can be estimated [162]. Indications and effect profiles can be predicted before a single molecule is synthesized [163]. As our data storage capabilities also increased, collection of experimental data into massive databases became available, for both small molecules (like DrugBank [164] and PubChem [165]) and proteins (like UniProt [166] and HPRD [167]), that can serve as the basis of high throughput *in silico* methods.

In addition to the discovery of novel molecular entities, in recent decades drug repurposing, i.e., approval and usage of existing compounds for new indications, has gained prominence. While this has also started with the employment of classical clinical analysis, it was mostly reliant on serendipitous discoveries of side effects (e.g., using aspirin in the treatment of cancer [168,169]). Our group has previously evaluated the effectiveness of aspirin, statins and other drugs with purported repositioning potential in cancer specifically for SCLC, based on clinical data [170]. High throughput *in vitro* methods for screening were developed, but since *in silico* techniques aiming to predict effect profiles work the same for approved molecules and novel ones, they require no special adjustments and present a more easily applicable toolset for systematic screening efforts [171].

1.4.2. Modeling biological systems

Approaching the drug-organism interaction from the other direction, modeling the reaction of biological systems to outside intervention can highlight molecular targets, as well as provide insight into the nature of the unperturbed system. Databases of potential or extant drugs can then be scanned for agents capable of modulating the behavior of the novel targets.

One fairly intuitive way of computationally representing complex systems is through networks. This approach emerged from the mathematical field of graph theory and has gained ground in the early 2000s [172,173]. Focusing on the interconnectedness of components, rather than the mechanism of those interactions, provides a level of

abstraction that bypasses hard to measure biochemical parameters, but nevertheless reveals useful information about the system [174]. It also allows for the easy investigation of the perturbation of multiple targets at once, which is crucial in the understanding of the complete effect profile of a given drug and in the development of combinatorial therapies [175].

In the specific case of macrophage polarization, we are investigating a process that enables the cell to adapt to the needs of its surroundings. If we aim to study it, we have to create a model of that environment. Doing so comprehensively *in vitro* would mean coculturing multiple different cell types, adding numerous small molecules to the medium and monitoring them [176]. That is why most researchers focus on the effect of a few specific signals, outside the broader context present *in vivo* [177,178]. Using a computational, *in silico*, model circumvents those problems, as it gives us full control of the experimental conditions.

2. Objectives

- Characterize the immune cell population (especially TAM and MDSC) of the SCLC TME, according to neuroendocrine subtypes and localization in tumor compartments to identify influential cell types suitable for modulation.

- Analyze the gene expression patterns of SCLC to identify molecular targets in tumor subtypes according to immune cell infiltration and neuroendocrine (NE) marker expression status (low vs high).

- Build an *in silico* model of tumor associated macrophage polarization in response to cytokines and other small molecule transmitters in the tumor microenvironment to facilitate cancer research and therapy development in the field.

- Identify elements of signal transduction in macrophages as potential drug targets in order to modulate the polarization process, and counter or diminish the immunosuppressive effect of macrophages in the TME.

- Evaluate, *in silico*, the potential of combination therapies versus the single-target approach in macrophage repolarization.

- Create a user friendly and collaborative platform collating and presenting the latest drug target information to enhance SCLC drug target validations and drug repurposing.

3. Methods

3.1. Exploring the Microenvironment of SCLC

3.1.1. Patient Population

In our retrospective study, we included surgically resected and histologically diagnosed samples from 1978 to 2013, collected at the National Korányi Institute of Pulmonology (Budapest, Hungary). Of the 219 samples available, matched lymph node metastases were included in 32 cases, and we focus our study on the analysis of these paired samples. A board-certified pathologist has histologically confirmed the diagnosis of SCLC. 27 patients had stage I or stage II SCLC, the remaining 5 had stage IIIA. An exploration of the clinicopathological characteristics has been previously reported [179].

3.1.2. Sample Preparation

Formalin-fixed, paraffin-embedded (FFPE) tissue samples were prepared immediately after the resection procedure. Fixation was performed in 4% formalin for 2 hours in room temperature, followed by an additional 48 hours in 4°C and then embedding into paraffin blocks. These FFPE blocks were used in the construction of a tissue microarray (TMA), according to previously described protocols [180]. The specifics in our study were as follows. We created 5-micron sections with an HM-315 microtome (Microm, Boise, ID, USA), which were then placed on charged glass slides (Colorfrost Plus, #22-230-890, Fisher, Racine, WI, USA). A board-certified pathologist reviewed the slides and identified tumor borders after staining with hematoxylin and eosin on an automated platform (Tissue-Tek Prisma, Sakura, Osaka, Japan). 1-mm punches were then taken from donor tissue blocks, 2 each from primary tumors and 1 each from lymph node metastases (MP10 1.0 mm tissue punch on a manual TMA instrument, Beecher Instruments, Sun Prairie, WI, USA). These were seated into a paraffin block in a positionally-encoded array format.

3.1.3. Immunohistochemistry and -fluorescence

For the purpose of immunohistochemistry 5-micron slices were cut from the TMA blocks and then processed using a Leica Bond RX autostainer. The following antibodies were used:

- against CD68: used as a pan-macrophage marker, mouse monoclonal (diluted 1:300, ab201340)
- against CD163: used as an M2 marker, rabbit polyclonal (diluted 1:400, ab87099)
- against CD33: used as an MDSC marker, mouse monoclonal (diluted 1:200, ab11032)

All three were purchased from Abcam (Cambridge, UK). The Bond Polymer Refine Detection kit (#DS9800) was used to stain the slides, according to Leica IHC Protocol F. Epitope retrieval was performed by a 20 minute exposure to the epitope retrieval 1 (low pH) solution. A Tissue-Tek Prisma automated platform was used to perform clearing and dehydration of the slides, followed by cover slipping with a Tissue-Tek Film coverslipper. In the case of double stainings, the ImmPRESS® Duet Double Staining Polymer Kit (MP-7724, VectorLabs, Burlingame, CA, USA) was utilized, with the HRP Anti-Mouse IgG-brown, and AP Anti-Rabbit IgG-magenta secondary antibodies, counterstained with hematoxylin.

Double immunofluorescence was performed with secondary fluorescently labeled antibodies Alexa 488 anti-rabbit IgG and Alexa 546 anti-mouse IgG (Invitrogen, Carlsbad, CA, USA), targeting epitopes of CD68 and CD163, respectively. Autofluorescence was eliminated with TrueBlack® Lipofuscin Autofluorescence Quencher (Biotium, Fremont, CA, USA) from FFPE samples.

3.1.4. Cell Counting and Analysis

We used an Olympus BX53 upright microscope to capture images of TMA sections. 20 MP resolution images were taken with a DP74 color CMOS camera, using 10x and 20x magnification objectives. The Olympus CellSens Dimensions Software package was used for morphometric analysis. Area annotation was performed manually, as described in, indicating the tumor nest and stroma [111]. To summarize, sections from two separate punches were retrieved for primary tumors, and one for metastases to create the TMA-s. Two different 5µm slices, at least 100µm apart, were quantified from all TMA blocks. Readings from different slices of the same TMA punch were averaged. $CD45^+$, $CD3^+$, $CD68^+$ and $CD163^+$ cells were manually counted by two independent observers, using the cell counter plugin of ImageJ [181]. Due to the low cell density, records of CD33 expression were binned (0 / 1-10 / 11-20 / 21+). MHCII expression was described with an ordinal categorical scale, ranging from 0 to 4.

We have defined high and low levels of immune infiltration, based on $CD45^+$ and $CD3^+$ cell density measured previously by our group [111]. We implemented a threshold taking into consideration the distribution of values observed in our samples and their median absolute deviation (MAD). To be classified as an infiltration-low, a sample has to be low-CD3 in both the tumor nest and stroma compartments and low-CD45 for at least one component. To be classified as an infiltration-high, a sample has to be high-CD3 in either compartment and also high-CD45 in either compartment.

For all density distributions the Kolmogorov-Smirnov test was used as a test of normalcy, and none of them were determined to be normal. Accordingly, we used the nonparametric Wilcoxon signed rank test to compare punches from the same patient (as matched pairs). We found no significant differences, and thus used the mean of the two cores in all analyses. Comparisons between density distributions of $CD68^+$, $CD163^+$, and $CD33^+$ cells from different circumstances (NE-high vs. NE-low, primary tumor vs. metastasis, nest vs. stroma) were performed with the Wilcoxon rank sum test, using two-sided p-values. Correlations between densities and expression levels were calculated using Spearman's ϱ. For both the significance threshold was set at $p=0.05$.

3.1.5. RNAseq Analysis

We have utilized the HTG EdgeSeq Targeted Oncology Biomarker Panel to extract RNA expression data from our FFPE tissue samples [182]. The panel contains 2549 genes related to cancer. Samples were run as singletons, and results were validated with positive and negative process controls. Expression levels of neuroendocrine genes were used as a basis for the NE-high or NE-low classification of samples, as described previously [16,179,183].

3.2. Modeling Macrophage Polarization

3.2.1. Model Design

Since we are interested in the effect of therapeutic intervention, we need a model that can predict the effects of changes to given, specific elements of the system. Anything that can be targeted has to be represented separately, i.e., it needs to be possible to implement external changes to each without changing the rest of the model. That is why I chose a network-based model.

In order to represent a process and not just the general relationships of elements, data on interactions needs to include directionality and distinguish between activation and

inhibition. In other words, edges need to be directed and signed. We also need to decide on a level of complexity. Theoretically even biochemical reaction data can be directly incorporated into a network framework, with differential equations governing changes. However, experimental data is prohibitively sparse and not uniformly measured. Taking into account the planned scale of the model, we have opted for a simpler representation, a Boolean network with logical gates. This is a well-established method that allows for the integration of diverse data sources [184], and for added complexity in the situations simulated, like the systematic examination of multi-target therapies [175].

3.2.2. Network Elements

3.2.2.1. Nodes

Our aim is to model the response of the cell to outside signals. This defines a clear input: extracellular signaling molecules. It is also practical to choose a well-defined output: a set of entities that will represent the response (polarization) of the cell. While there certainly are proteins that exhibit changes in activity, we know that such a critical change to the cell's functionality involves changes to gene expression. Protein activity and gene function both influence each other, but modeling the complexity of that feedback system is outside the scope of the current study. Using gene expression as output provides a natural endpoint.

We have also started the definition of nodes with the two sides of inputs and outputs, as they form the frame of our model. We searched the literature for primary research articles on macrophage polarization that provide experimental evidence about the effects of potential inputs (extracellular stimuli), and outputs (gene expression) [159,177,185]. We prioritized components that are supported by multiple references to raise the confidence level of the data and make verification feasible. The need for manual curation also imposed a limit on model size, making this method more fruitful than paring down an extensive list of potential components from a large database. Genes without sufficient information on the transcription factors regulating them (at minimum a set of TF-s that are necessary and sufficient for expression) were excluded. This included VEGFA, which undergoes splicing events that markedly alter its function, but the proteins responsible are not well described [186].

In order to connect the two sides of the model, we collected the elements of major pathways from the KEGG Pathway database [187]. We limited our search to pathways

that are researched in such detail that we could expect to extract an unbroken and functional series of direct connections from the available literature and data. The Jak/STAT, MAPK, PI3K/AKT, and TLR pathways were selected, as this group contains all input and output points of our system and meaningfully connects them. To ensure that any combinatorial effects and crosstalk between the pathways is present in the model, first neighbors of these core nodes that interact with components from at least two pathways were added, based on the databases listed in ch. 3.2.2.2.. The list of nodes was also reviewed based on our verification criteria (see ch. 3.2.3.4.). We have found criteria that could not be satisfied with only the nodes collected in the above, systematic manner. In these cases, we have analyzed the literature about the expression of the genes in question, and upstream signaling elements as necessary, to identify the source of the discrepancy. In some cases, functional components were found to be missing from the model and were then included as additional nodes (see ch. 4.2.2.).

We have also checked the relevance of each node and excluded proteins that do not change in activity in macrophages. On one end are proteins that show no expression in macrophages. This is according to the Gene Atlas database (accessed via biogps.org) [188]. On the other are those that have constitutive activity in this cell type (e.g., PU.1, a transcription factor). These were considered to be essential for either the survival of the cell or upholding its identity as a macrophage, making them unfit to be targeted with therapeutic intervention. Thus, they would have been nodes that are active in all cases and states of the model and would hold no information whatsoever.

The accurate representation of certain proteins and their processes in our Boolean system has necessitated the addition of a number of “technical” nodes. These denote complexes and altered forms whose behavior could not be described with only the proper choice of edge weights. Furthermore, we have grouped certain proteins into one node if their functionality did not differ on a scale that could be represented in our system. For example, we have included only a single “PI3K” node to account for the complex of multiple separate protein subunits. Interactions of group members were included as interactions of the whole group.

The entire list of nodes, their groupings and expression levels are presented in Supplementary Table 1 of [189].

3.2.2.2. Edges

To define our edges, we first collected and collated information from the STRING [190] and SignaLink2 [191] databases. Since we are looking for direct interactions, we have limited the data loaded from the STRING database to those tagged as "binding". Both databases contain data for which evidence is circumstantial or weak: STRING often lists connections that are based on the interactors' presence in the same pathway, and SignaLink2 contains edges that are supported only by *in silico* predictions. We did not include these. During the later stages of model construction, we have also utilized the HPRD database to check individual interactions [167]. We did not find a database of transcription factor - gene interactions suitable for our needs, and thus those edges are based on a systematic manual search of the literature. Since the databases do not contain (unequivocal) information on the direction and sign of edges, this information was collected separately as part of the manual curation of the system. Evidence was collected with the aim of describing a human macrophage, with evidence in other cell types usually rejected. Exceptions to this were made only if it served to fulfill verification criteria (see chs. 3.2.3.4. and 4.2.2.).

With regards to the interactions represented by edges, it should be noted that sub-protein elements of signal transduction (Ca^{2+}, PIP_3) were not given separate nodes. In addition, physical interactions within larger complexes were omitted, based on the analysis of the information flow in the complex. E.g., while MyD88 and TRAF6 have a physical bond in vivo, their relationship is already functionally described in the MyD88 → IRAK1 → TRAF6 set of edges. These bonds and scaffold proteins serve an important function in the kinetics of the formation of complexes, but unless a component of the model is able to completely disrupt the binding, their effects are too subtle to include in our Boolean system.

The edges are also weighted in order to encode how multiple incoming edges affect the activity of their target, by effectively creating logic gates. Thus, they do not represent parameters of the binding event or enzymatic action, but rather dependencies. If a node has two incoming edges of weight 0.5, these interactions are assumed to be both necessary for the activation of the node (rather than, e.g., both being able to create 50% activity), forming an AND gate (see Eq.1. in ch. 3.2.3.1.). Inhibition is represented by

negative weights, and such edges are otherwise evaluated in the same manner as activating ones.

The complete list of edges, including references in support of them, is presented in Supplementary Table S2 of [189].

3.2.3. Model Evaluation

Calculations were performed with MatLab (The MathWorks, Inc.). Scripts are available as Supplementary File S5 of [189].

3.2.3.1. State progression

The model starts each run with all nodes inactive, except for those constitutively active for technical reasons and any input nodes chosen for that particular instance. The activation state of these nodes is kept constant. From this starting point the system advances in discrete steps. The new activation state of each non-fixed node is calculated from the previous network state and all of them are evaluated in each step; this is called a synchronous update scheme. The nodes that have an impact on the state of a particular node are the ones sending edges to it. Their concerted effect is represented by a logical gate and is encoded in the weight of those edges.

These steps are continued until a stable cycle of network states is reached. This set of states is called an attractor, more specifically a limit cycle if there is more than one constituent state and a fixed point of there is only one. To recognize attractors, we have used an implementation of Brent's cycle detection algorithm [192]. The output of the model is always evaluated after an attractor has been reached. We base the mathematical representation of this ruleset on the one published in [193]. Subsequent system states are calculated as:

$$S_{t+1} = thr\left(W \cdot S_t - \Theta\right) \qquad \text{[Eq.1.]}$$

where S_x is the state of the system at step x, represented as a binary column vector, W is a square weight matrix containing all edge weights (with nonexistent edges having a weight of 0), Θ is a vector of threshold values for each node and thr is a threshold function defined as: [if $x \geq 0$: thr(x)=1, otherwise thr(x)=0]. Constitutive node states are implemented by changing the threshold value for them (in Θ) to ± 100, making them independent of incoming edges or their lack thereof.

3.2.3.2. Polarization index

The output of a particular run is a gene expression pattern, encoded as the activation state of the output nodes. We chose to process this into a continuous index value representing polarization state, in accordance with the spectrum model of macrophage polarization [155]. We refer to this as the polarization index, or pI, and calculate it as:

$$pI(i)=\frac{A_1(i)}{T_1}-\frac{A_2(i)}{T_2} \qquad \text{[Eq.2.]}$$

where $A_x(i)$ is the number of active outputs of type x given input i for fixed point attractors, and the sum of the ratio of states in which each output of type x is active for all such outputs given input i for limit cycles. T_x is the total number of outputs of type x. Type 1 genes push polarization in an inflammatory direction (towards an M1-like state), and type 2 genes promote a tissue-protective polarization (towards an M2-like state). In our model the outputs designated type 1 are: CD64, CD68, CIITA, CXCL10, IFNβ, IL-12A, IL-12B, IL-1B, IL-6, iNOS, and TNFα. The outputs considered to be type 2 are: CCL17, CCL22, CCL24, CD209, MERTK, MRC1, and TGFβ.

3.2.3.3. Synergy index

In the simulations where we inhibit two nodes simultaneously, we define a measure of synergy, i.e., how different is the result of these inhibitions from what we would expect based on their individual effects. We term this the synergy index, or synI, and calculate it as:

$$synI(A,B,i)=\frac{\left|\Delta pI(AB,i)\right|}{max\left(\left|\Delta pI(A,i)\right|+\left|\Delta pI(B,i)\right|,\tau\right)} \qquad \text{[Eq.3.]}$$

where ΔpI(X,i) is the change in polarization index due to the inhibition of node(s) X compared to no inhibition under the same input conditions, i. τ is an adjustment parameter included to avoid extreme index values in cases where ΔpI values are low for single inhibitions, as these would be misleading. In our work we use τ=0.1, but this choice is arbitrary.

3.2.3.4. Verification

The aim of this model is to link external stimuli to changes in gene expression. Thus, the most direct way to verify that it reflects the real-world workings of the system it represents is via comparison to experiments measuring the same. There is not enough data in literature about changes to protein activity levels during these studies to include such in our evaluation, and so we have to restrict the verification to inputs and outputs only. There are some cases where multiple of our outputs were measured in response to one of the inputs, but keeping this linkage would mean we would have to evaluate them on a per-study basis, which could introduce a bias we would have to control for. Thus, we verify the model with individual input-output pairs supported by *in vitro* experiments. We only take into account results that are clearly stimulatory or inhibitory, the former satisfied by the gene node being active in response to the given input alone, the latter by the gene node being inactive. Articles that report no significant change in expression levels were not included. We have collected evidence for 55 input-output pairs. The pairs and the PMIDs of the articles in support of them are presented in Supplemental Table S3 of [189].

3.3. Online data collation tool

Our data retrieval and integration utility is built with the R language and produces an HTML output viewable in any browser. A target list can be provided as a local TSV file or online as a Google Sheet document. Targets should be specified with their HUGO (Human Genome Organization) name and UniProt ID. The first R script (clue.R) loads this list, then accesses the REST API of clue.io and for each listed element looks for components in its database, i.e., any information about repurposing attempts. Entries without a clue.io record are excluded from further searches. This data is passed to the next script as an RDS file (a format specific to the R language). In the next step dataPatch.R collects additional data from various sources. It automatically searches the FDALabel service and the website of the European Medicines Agency (EMA) and filters the results to provide direct links to relevant drug labels. Using the UniProt ID, data about the target is collected through the UniProt REST API, including Gene Ontology (GO) terms from the molecular function and cellular component categories, and references to STRING and Reactome. Using the compound name found in clue.io, a search request is sent to the PubMed database. Results are filtered for randomized controlled trials, clinical trials,

reviews, systematic reviews and meta-analyses and the top 3 according to the best match algorithm of PubMed are recorded. A third R script (renderWebPage.R) is responsible for creating a human-readable output. It collects related information from different sources into one group (like multiple mechanism of action (MoA) items or outgoing links to similar resources like DrugBank and PubChem) and converts the data table structure into a hierarchical presentation format. A more in-depth explanation of underlying functions is available at https://cycle20.github.io/EZCancerTarget/index.html, and all scripts, version descriptions and the runtime environment can be downloaded for free at https://github.com/cycle20/EZCancerTarget.

4. Results

Primary tumors and metastases were classified into NE-high and NE-low categories. The NE-high subtype was more prevalent in the cohort, with 20 primary and 24 metastatic tumors falling into this group. There were 11 primary and 8 metastatic samples in the NE-low group. Next, we characterized the samples in regard to immune infiltration level. In our analysis, 56% of infiltration-high tumors were classified NE-low, and 87.5% of infiltration-low tumors as NE-high.

4.1. Myeloid cells in the TME of SCLC

4.1.1. Distribution

The distribution of $CD33^+$, $CD68^+$ and $CD163^+$ cells shows a particular pattern across our axes of interest: tumor nest/stroma, primary/metastatic and NE-high/NE-low [fig. 1., fig. 2.]. By comparing pairs of data that differ in one attribute (e.g., CD86 in the stroma of primary tumors in NE-high vs NE-low samples), we have observed the following. First, the stroma has two properties in contrast to the tumor nest: overall immune infiltration is significantly higher ($p<0.008$ in all cases, for all myeloid cell types), and it has $CD33^+$ cells (though fewer in number than other immune cells [fig. 1. (I)]). Second, in primary NE-low tumors, we can detect a higher density of myeloid cells, when compared to their NE-high counterparts [fig. 1. (J, K)]. Specifically: a significantly higher density of $CD68^+$ and $CD33^+$ cells in the stroma ($p=0.048$ and 0.019, respectively), and a significantly higher density of $CD68^+$ and $CD163^+$ cells in the tumor nest ($p=0.032$ and 0.003, respectively) [fig. 2.].

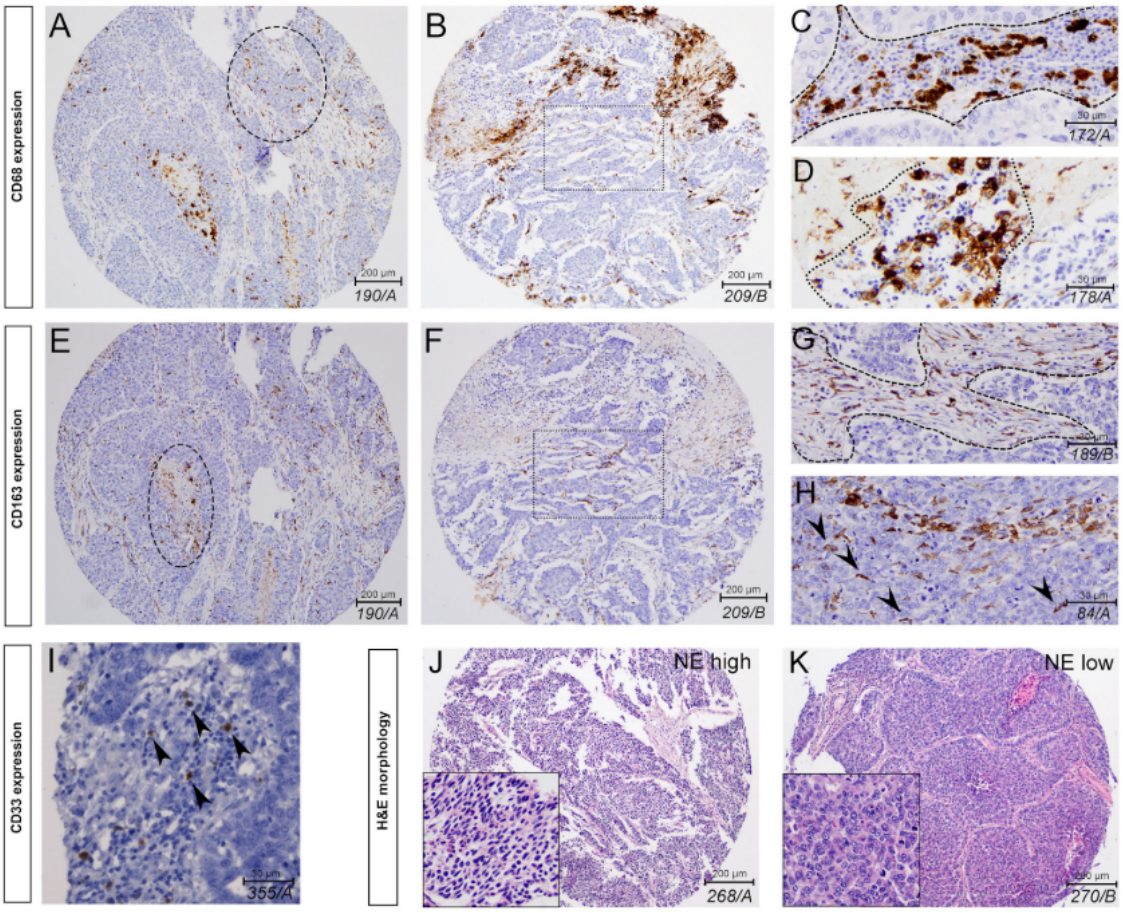

Figure 1. Immunohistochemical analysis of myeloid markers in SCLC tissue samples. Samples are formalin-fixed and paraffin-embedded (FFPE). Myeloid cells show multiple morphologies. Both amoeboid and ramified cells express CD68 (A-D), while CD163^{+} cells are mostly ramified and exhibit long processes (G). Both markers show preferential expression in the stroma compartment (ROI-s marked on C, F, and G). CD163 expression is particularly sparse in the tumor nest (arrowheads on H). In cases of high immune infiltration, CD68 can be found in the nest compartment (ROI on A). Both macrophage markers also appear in necrotic areas (ROI-s marked on D and E). CD33^{+} cells are present exclusively in the stroma, and only in low numbers (arrowheads on I). On images J and K hematoxylin and eosin staining shows the histologic characteristics of neuroendocrine (NE) high and low tumors, respectively. (Source: [194]*, used according to the Creative Commons Attribution (CC BY) license.)*

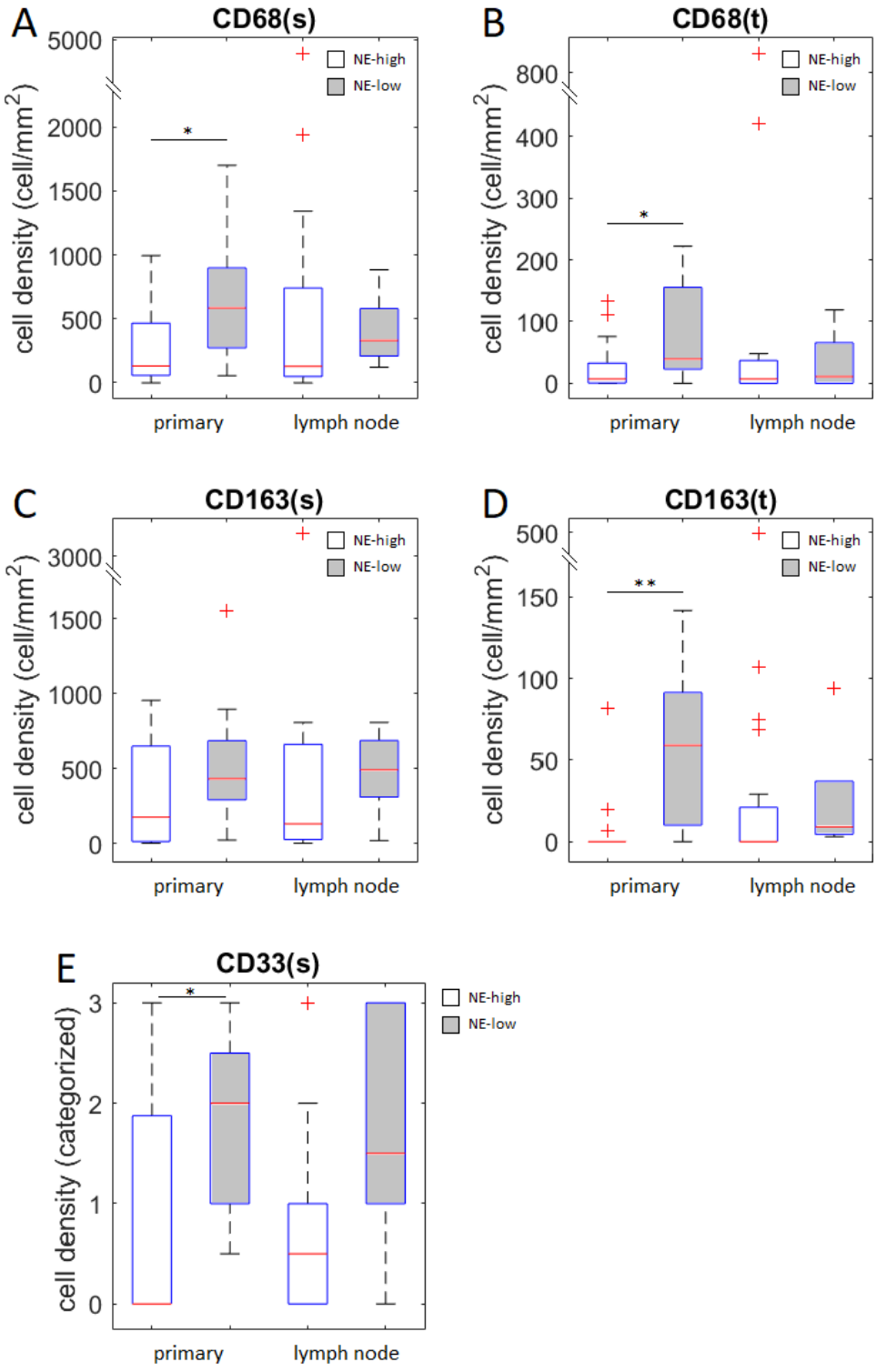
A
CD68(s)
cell density (cell/mm2)
5000
2000
1500
1000
500
0
*
NE-high
NE-low
primary
lymph node
B
CD68(t)
cell density (cell/mm2)
800
400
300
200
100
0
*
NE-high
NE-low
primary
lymph node
C
CD163(s)
cell density (cell/mm2)
3000
1500
1000
500
0
NE-high
NE-low
primary
lymph node
D
CD163(t)
cell density (cell/mm2)
500
150
100
50
0
**
NE-high
NE-low
primary
lymph node
E
CD33(s)
cell density (categorized)
3
2
1
0
*
NE-high
NE-low
primary
lymph node

➢ Figure 2. Comparison of cell density data of myeloid cells in different SCLC subtypes and split between the stroma and tumor nest compartments. $CD68^+$ cell numbers are significantly increased in primary NE-low tumors, compared to NE-high (A, B). While $CD163^+$ cell density does not show significant differences in the stroma across subtypes and compartments (C), it is significantly elevated in the nest of primary tumor sites of NE-low cases (D). CD33 did not appear in the tumor nest. In the stroma, its levels are increased in primary NE-low tumors (vs. primary NE-high) (E). There were no significant differences in CD68, CD163, and CD33 expression patterns of NE-high and NE-low cases in lymph node metastases (A-E). Data was obtained with immunohistochemistry from formalin-fixed, paraffin-embedded (FFPE) samples, organized into a tissue microarray. Values for a given sample are the average of two slices from the same punch. Values measured in the stroma are indicated with (s) in the title (A, C, E), while those from the tumor nest are labeled (t) (B, D). Grouping based on neuroendocrine marker expression is shown with the box color: clear for NE-high and gray for NE-low. For CD68 and CD163 (A-D), cell density is measured in cell/mm^2. In the case of CD33 (E), density was measured as distinct categories labeled from 0 to 3. In all figures the red line represents the median of values, the box ranges from the 25th to the 75th percentile and whiskers stretch to the minimum and maximum values (ignoring outliers). Red (+) marks indicate outliers, defined here as values further from the closest edge of the box (25th or 75th percentile) than 1.5 times the height of the box. Vertical axes in A-D have a break point (marked with \\) in order to accommodate all outliers without compromising the presentation of the bulk of the data. (*) marks $p<0.05$ and (**) $p<0.01$, according to the Wilcoxon rank sum test. (Candidate's own figure, unpublished)

4.1.2. Associations with other immune markers

Previously, our group has also measured CD45 (as a pan-leukocyte marker), CD3 (as a T-cell marker) and the major histocompatibility complex II (MHCII) expression of tumor cells [111]. Here, we have analyzed the correlations between these factors and myeloid cell markers [fig. 3.].

We observe that all significant correlations are positive. CD68 shows negative association to all other markers in NE-low metastases, in the stroma and nest separately (ϱ=-0.314 to -0.872), but these are not significant ($p>0.05$), possibly affected by the low number of observations (n=5 or 6). CD45 and CD3 show consistently high correlation in all cases (min ϱ=0.821). In primary tumors, evaluating the stroma and the nest together, all 4 cell types have fairly high correlation, with values slightly higher in NE-low cases. In lymph node metastases this is limited to NE-low tumors and excludes CD68. If we stay focused on primary tumors, but look at the tumor nest separately, all markers show consistently high correlation, including tumor MHCII expression (CD45/CD3 ϱ=0.928, for all others ϱ=0.703 to 0.812). In the stroma of primary tumors CD3, CD45 and CD163 are strongly correlated (min ϱ=0.811), with CD68 and MHCII showing lower levels of association to other markers.

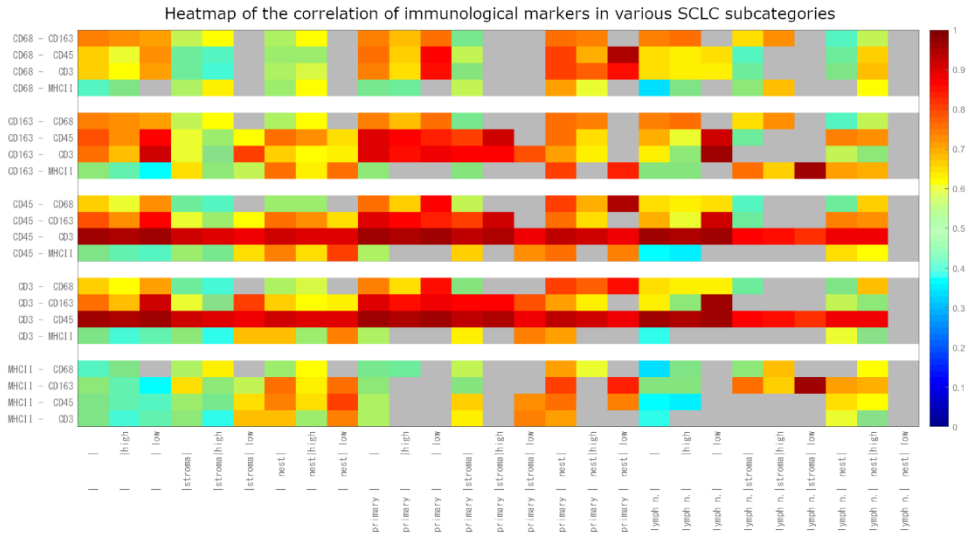

Figure 3. Heatmap of the correlation of immunological markers in various subsets of SCLC samples. The markers being compared are CD68, CD163, CD45, and CD3 on immune cells and MHCII on tumor cells. The pair of markers being compared is indicated on the vertical axis (one group for each marker), and the subsets on the horizontal axis. If a category is left blank, both options for that category (subtype, compartment or

localization) were taken into account. "high" and "low" refer to neuroendocrine (NE) marker levels. "lymph n." refers to lymph node metastasis, in contrast to the "primary" tumor site. Color corresponds to the value of Spearman's ϱ, with the scale indicated on the bar on the right. No value is presented (marked in gray) for cases where the correlation is non-significant ($p>0.05$). There are a number of "hot spots" with high correlation values. CD3 and CD45 correlate strongly over all categories. Without categorization with regards to nest/stroma and primary/lymph node, all immune cell markers correlate moderately or better with each other. The situation is similar if we look at only primary tumors, with a few exceptions, including cases where MHCII also correlates with the other markers (notably primary/nest/-). CD163 correlates strongly with CD3 and CD45 in the lymph node/-/NE-low case. (Candidate's own figure, unpublished)

4.2. Boolean Network Model of Macrophage Polarization

4.2.1. Characteristics

We have built a network that includes 106 nodes and 217 edges between them. Of the nodes, there are 9 input and 22 output, with 75 inner nodes connecting them [fig. 4.]. One of the fundamental characteristics of a network is its degree distribution. (The degree of a node is the number of edges connected to it.) Protein-protein interaction networks have been observed to fall into a specific category regarding this in most cases. They exhibit a so-called scale-free architecture, where the degree distribution follows a power law [195]. We have examined our system to check whether it also follows this trend [fig. 5. (A)]. The disparity in the case of degree = 1 can be explained by the fact that this is a control network. A degree of one is restricted to input and output nodes only, as all others are required to have at least one incoming and one outgoing edge. The only exception to this are the JAK-s that have no inputs, as their nodes are constitutionally active for technical reasons, and out of them only JAK3 has only 1 edge. This limitation is responsible for the lower-than-expected frequency. The other difference is the overrepresentation of nodes of degree = 4. While a direct cause is hard to ascertain, we observe that most technical nodes (8 out of 11) have this trait. Excluding technical nodes from calculations fails to bring the number in line with expectations. If we declare degree = 1 and degree = 4 outliers and exclude them, the network fits a scale-free distribution ($R^2 = 0.80$).

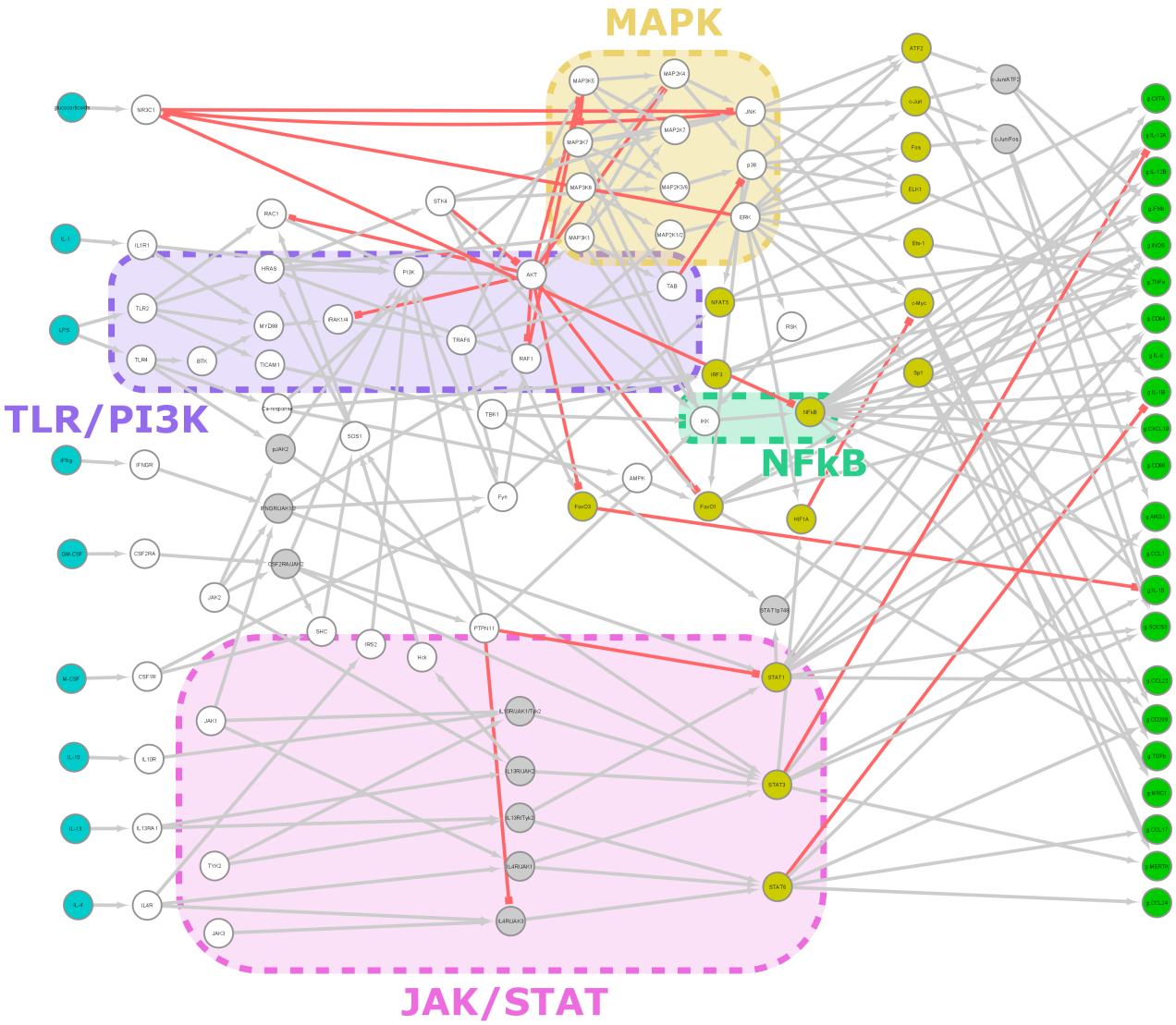
MAPK
TLR/PI3K
NFkB
JAK/STAT

➢ *Figure 4. Visual representation of the macrophage polarization network. Certain categories of nodes are colored (teal: input, green: output, yellow: transcription factors, gray: technical nodes). Red edges indicate an inhibitory effect. Signaling pathways are highlighted with colored boxes. The image was created with the aid of Cytoscape. (Candidate's own figure, published in* [189]*, used according to the Creative Commons Attribution (CC BY) license)*

To rule out that our selection of nodes created any major distortions in the pathways examined, we checked the betweenness centrality of nodes [fig. 5. (B)] and confirmed that we cannot find any component with an anomalously heightened value. Looking at the attractors reached, in the case of the unperturbed model and single inhibitions, all of them are steady state. This is to be expected, based on our decision to not include major feedback loops. This changes and a few limit cycles appear (2894, 0.26%) with the simultaneous inhibition of two nodes, showing that the model is not completely bereft of cyclical substructures. In order to double-check that all interactions in the model can happen in an actual cellular environment, we have pulled localization data for all components from the Gene Ontology database [196,197] [fig. 5. (C)]. All interactions are theoretically possible in the cytosol, nucleus or the plasma membrane.

4.2.2. Verification

When the verification criteria were first applied to the model during development, the output had an approximately 65% match with it. Differences between the two were used to spot incorrect or incomplete parts of the model. There were three major points of difference that involved the addition of new nodes. The protein node HCK was introduced to reconcile the model with the IL13→$CD209^+$ criterion [178]. There was support for an IL13→Akt connection, but not in macrophages [198]. Investigating this link led us to HCK, and it was then included based on the support for the overall input-output link established in macrophages. The GM-CSF→$CIITA^+$, $iNOS^+$ criteria [199,200] could not be satisfied within the framework at the time, and this prompted the search for a "missing" node and later addition of the transcription factor NFAT5. The node of STK4 was added and removed multiple times during the fine-tuning of the system, due to insufficient data about its direct connections and was kept in the published version of the model based on its effects on verified input-output connections. The final model shows a 94.55% match with the verification criteria (52 of 55).

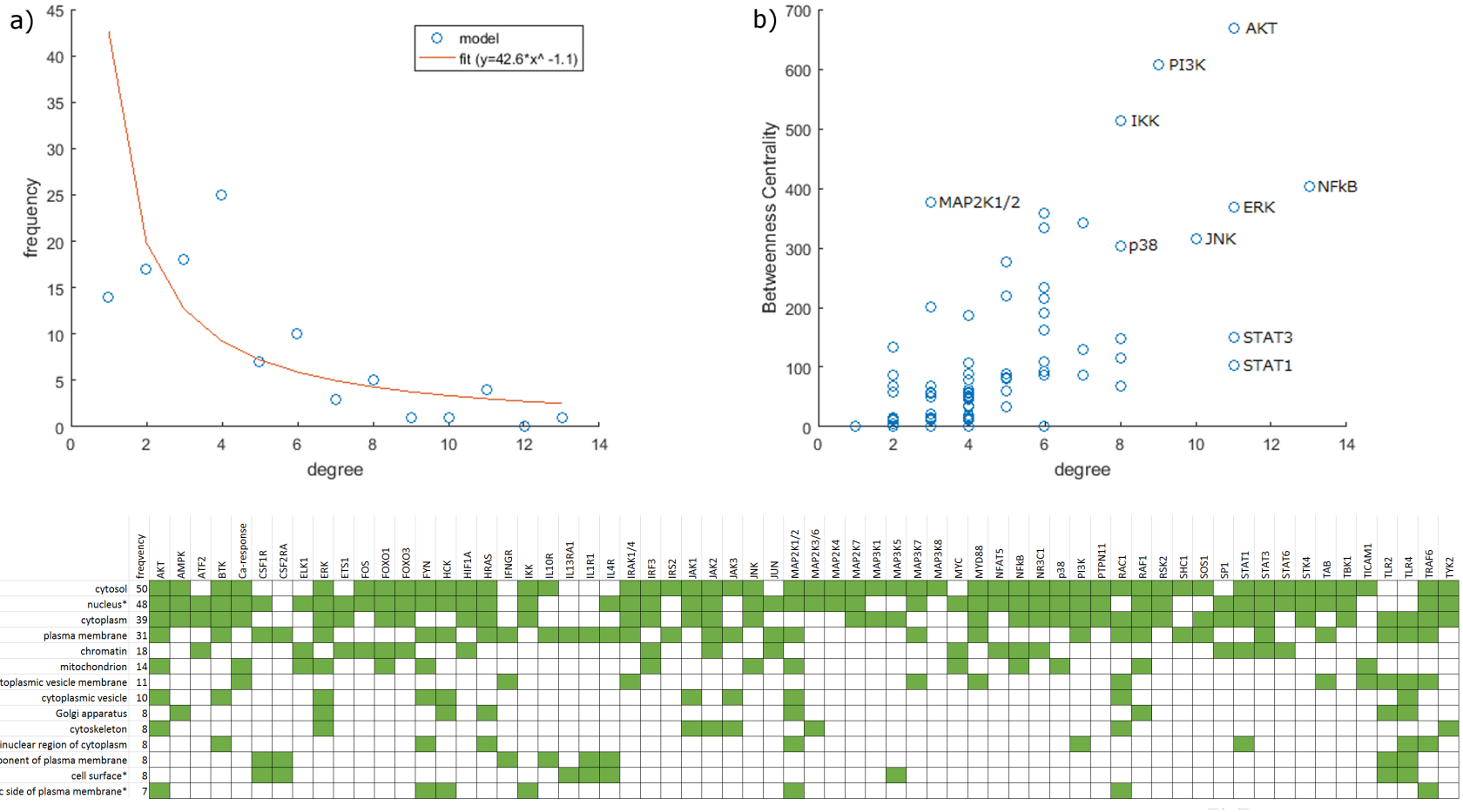
a)
model
fit (y=42.6*x^ -1.1)
frequency
degree
b)
Betweenness Centrality
degree
AKT
PI3K
IKK
NFkB
MAP2K1/2
ERK
JNK
p38
STAT3
STAT1
c)
frequency
AKT
AMPK
ATF2
BTK
Ca-response
CSF1R
CSF2RA
ELK1
ERK
ETS1
FOS
FOXO1
FOXO3
FYN
HCK
HIF1A
HRAS
IFNGR
IKK
IL10R
IL13RA1
IL1R1
IL4R
IRAK1/4
IRF3
IRS2
JAK1
JAK2
JAK3
JNK
JUN
MAP2K1/2
MAP2K3/6
MAP2K4
MAP2K7
MAP3K1
MAP3K5
MAP3K7
MAP3K8
MYC
MYD88
NFAT5
NFkB
NR3C1
p38
PI3K
PTPN11
RAC1
RAF1
RSK2
SHC1
SOS1
SP1
STAT1
STAT3
STAT6
STK4
TAB
TBK1
TICAM1
TLR2
TLR4
TRAF6
TYK2
cytosol 50
nucleus* 48
cytoplasm 39
plasma membrane 31
chromatin 18
mitochondrion 14
cytoplasmic vesicle membrane 11
cytoplasmic vesicle 10
Golgi apparatus 8
cytoskeleton 8
perinuclear region of cytoplasm 8
integral component of plasma membrane 8
cell surface* 8
cytoplasmic side of plasma membrane* 7

➢ *Figure 5. General statistics of the in silico protein-protein interaction network, representing overall structural properties (degree distribution (a), betweenness centrality of nodes (b)) and co-localization of components (c).* ***a)*** *Degree distribution. A power law curve was fitted ($R^2 = 0.80$) to the data with degrees 1 and 4 ignored as outliers (red line). This supports that our network has a "small world" property, a characteristic feature of most biological networks.* ***b)*** *Betweenness centrality against degree per node. Nodes of possible interest are labeled. All nodes emerging this way are known to be of central importance, meaning that our network does not overrepresent minor actors and pathways.* ***c)*** *Cellular localization of model components. For each protein data from the Gene Ontology database was extracted. Here the terms were extended to include all sub-terms (those connected with one or more "is_a" relations). In the cases marked with an asterisk, certain terms connected by a "part_of" relation were also merged: "nucleoplasm" and "nuclear body" were merged into "nucleus", "external side of plasma membrane" was merged into "cell surface", and "extrinsic component of cytoplasmic side of plasma membrane" was merged into "cytoplasmic side of plasma membrane". The components of the network co-localize into major subcellular compartments, supporting that direct interaction between them is feasible in vivo. (Candidate's own figure, published in* [189]*, used according to the Creative Commons Attribution (CC BY) license)*

We have also examined how internally consistent the assignment of inputs and outputs to polarization directions is. We calculated a polarization index for the input nodes too, analogous to what we defined for the outputs (see ch. 3.2.3.2.), for all input combinations, based just on their assignment. Then we compared the two indices [fig. 6.]. While the correlation between them is moderate, with a Pearson r of 0.58, the tendency we expected from their relation is apparent. In addition, a slight clustering of the output pI values can be observed. This is not an inherent attribute of how the index is constructed, as the value set is close to continuous. There are three subsets, one each that shows polarization towards an M1-like and an M2-like state, and one that is transitory or uncommitted. There is only a relatively narrow band of input-pI where both committed subgroups are present, at input-pI = 0 and slightly below that. The subgroups also separate on the output-pI axis, with transition points at approximately ±0.2. We use these values in the definition of repolarization (see ch. 4.3.2.).

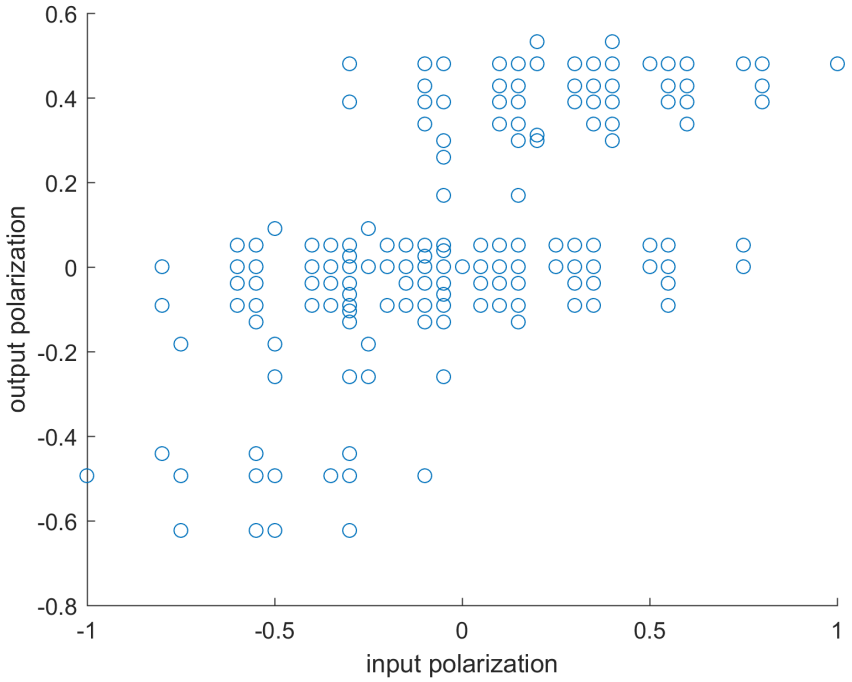

Figure 6. Relating input and output polarization of a macrophage in the BCN model. Each instance of a unique input combination is represented by a circle. A significant moderate correlation between the two indices can be clearly observed (Spearman's $\varrho=0.555$, $p=1.09\times10^{-42}$*). This supports that the model does not deviate severely from our current knowledge of the high-level functions (i.e., promotion of M1-like or M2-like behavior) of these components. (Candidate's own figure, published in* [189]*, used according to the Creative Commons Attribution (CC BY) license)*

4.3. Molecular Targets

4.3.1. Targeted RNA seq of SCLC tissue samples

After identifying four tumor subsets (see ch. 4.), we looked for potential molecular targets by comparing gene expression values between them. To visualize particularly enhanced or repressed genes, we created volcano plots [fig. 7.]. The comparison of primary and metastatic samples shows only few points of significant difference [fig. 7. (F)], and thus for the other plots we pooled their data. To establish the differences between the major subgroups, we plotted all NE-high versus all NE-low and all infiltration-high versus all infiltration-low samples [fig. 7. (A, B)]. As an infiltration-high TME is expected to be more susceptible to immunotherapy, we were also interested if we could focus such efforts based on NE status [fig. 7. (C)]. Since the NE subtypes are already gene expression based, we also wanted to explore any more subtle differences within these groups, in relation to immune infiltration status [fig. 7. (D, E)].

The volcano plot analysis highlighted certain gene sets. In the case of NE subgroups, the following show a heightened expression compared to the other subgroup. In NE-low: ANXA1, CD44, CD70, CXCR2, FCGR1A, HLA-B, IFI27, ITGAM, ITGB6, ITGB4, KRT5, MYC, MMP7, YBX3. In NE-high: CDH2, CHGA, FGF5, GRP, ISL1, NCAM1, NKX2, SOX3, SYP. Genes in the NE-high group are mainly neural or neuroendocrine differentiation factors. The immune-infiltration based subgroups exhibit higher levels of the following genes. In infiltration-high: CD70, CXCL9, CXCR2, FCGR1A, GZMA, HLA-B, MMP7, ITGAM, IFI27, YBX3. In infiltration-low: CDH2, CHGA, FGF5, GRP, IL9, INS, ISL1, NCAM1, SYP. The NE-high and infiltration-low lists show considerable overlap. These cross-subtype similarities are further explored on the Venn diagrams of [fig. 8.]. We have collected emerging potential molecular targets that already have drugs available for them (in clinical trials or launched) in Supplementary Table S6 of [194].

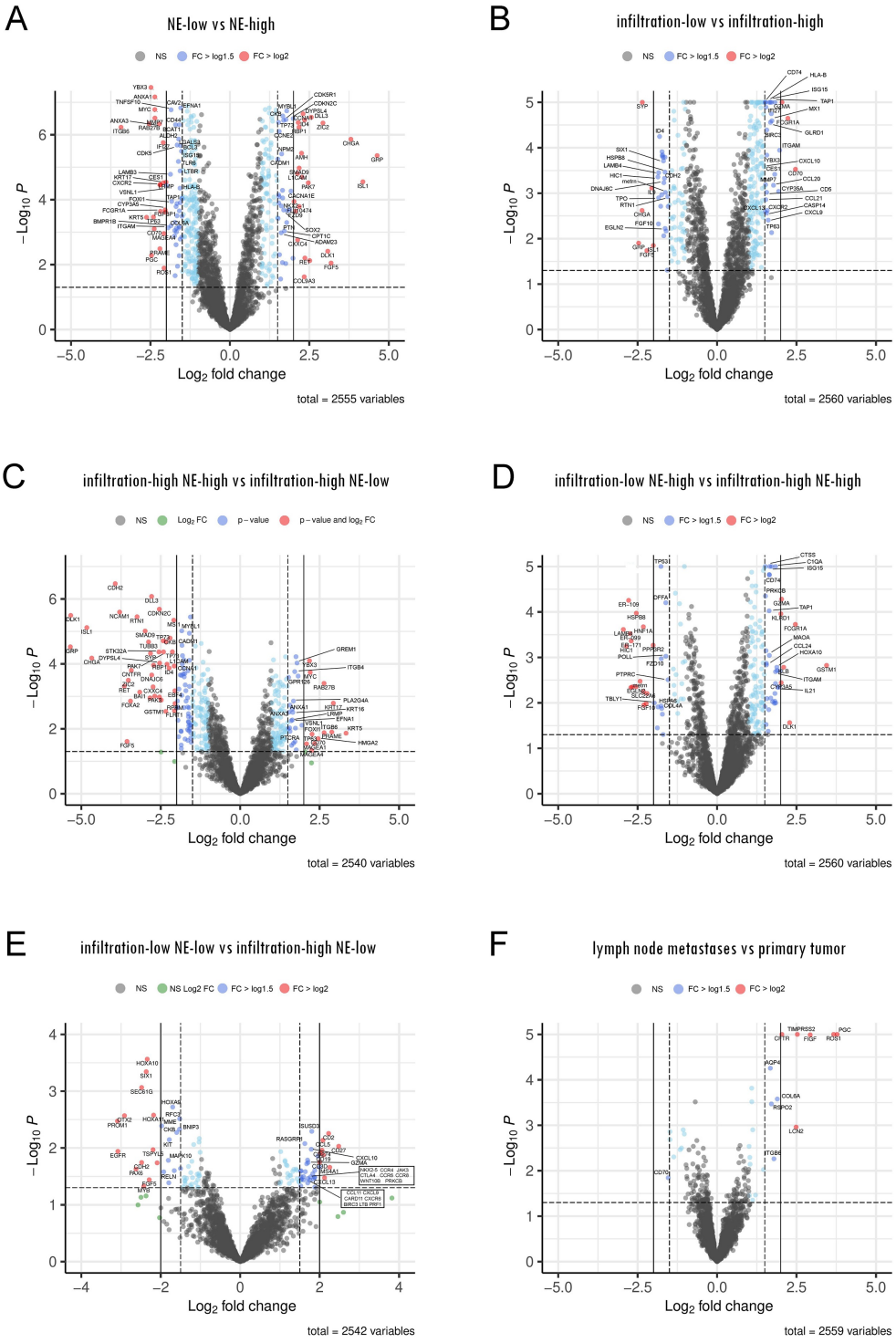
A
NE-low vs NE-high
NS
FC > log1.5
FC > log2
−Log10 P
Log2 fold change
total = 2555 variables
B
infiltration-low vs infiltration-high
NS
FC > log1.5
FC > log2
−Log10 P
Log2 fold change
total = 2560 variables
C
infiltration-high NE-high vs infiltration-high NE-low
NS
Log2 FC
p − value
p − value and log2 FC
−Log10 P
Log2 fold change
total = 2540 variables
D
infiltration-low NE-high vs infiltration-high NE-high
NS
FC > log1.5
FC > log2
−Log10 P
Log2 fold change
total = 2560 variables
E
infiltration-low NE-low vs infiltration-high NE-low
NS
NS Log2 FC
FC > log1.5
FC > log2
−Log10 P
Log2 fold change
total = 2542 variables
F
lymph node metastases vs primary tumor
NS
FC > log1.5
FC > log2
−Log10 P
Log2 fold change
total = 2559 variables

➢ *Figure 7. Comparing the RNA expression patterns of different SCLC subtypes with volcano plots. Between the patterns in primary sites and metastases (F) there are very few genes showing a considerable difference. Based on the level of infiltration (B) a handful of genes get highlighted but based on NE status (A) we can see a higher number of genes, many with higher fold change and significance. Contrasting subtypes based on both (C-E) yields different sets of genes. Dots represent individual genes. On the horizontal axis is the base 2 logarithm of the fold change (FC). On the vertical axis is the base 10 logarithm of the p value from a Mann-Whitney U test, multiplied by -1. Points with* $p < 0.05$ *are colored based on their FC and some are also labeled. Those with* $\log_2 FC > 1$ *are light blue,* > 1.5 *are blue, and* > 2 *are red. A plot title of "A vs B" means that FC was calculated from B/A, putting the genes overexpressed in category A on the left side of the plot. (Candidate's own figure, modified after* [194]*, used according to the Creative Commons Attribution (CC BY) license.)*

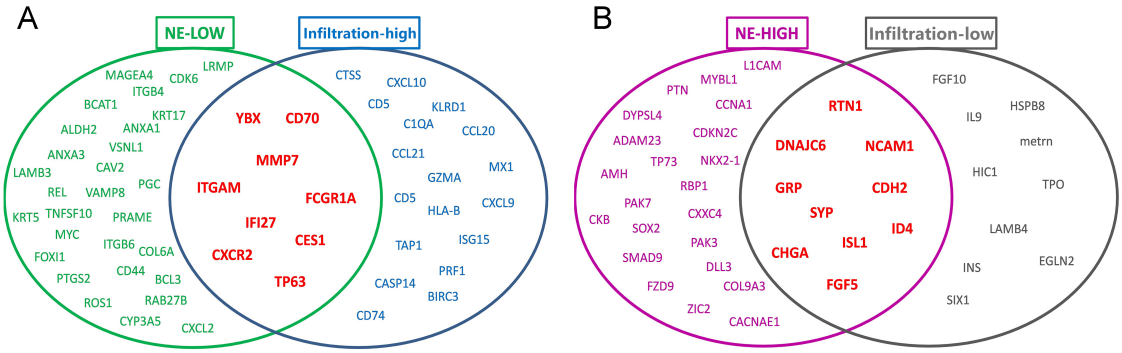

Figure 8. Genes with differential expression in SCLC subtypes by neuroendocrine type and level of immune infiltration. Genes listed in a given set are upregulated in the noted subtype, in comparison to its respective counterpart (infiltration-high vs low, NE-high vs low). (Candidate's own figure, modified after [194]*, used according to the Creative Commons Attribution (CC BY) license)*

4.3.2. in silico simulations

To highlight potential targets in macrophages for drugs aimed at repolarization, we have simulated therapeutic intervention by blocking proteins in the network (making the node constitutively inactive). We evaluate the effect of these perturbations by looking at the change in the polarization index. We have simulated single inhibitions [fig. 9.] and combinations of two [fig. 10.], with all possible input combinations. In the latter case we improve the characterization of the effect with the synergy index (for a description of these indices, see chs. 3.2.3.2. and 3.2.3.3.).

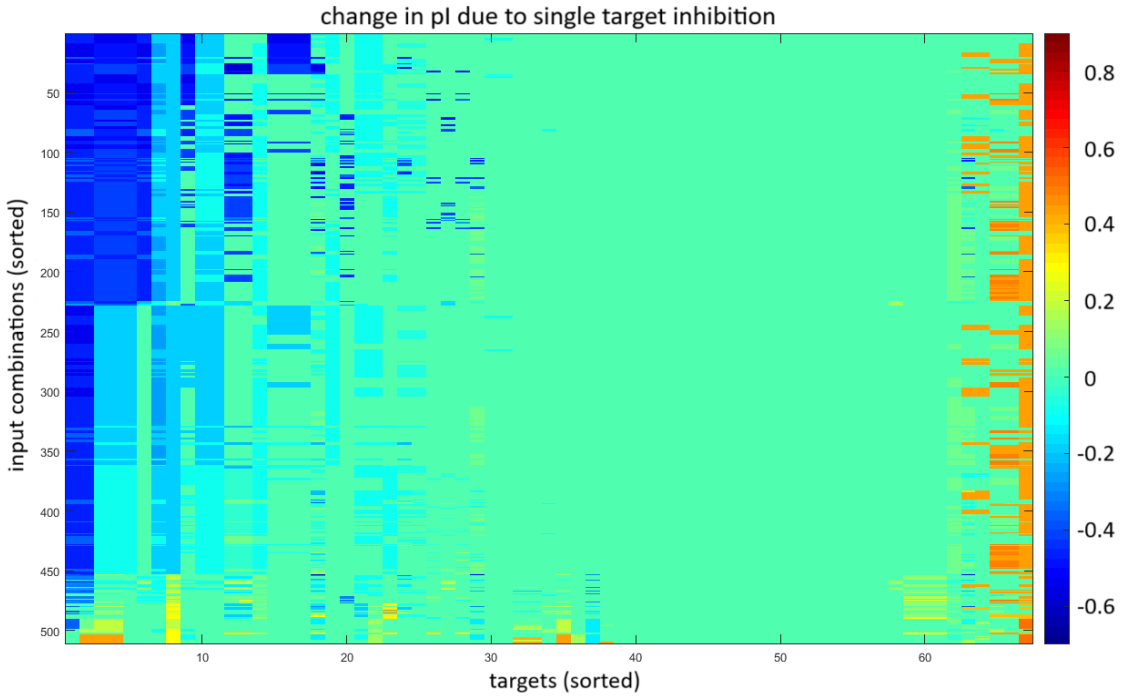

Figure 9. Effects of single-target inhibition on the polarization index. On the horizontal axis we see the 67 potential target nodes. Input and output nodes were not included, with the exception of the TLR receptors. On the vertical axis are listed all 511 input combinations. The order of entities on both axes has been chosen for presentation purposes of this heatmap, and are based on the first principal component of the data shown here. Two regions of interest (ROI) are highlighted. ROI#1 contains instances predominantly shifted toward an M2-like state, while ROI#2 contains ones shifted toward an M1-like state by the perturbation. However, both contain a considerable amount of essentially unperturbed instances, and cover a rather small portion of targets (approx. 30% and 7%, respectively). (Candidate's own figure, published in [189]*, used according to the Creative Commons Attribution (CC BY) license)*

We also need a numerical definition of repolarization. We have seen in [fig. 6.] that ±0.2 is a pI threshold that roughly separates groupings of more extremely polarized states from those with no clear direction of polarization. Thus, we consider a perturbation to have caused repolarization if both the unperturbed and perturbed states reach an attractor that has a pI with an absolute value >0.2 and they have opposite signs. This necessitates a change in the polarization index (ΔpI) of over 0.4, but most of the perturbations showing such a great shift fail to affect repolarization.

In the case of single target inhibition, we have examined a total of 34 237 cases (67 targets over 511 input combinations). There are quite a few that show abs(ΔpI)>0.4; we see 790 cases with a shift towards an inflammatory state and 2210 in the opposite direction. These constitute 2.31% and 6.46% of all cases, respectively. However, of these perturbations with considerable effect, only a total of 4 repolarize the cell, all of them towards an M1-like state and none in the other direction.

We see a different outcome with the simultaneous inhibition of two targets. Among the 1,129,821 possible cases (2211 target combinations over 511 input combinations) we have checked, we have found a total of 528 that result in repolarization. Of these 326 are towards an M1-like state and 202 towards an M2-like one. Given the sheer number of possibilities, this is still limited, comprising 0.79% and 0.16% of cases with an abs(pI)>0.4, respectively, but is a useful amount from a translational standpoint.

To further characterize these combinations, we calculate their synergy index (defined with Eq. 3. in ch. 3.2.3.3.) [fig. 10.]. The value of synI is indicative of the relationship between the pathways affected by the perturbations. Two completely independent pathways would result in a synI of 1. This is the result in 23.14% of the cases. If the index drops below 1, the targets are likely to be a part of the same pathway(s), serially connected, making blocking both of them at least partially redundant. This is the most common relationship, and we see this in 75.10% of cases. A synergy index over 1 indicates convergent pathways, creating effects that neither single inhibition could achieve alone. Only 1.76% exhibit such a true synergistic relationship.

Combinations with a repolarizing effect toward an M2-like state show a majorly different distribution of these categories. 200 of the 202 cases have a synI over 1. Most of these involve blocking NFAT5, even though that in itself has negligible impact, with a ΔpI just above -0.1. Even the targets that comprise the other half of these combinations

only shift the system to around pI=0. In the case of repolarizing toward an M1-like state, true synergistic combinations are rarer. The only node that can cause repolarization as a single target, STAT6, is part of 75.5% of all combinations that can achieve the same. But even in this case we see an increase in effectiveness. STAT6 alone can cause repolarization for only 4 input combinations (18% of inputs that lead to an M2-like end state), but combinations widen this range. Simultaneous inhibition of STK4 is effective for 10 inputs (45%) and blocking Sp1 leads to repolarization for 14 inputs (64%). Considering all dual inhibitions, 18 (82%) of inputs can be shifted into an M1-like polarization. We also have to note that in the few combinations that show synergy, there are some striking cases. Like JAK1 and JAK3 (or their complexes with IL4R), that alone have next to no impact on polarization (with a ΔpI of +0.05 and 0, respectively), but together can lead to a total ΔpI of +0.57 for certain inputs (either IL-10 or IL-1 combined with IL-4). The above also results in a distribution of synI different from both that of all combinations and those repolarizing in the other direction. The dominant category is synI=1, covering 77.9% of combinations (254). The ratio of synI>1 combinations is still higher than without filtering, but only reaches 11.7% (38) of repolarizing combinations.

All repolarizing combinations are listed in Supplementary Table S4 of [189].

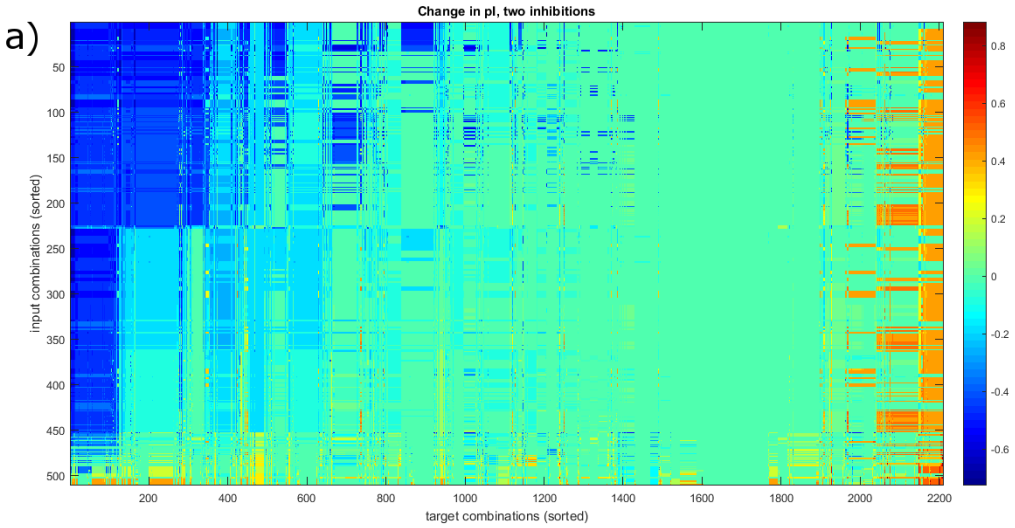
a)
Change in pI, two inhibitions
input combinations (sorted)
target combinations (sorted)

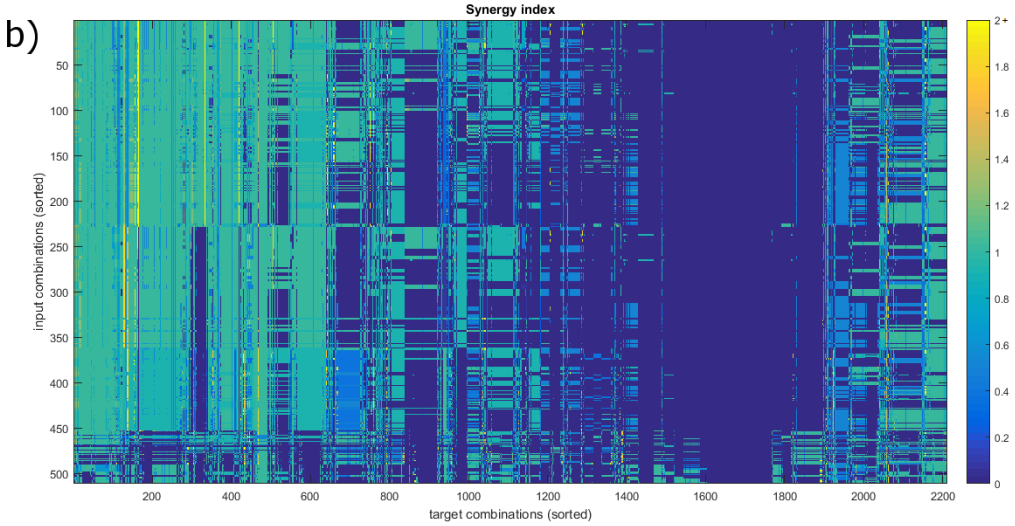
b)
Synergy index
input combinations (sorted)
target combinations (sorted)

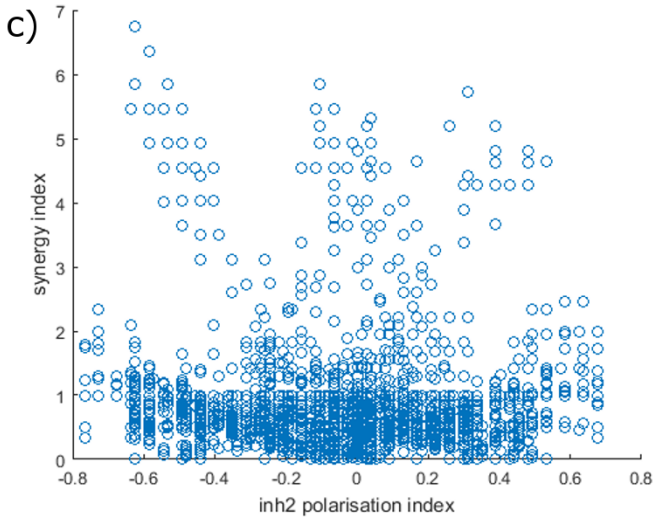
c)
synergy index
inh2 polarisation index

➢ *Figure 10. Perturbation of the system by simultaneous inhibition of two nodes.* ***a)*** *Shift in the polarization index. On the horizontal axis we see the 2211 potential target node combinations. Input and output nodes were not included, with the exception of the TLR receptors. On the vertical axis are listed all 511 input combinations. The order of entities on both axes has been chosen for presentation purposes of this heatmap, and are based on the first principal component of the data shown here. ROI-s are chosen as they were for fig. 9., showing combinations that push the model mainly in one direction. They are somewhat wider (37% and 11%, respectively), than in the case of single inhibitions, but not considerably.* ***b)*** *Heatmap of the synergy index. Axes and their sorting is the same as in a). The previously observable ROI-s are unclear here, high synergy instances do not necessarily overlap with those of high ΔpI. We can only distinguish an inert zone (highlighted), with no changes based on both ΔpI and synI.* ***c)*** *Plotting synI versus pI. The apparent upper limit (most observable below -0.2 pI) is an artifact of the τ adjustment parameter (see Eq.3. in 3.2.3.3.) not permitting synI to rise above ΔpI/τ. (Candidate's own figure, published in* [189]*, used according to the Creative Commons Attribution (CC BY) license)*

4.3.3. Drug repositioning data collation tool: EZCancerTarget

Our drug repositioning data collation tool is online and available to researchers. It aids in the acquisition and structuring of data stored in disparate large databases, greatly reducing the time and effort necessary to perform a thorough search. It also helps in avoiding errors that manual data entry can bring about. As it collects information during runtime, the results will always be up to date. Our novel approach of presenting data on both compounds and their biological targets side by side in the same data structure shortens the gap between these two sides of drug repurposing, usually detailed in separate databases.

The workflow is started on the project's Github page (https://github.com/cycle20/EZCancerTarget). To avoid problems stemming from multiple simultaneous users, those wishing to use the utility remotely (via the Google spreadsheet for input) have to receive authorization from the project administrator. It can also be installed locally, for which detailed guidance can be found at the link above. The spreadsheet includes links, with which users can start the script, follow progress and view the resulting web page [fig. 11.]. Information collecting and rendering the results takes approximately 30 minutes.

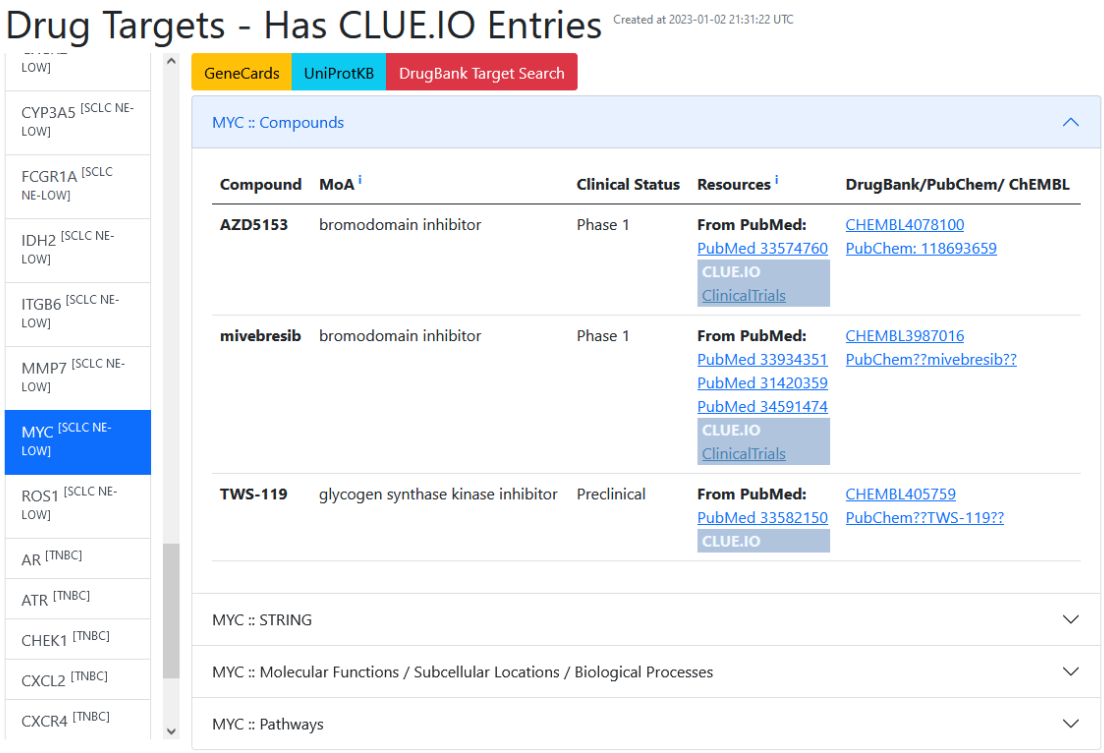

Figure 11. Example results page of EZCancerTarget. On the left side, targets used as input are listed, along with a user-defined label in brackets (optional). Clicking on one will bring up search results on the right. At the top outgoing links are given to other resources on the target. Compounds related to the target are listed along with mode of action (MoA) and clinical status. These can be explored further through the links in the last two columns. Additional data can be accessed by clicking the options below. (Candidate's own figure.)

5. Discussion

Small cell lung cancer (SCLC) is a highly progressive type of malignancy and advancements in its therapy have been unfortunately lacking. We believe that bridging the gap between knowledge gained from biological research and applied techniques in clinical practice is paramount.

As our understanding of tumor biology grows, the importance of the interplay between the immune system and tumor cells in the tumor microenvironment (TME) becomes ever more apparent. Cells of both lymphocytic and myeloid lineage appear in the TME, and their presence can be a boon as much as a bane [201–203]. However, the immune contexture (types, amount and localization of immune cells) of the TME is not fixed, as evidenced by its modulation by the cancer itself. This is accomplished through secretion of small molecules (like cytokines and chemokines) and other bioactive chemicals (e.g., reactive oxygen species (ROS)) and taking advantage of environmental factors (like hypoxic conditions). These can enable the tumor to not only neutralize particular immune cells, but to hinder immune clearance as a whole [204,205]. This also presents a potential new angle of attack for intervention that in recent years has garnered considerable attention in translational medicine and shows promising results [206,207].

Continuing previously published work from our group [111], we have further characterized the immune cell content of limited-stage (LS) SCLC using resected tissue samples [194]. Compared to immune cell densities reported in other types of lung cancer [208], we found that immune infiltration in SCLC is low not only for lymphocytes [111], but also myeloid cells, regardless of tumor compartment. We have also explored the association of neuroendocrine (NE) marker expression and overall immune infiltration ($CD45^+$ level). In the earlier results of the group from 2020, we saw that both overall infiltration, and specifically T lymphocytes ($CD3^+$, $CD8^+$), are significantly elevated in NE-low tumors, and in the stroma compartment [111]. Here we show that while there is some level of association between NE status and level of infiltration (most cases being either NE-low/infiltration-high or NE-high/infiltration-low), a considerable number of cases are either NE-low/infiltration-low or NE-high/infiltration-high. This could provide an explanation to the observation that subtype status alone is not a significant predictor of OS, in patients who underwent resection followed by adjuvant chemotherapy with or without thoracic irradiation [125]. Thus, genetic markers and immune contexture both

need to be taken into account separately for an accurate description of SCLC subtype for clinical purposes.

Here, we have shown that $CD68^+$ TAM-s are the most numerous leukocytes of the SCLC TME. Even compared to $CD3^+$ T-cells, their density is approximately two times higher [111]. Following the trends of overall infiltration [111], their numbers are significantly higher in the stroma (vs. the tumor nest), and in primary NE-low tumors (vs. primary NE-high). Another major group of myeloid cells, $CD33^+$ MDSC, are present only in the stroma, and in very small numbers, with a slight increase in NE-low tumors. This is in direct contrast with results from NSCLC, where high levels of MDSC-s were reported [209]. We have also observed that while the density of T-cells correlates highly with the level of overall immune infiltration in all compartments and subtypes, in the case of TAM-s, this linkage is restricted to primary tumor nests, hinting at additional mechanisms affecting their population.

Others have attempted to quantify immune cell populations in SCLC with single cell RNA sequencing [210–212]. While these studies report a higher T cell to myeloid cell ratio than our IHC results, this is likely due to the fact that nearly all of their samples show an NE-high phenotype (positive for ASCL1 and/or NEUROD1). We have seen that cells of monocytic origin ($CD68^+$ and $CD163^+$) are more numerous in NE-low tumors. Single cell analysis reveals the important fact that there is intratumoral heterogeneity in the expression of subtype markers, with one study linking tumor cells with an NE-low phenotype in otherwise mostly NE-high samples with stemness characteristics [211]. Further exploration of NE-low tumors with single cell resolution would be necessary to gain a comprehensive understanding of SCLC features.

In addition to their numerically superior presence in SCLC, macrophages exhibit an outstanding plasticity of function, accessed via a process called polarization. The result of this is nuanced, but two main directions can be recognized: an M1-like direction that promotes inflammation and an aggressive immune response, and an M2-like direction that coordinates tissue repair and angiogenesis. This ability to adopt either tumoricidal or immunosuppressive functionality might explain why overall TAM infiltration level does not associate with OS [15]. In relation to SCLC subtypes, we observed that in primary NE-low tumors the amount of TAM-s showing an M2-like polarization ($CD163^+$) is

significantly higher. This might counteract the effects of the overall higher infiltration in this subtype.

These results highlight macrophages as key players in the SCLC TME and promising targets for immunotherapy. While therapies attempting to lower the number of M2-like, negatively modulated cells, either by impeding their recruitment or directly affecting depletion [213], have merit, repolarizing immunosuppressive TAM-s would have a much more potent effect by also introducing additional tumoricidal immune cells to the TME [214].

To better understand macrophage function and to find ways to affect their polarization status, we have established a computational network model of intracellular events in the early stages of polarization [189]. Interactions were assembled based on PPI databases, and then were curated and expanded with a systematic search of available literature. It is validated against published primary research results that measured the connections between our inputs and outputs and displays the properties that can be expected of such a network. We have used this network to investigate the system both unperturbed and with modifications simulating small inhibitory molecules used as drugs. With these we have observed that monotherapies are not well suited to achieving repolarization, but the combined inhibition of two targets presents multiple effective options that in most cases are based on a synergistic effect, i.e., the combination being more potent than the sum of their components. This observation is in keeping with the previous results of Fumia and Martens, who found in their model of tumor cells that single-target interventions are ineffective at changing the state of the cell [193]. We have also investigated the level of synergy between targets in our dual inhibition scenarios, as it is indicative of their relative position in the network. We observe that the pathways responsible for different polarizations differ not only in the identity of their members but follow a different logic and network architecture. Pathways promoting an M1-like state show a convergent structure, while those promoting an M2-like state rely more on parallel lines of signal transduction.

In order to functionally model signal transduction events, our model includes directed and signed edges. We had to collect the necessary data for this manually from the literature, as the available extensive databases like STRING [190] or HPRD [167] do not contain this kind of information, as they rely on high-throughput techniques that do not

provide these parameters. Indeed, most PPI-based network models are undirected and unsigned. There have been recent attempts at developing an automated method to predict these attributes, and they have shown that including edge direction and sign information enhances the performance of drug target and cancer driver mutation predictions [215,216].

We have aimed to create our output such that it can work with various methods of interpretation and is not limited to what we present in conjunction with the model. This is a break from the norm of hardwiring the states of interest into the model structure as a few nodes, usually with a relatively low degree [193,217,218]. Our 27-node gene expression pattern is able to represent a large variety of subpopulations, in accordance with the spectrum model of macrophage polarization [155]. Its flexibility also makes it easier to expand or modify to incorporate new data, or to integrate it into a larger scale model.

Others have also published *in silico* models of intracellular processes inside macrophages. Palma and colleagues presented a simple model with 14 inner nodes [219], which was then extended later to 21 nodes by another team [218]. As they span a similar functional space as our model, this also means that they often include indirect interactions as edges and exclude components based on their perceived importance. In order to include all possible targets and to create a more detailed model, we have incorporated 92 intracellular proteins, grouped into 64 inner nodes in our system and allow indirect interactions very sparingly. There are two more recent models that have a high level of detail [220,221], but both limit their analysis to single-node inhibition. As we have shown, targets that are effective as part of a combination would often be overlooked by screening for individual targets. Single-target inhibition also differs more from real world situations, both because of treatment practices, and because perfectly single-target small molecule inhibitors are practically nonexistent.

In our search for molecular targets, we first focused on the SCLC cells themselves. We have categorized our samples on the NE-high/low and infiltration-high/low axes and compared the expression profiles of the resulting subgroups. The expression of Annexin A1 (ANXA1) is heavily upregulated in NE-low tumors but shows no association with immune infiltration status. ANXA1 contributes to immunosuppression, with an effect that resembles glucocorticoids, positively affecting TGFβ signaling and wound healing, and suppressing inflammation [222]. Its upregulation, and its correlation with a

poor prognosis has been shown in other types of cancer too: in gastric cancer [223], in hepatocellular carcinoma [224], in melanoma [225], and in adenocarcinoma of the lung [226]. In breast [227] and colorectal [228] cancer high ANXA1 expression has been linked to an increased resistance to chemoradiotherapy. In addition, there is evidence of its involvement in tumor invasion and metastasis, through the role it plays in macrophage polarization and epithelial-mesenchymal transition [229,230]. On the molecular level, this involves an enhancement of CXCR4 and matrix metalloproteinase (MMP) expression, via an increase in IκB kinase (IKK) and thus NFκB activity [231]. Our own findings also support this: we have observed a higher expression of ANXA1 in tumors with a high density of $CD163^+$ (M2 TAM) cells [194].

Our analysis of gene expression patterns has also highlighted the receptor-ligand pair of CD27 and CD70, both showing upregulation in the NE-low and infiltration-high categories. CD27 is a member of the TNF receptor superfamily that promotes T-cell proliferation by activating the NFκB pathway [232]. The expression of its natural ligand, CD70, is a main factor in the regulation of CD27 activity, and is therefore controlled and transient, appearing mostly on subpopulations of activated lymphocytes in physiological conditions [233–235]. Expression of CD70 has been observed in glioblastoma [236], non-Hodgkin lymphoma [237], renal cell carcinoma [238], and NSCLC [239]. It was also shown that the presence of CD70 on tumor cells increases the presence of regulatory T-cells (Treg), and thus supports tumor growth, by supporting their survival [240], and by inducing regulatory function in $CD25^-$ T-cells through activation of FoxP3 [237].

There are a number of other genes that our search has highlighted as being differentially expressed in NE-low tumors and there is evidence in the literature corroborating their involvement in the TME and tumor progression. CXCR2 has been linked to poor prognosis in NSCLC [241,242]. Also in NSCLC, MMP7 level has been reported to be associated with proliferation of tumor, resistance to chemotherapy and unfavorable prognosis [243]. Our data shows that MMP7 is more prevalent in NE-low tumors, but is not linked to the level of immune infiltration. ITGB6 associates with ITGAV to form a receptor recognizing, among others, fibronectin and latency associated peptide (LAP), able to promote tumor cell invasion [244] and immunosuppression through the release of TGFβ [245]. We also have to mention TP63, a protein associated

with the cell cycle, that has shown high expression in our study, but has been reported as a tumor suppressor in NSCLC [246].

We have also identified proteins differentially expressed in NE-low tumors that have not yet been connected to cancer, but based on their known functions their involvement is likely, making them promising targets of future research. The nucleotide-binding protein YBX3 is described in relation to cold shock, but also binds to and represses the promoter of GM-CSF [247], and can thus potentially influence TAM behavior. High-affinity IgG Fc receptor 1A (FCGR1A) levels have not been reported before in cancer, and here we show high relative expression in both NE-low and infiltration-high tumors. The receptor is involved in antigen presentation and is reported to be of import in monoclonal antibody therapies [248].

Using our computational model, we have investigated the possibility of targeting proteins in macrophages to counteract the immunosuppressive effects of the TME that push their polarization in an M2-like direction. We have observed that inhibition of multiple targets simultaneously outperforms single-target approaches, often in a synergistic manner, i.e., proving more effective than the sum of individual effects. As part of combinatorial target-pairs, STAT6, JAK1 and JAK3 emerged as primary candidates, with Tyk2, STK4 and Sp1 also showing potential to a lesser extent.

STAT6 is a major transcription factor, and the only target whose inhibition could create repolarization in our model as a single target. There are molecules already in use in oncotherapy, imatinib [249] and gefitinib [250], that have been shown to influence STAT6 phosphorylation and polarization in TAM. There is also one study using STAT6 inhibition as part of combinatorial therapy [251]. Their secondary target is IKKβ, and they show that simultaneous inhibition is more effective in creating repolarization, though the effect is not necessarily synergistic, which is in line with the prediction of our model (see Supplementary Table S4 of [189]).

We have seen in our simulations that the inhibition of JAK family members by themselves can have a limited effect on polarization, affecting repolarization only when paired with another target. One explanation would be that their function is context-dependent and can simultaneously affect pathways acting cross-purposes. This is supported by the results of previous efforts at targeting the family with therapeutics. Tofacitinib targets JAK1 and JAK3 (with a minor effect on JAK2), has been tested for use

in rheumatoid arthritis and other inflammatory diseases [252], and shows anti-inflammatory effects, via a modulation of immune cells. In the case of macrophages, it is most likely that these are achieved by interfering with the JAK1-STAT1 interaction, without much contribution via JAK3 [253]. In contrast to this, in other scenarios the same drug has shown an ability to block STAT6 function [254], and anti-angiogenic effects [255], both indicating a shift towards M1-like functions from a macrophage perspective.

Less is known about the other two targets in this context. Modulation of STK4 function has shown contradicting results. Both inhibition by malibatol A [256], and activation with adapalene [257] was reported to create a shift toward anti-inflammatory functions in macrophages. Sp1 was explored as a target in multiple forms of cancer [258–260], but its connection with or effect on TAM-s was not investigated.

As it might be of importance in inflammatory diseases, we have also searched for targets that would push the system in the other direction, toward an M2-like state, and NFAT5 has emerged as a protein of interest. Arctigenin has been shown to inhibit NFAT5 and have an anti-inflammatory effect through the modulation of cardiac macrophage function [261]. In our model, individual inhibition of NFAT5 was insufficient to affect repolarization. This discrepancy might be due to our exclusion of feedback routes. As a secondary effect, dependent on the inhibition of NFAT5, a decrease in the phosphorylation of STAT1 and JAK2 has also been reported [261], which might strengthen the overall impact of the drug. Based on the localization and function of these proteins, the most likely path of effect between them and NFAT5 would be via the modulation of the gene expression of a third element, creating a (possibly autocrine) loop.

According to the Essential Genes database of the International Mouse Phenotyping Consortium [262,263], KO of the targets we have identified in both studies is not cytotoxic or lethal, thus their inhibition via drugs should be viable. They had no data available for CD70, but double knockout mice have been created [264] and no systemic defects were reported.

We also have to consider the limitations of our work. The *in vitro* studies were retrospective, and we do not have access to sufficient data on outcomes. Thus, we are unable to link our findings with prognoses. In addition, our data comes exclusively from limited-stage SCLC, and thus our results are not necessarily descriptive of advanced-stage

malignancies. However, surgical resection is not recommended in extended stage disease, lowering sample availability. Tissue samples acquired by bronchoscopy are prohibitively small. Post mortem sample collection brings in biases and cohort homogeneity is low (e.g., in terms of treatments received). The cohort size and the individual sample sizes are also not extensive. The genes ASCL1, NEUROD1, POU2F3 and YAP1 were not yet known as subtype markers during the data collection phase of our study and thus were not included in the genetic panel used. However, they show substantial overlap with NE status [17], and the low cohort size would preclude us from drawing statistically significant conclusions from the 4 genetic [183] or 7 histologic subtypes [15] defined by them. To provide a thorough characterization of the SCLC subsets we identified, especially on the genetic level, further studies with higher case numbers will be necessary. Targets identified on the transcriptomic level will need to be confirmed on a proteomic level with *in situ* experiments before use in pharmacological studies.

In the case of the *in silico* model, its design constricts what aspects of polarization it can handle. The BCN presented ignores questions of time altogether. The speed of interactions is presumed the same by omission of a parameter to account for it, due to this information being inaccessible on the scale of our model. Beyond not being able to predict the speed of reaching a polarized state, this also makes it impossible to represent certain signaling circuits that depend on signal duration, like the interaction of IL-10 and IL-6 [265]. We assume that gene expression is slower than signal transduction by orders of magnitude and limit our system to the early response by excluding events requiring protein synthesis. Some of these are known to create feedback loops and affect subsystems not exhaustively represented in our network. One such is the metabolic state of the macrophage, known to be involved in polarization [266] and interactions with other parts of the TME [267]. Using binary values to represent node activity means that encoding intensity levels would be problematic, and the current model ignores them entirely. We also did not consider the possibility of activating proteins with an intervention [268]. Due to the low intensity resolution and the lack of a time scale, we cannot draw conclusions about the *in vivo* stability of the resulting state, and we also do not gain insight into mechanisms that adjust the longevity of it. In addition, verification is limited by the available data. The majority of experiments we utilize connect one input with one output, an approach taken by others facing similar issues too [269]. To be more

thorough, combinations of both inputs and outputs would have to be considered, but such data is not available at the time of writing and performing a series of systematically chosen high-throughput *in vitro* experiments to provide them is out of the scope of this project.

6. Conclusions

- $CD33^+$ MDSC in the stroma, and $CD163^+$ M2-like TAM cells in the tumor nest are significantly more prevalent in NE-low SCLC, compared to NE-high, establishing an immunosuppressive TME with potential future therapeutic applications.
- In primary tumors, leukocyte numbers correlate with both macrophage markers (CD68 and CD163) in the nest, but in the stroma only with CD163, i.e., M2-like cells, implying distinct mechanisms of colonization in different tumor compartments.
- Interventions aimed at tipping the balance of immune infiltration and suppression are expected to be particularly effective in CD68- and CD163-high subsets of NE-low tumors. We identified CD70, ANXA1, FCGR1A, ITGB6, MMP7, YBX3 and CXCR2 as potential targets for this purpose.
- NE-low and infiltration-high tumors showed highly similar expression profiles at both primary sites and lymph node metastases. Smaller subgroups of NE-high, but phenotypically infiltration-high and NE-low, but phenotypically infiltration-low tumors exist, with distinct expression profiles.
- Our *in silico* model can replicate experimentally observed cell behavior in its scope and shows the expected characteristics of a complete network encompassing the selected pathways involved in macrophage polarization.
- When aiming to affect repolarization, interventions designed against a single target are suboptimal compared to treatments simultaneously targeting two intracellular actors. Individual targets in combination therapies might not show a significant effect on cellular state on their own.
- When attempting to repolarize cells into an M1-like state, our model highlights STAT6, JAK1 and JAK3, and to a lesser extent Tyk2, STK4 and Sp1 as potential targets. When trying to push the system toward an M2-like state, NFAT5 emerges as a point of interest.
- We created a platform for drug repurposing in oncopharmacology that is accessible and expandable by the international research community, intended to aid research into SCLC and other highly aggressive malignancies.

7. Summary

Translational research of the tumor microenvironment (TME) is an emerging field of study that has resulted in therapeutic developments in multiple types of cancers recently. Our understanding of the TME of small cell lung cancer (SCLC) is incomplete, severely limiting therapeutic prospects and the application of the newest advances in the field. We aimed to gain new insights about the immune cells in the SCLC TME, with special attention to tumor-associated macrophages (TAMs) and their polarization state, to reveal molecular targets for therapeutic intervention.

First, we characterized the cellular environment regulating anti-tumor immunity in limited-stage neuroendocrine (NE)-high and NE-low SCLC subsets, including lymph node metastases. Immunohistochemical labeling and cell counting on TMAs (tissue microarrays) showed that overall immune-infiltration is low, and that TAMs are the most abundant cell type in the tumor nest TME, exceeding $CD3^+$ T-cells. Also, the amount of $CD163^+$ M2-polarized TAMs is significantly higher in NE-low (vs. NE-high) tumor nests. TAM density shows a strong positive correlation with CD45 and CD3 in primary tumor nests, but not in the stroma. We identified potential molecular targets based on our expression data in NE-low and infiltration-high tumor subsets.

Next, we propose an *in silico* approach aimed at understanding the intracellular systems driving polarization and their dependence on extracellular cues. We create and verify a Boolean Control Network model, connecting extracellular signals with the gene transcription to model the early response in macrophages. We observe that inflammatory and regenerative pathways show a difference in architecture. Based on simulations of therapeutic intervention, we conclude that inhibition of single targets is insufficient to change an established polarization in most cases. Inhibition of multiple targets (often with an individually weak effect) is necessary, with STAT6, JAK1 and JAK3 emerging as important targets to push toward M1 and NFAT5 toward M2.

To facilitate the use of large databases we present a novel, open access platform aimed at drug repurposing that we call EZCancerTarget, aggregating data from databases such as PubChem, DrugBank, PubMed, and EMA, complete with biological background information and literature citations for every target from UniProt, String, GeneCards and more. The content of the platform can be expanded or replaced by users to suit their purposes.

7.1. Összefoglalás (Summary in Hungarian)

A tumor mikrokörnyezetre (TME) fókuszáló transzlációs kutatások újszerű megközelítést jelentenek és több ráktípusban is terápiás lehetőségeket tártak fel. A kissejtes tüdőrák (SCLC) mikrokörnyezetének megismerése segíthet új terápiás célpontok azonosításában. Kutatásunk az SCLC TME megértését célozta, különös tekintettel altípusaira, az infiltráló makrofágokra (TAM) és azok polarizációjára.

Először a tumorellenes immunválaszért felelős immunsejtek előfordulását vizsgáltuk neuroendokrin markerekben (NE) magas és NE-alacsony, limitált stádiumú SCLC-ben és nyirokcsomó áttéteiben. Immunhisztokémiával jelölt szövetmintákon kimutattuk, hogy az SCLC egy alacsony immun infiltráltsággal jellemzhető daganat. Ebben a kontextusban fontos megállapításunk hogy más daganatokkal szemben a TAM-ok alkotják a legnépesebb populációt, megelőzve a $CD3^+$ sejteket is. Az M2 polarizált $CD163^+$ sejtek száma szignifikánsan magasabb az NE-alacsony tumor fészkekben. A TAM sűrűség erős pozitív korrelációt mutat a CD45 és CD3 markerekkel elsődleges tumor fészkekben, de a környező strómában nem találtunk hasonló összefüggést. Expressziós adatok alapján lehetséges farmakológiai célpontokat azonosítottunk NE-alacsony és immun-oázis tumorokban.

A makrofágok polarizációs folyamatait és azok külső jelekkel való összefüggését *in silico* megközelítéssel vizsgáltuk. Létrehoztunk és verifikáltunk egy Boolean Control Network modellt, mely összeköti a sejten kívülről érkező jeleket a korai válasz során jelentkező génexpressziós változásokkal. Megfigyeltük, hogy a proinflammatorikus és regeneratív útvonalak felépítésük jellegében is különböznek. Terápiás beavatkozásokat szimulálva arra a következtetésre jutottunk, hogy egyetlen célpont gátlása nem elégséges a polarizáció megváltoztatásához, két megfelelő (önmagában akár elenyésző hatású) célpont egyidejű gátlásával viszont elérhető. M1 irányba történő modulációnál a STAT6, JAK1 és JAK2, M2 irányba pedig az NFAT5 fehérjék szerepe emelkedett ki.

Új célpontok azonosítására irányúló kutatások támogatására és hatóanyag indikációk újratervezésére (drug repurposing) felépítettünk egy nyíltan elérhető online eszközt, az EZCancerTarget-et. Ez számos adatbázis, köztük a PubChem, DrugBank, PubMed és EMA adatait összesíti gyógyszer(jelölt)ekről és gazdagítja biológiai háttérinformációkkal célpontjaikról a UniProt, String, GeneCards és más forrásokból.

8. References

1. Bray F, Ferlay J, Soerjomataram I, Siegel RL, Torre LA, Jemal A. Global cancer statistics 2018: GLOBOCAN estimates of incidence and mortality worldwide for 36 cancers in 185 countries. CA Cancer J Clin [Internet]. 2018 Nov;68(6):394–424. Available from: http://www.ncbi.nlm.nih.gov/pubmed/30207593
2. Siegel RL, Miller KD, Wagle NS, Jemal A. Cancer statistics, 2023. CA Cancer J Clin. 2023 Jan;73(1):17–48.
3. Ou SHI, Ziogas A, Zell JA. Prognostic factors for survival in extensive stage small cell lung cancer (ED-SCLC): the importance of smoking history, socioeconomic and marital statuses, and ethnicity. J Thorac Oncol [Internet]. 2009 Jan;4(1):37–43. Available from: http://www.ncbi.nlm.nih.gov/pubmed/19096304
4. Varghese AM, Zakowski MF, Yu HA, Won HH, Riely GJ, Krug LM, Kris MG, Rekhtman N, Ladanyi M, Wang L, Berger MF, Pietanza MC. Small-cell lung cancers in patients who never smoked cigarettes. J Thorac Oncol [Internet]. 2014 Jun;9(6):892–6. Available from: http://www.ncbi.nlm.nih.gov/pubmed/24828667
5. Oze I, Hotta K, Kiura K, Ochi N, Takigawa N, Fujiwara Y, Tabata M, Tanimoto M. Twenty-seven years of phase III trials for patients with extensive disease small-cell lung cancer: disappointing results. PLoS One [Internet]. 2009 Nov 13;4(11):e7835. Available from: http://www.ncbi.nlm.nih.gov/pubmed/19915681
6. SEER. Cancer Statistics [Internet]. 2023 [cited 2023 Mar 14]. Available from: https://seer.cancer.gov/statistics/
7. Howlader N, Forjaz G, Mooradian MJ, Meza R, Kong CY, Cronin KA, Mariotto AB, Lowy DR, Feuer EJ. The Effect of Advances in Lung-Cancer Treatment on Population Mortality. N Engl J Med. 2020 Aug 13;383(7):640–9.
8. Horn L, Mansfield AS, Szczęsna A, Havel L, Krzakowski M, Hochmair MJ, Huemer F, Losonczy G, Johnson ML, Nishio M, Reck M, Mok T, Lam S, Shames DS, Liu J, Ding B, Lopez-Chavez A, Kabbinavar F, Lin W, Sandler A, Liu S V, IMpower133 Study Group. First-Line Atezolizumab plus Chemotherapy in Extensive-Stage Small-Cell Lung Cancer. N Engl J Med [Internet]. 2018 Dec 6;379(23):2220–9.
   Available from: http://www.ncbi.nlm.nih.gov/pubmed/30280641

9. George J, Lim JS, Jang SJ, Cun Y, Ozretia L, Kong G, Leenders F, Lu X, Fernández-Cuesta L, Bosco G, Müller C, Dahmen I, Jahchan NS, Park KS, Yang D, Karnezis AN, Vaka D, Torres A, Wang MS, Korbel JO, Menon R, Chun SM, Kim D, Wilkerson M, Hayes N, Engelmann D, Pützer B, Bos M, Michels S, Vlasic I, Seidel D, Pinther B, Schaub P, Becker C, Altmüller J, Yokota J, Kohno T, Iwakawa R, Tsuta K, Noguchi M, Muley T, Hoffmann H, Schnabel PA, Petersen I, Chen Y, Soltermann A, Tischler V, Choi CM, Kim YH, Massion PP, Zou Y, Jovanovic D, Kontic M, Wright GM, Russell PA, Solomon B, Koch I, Lindner M, Muscarella LA, La Torre A, Field JK, Jakopovic M, Knezevic J, Castaños-Vélez E, Roz L, Pastorino U, Brustugun OT, Lund-Iversen M, Thunnissen E, Köhler J, Schuler M, Botling J, Sandelin M, Sanchez-Cespedes M, Salvesen HB, Achter V, Lang U, Bogus M, Schneider PM, Zander T, Ansén S, Hallek M, Wolf J, Vingron M, Yatabe Y, Travis WD, Nürnberg P, Reinhardt C, Perner S, Heukamp L, Büttner R, Haas SA, Brambilla E, Peifer M, Sage J, Thomas RK. Comprehensive genomic profiles of small cell lung cancer.
Nature [Internet]. 2015 [cited 2023 Jul 13];524(7563):47–53. Available from: https://www.ncbi.nlm.nih.gov/pmc/articles/PMC4861069/

10. Sen T, Tong P, Stewart CA, Cristea S, Valliani A, Shames DS, Redwood AB, Fan YH, Li L, Glisson BS, Minna JD, Sage J, Gibbons DL, Piwnica-Worms H, Heymach J V, Wang J, Byers LA. CHK1 Inhibition in Small-Cell Lung Cancer Produces Single-Agent Activity in Biomarker-Defined Disease Subsets and Combination Activity with Cisplatin or Olaparib. Cancer Res [Internet]. 2017 Jul 15;77(14):3870–84.
Available from: http://www.ncbi.nlm.nih.gov/pubmed/28490518

11. Gazdar AF, Carney DN, Nau MM, Minna JD. Characterization of variant subclasses of cell lines derived from small cell lung cancer having distinctive biochemical, morphological, and growth properties. Cancer Res. 1985 Jun;45(6):2924–30.

12. Sorenson GD, Pettengill OS, Brinck-Johnsen T, Cate CC, Maurer LH. Hormone production by cultures of small-cell carcinoma of the lung. Cancer. 1981 Mar 15;47(6):1289–96.

13. Borromeo MD, Savage TK, Kollipara RK, He M, Augustyn A, Osborne JK, Girard L, Minna JD, Gazdar AF, Cobb MH, Johnson JE. ASCL1 and NEUROD1 Reveal

Heterogeneity in Pulmonary Neuroendocrine Tumors and Regulate Distinct Genetic Programs. Cell Rep. 2016 Aug 2;16(5):1259–72.

14. Gay CM, Stewart CA, Park EM, Diao L, Groves SM, Heeke S, Nabet BY, Fujimoto J, Solis LM, Lu W, Xi Y, Cardnell RJ, Wang Q, Fabbri G, Cargill KR, Vokes NI, Ramkumar K, Zhang B, Della Corte CM, Robson P, Swisher SG, Roth JA, Glisson BS, Shames DS, Wistuba II, Wang J, Quaranta V, Minna J, Heymach J V, Byers LA. Patterns of transcription factor programs and immune pathway activation define four major subtypes of SCLC with distinct therapeutic vulnerabilities. Cancer Cell. 2021 Mar 8;39(3):346-360.e7.
15. Dora D, Rivard C, Yu H, Pickard SL, Laszlo V, Harko T, Megyesfalvi Z, Gerdan C, Dinya E, Hoetzenecker K, Hirsch FR, Lohinai Z, Dome B. Protein Expression of immune checkpoints STING and MHCII in small cell lung cancer. Cancer Immunol Immunother. 2023 Mar;72(3):561–78.
16. Zhang W, Girard L, Zhang YA, Haruki T, Papari-Zareei M, Stastny V, Ghayee HK, Pacak K, Oliver TG, Minna JD, Gazdar AF. Small cell lung cancer tumors and preclinical models display heterogeneity of neuroendocrine phenotypes. Transl Lung Cancer Res. 2018 Feb;7(1):32–49.
17. Baine MK, Hsieh MS, Lai WV, Egger J V, Jungbluth AA, Daneshbod Y, Beras A, Spencer R, Lopardo J, Bodd F, Montecalvo J, Sauter JL, Chang JC, Buonocore DJ, Travis WD, Sen T, Poirier JT, Rudin CM, Rekhtman N. SCLC Subtypes Defined by ASCL1, NEUROD1, POU2F3, and YAP1: A Comprehensive Immunohistochemical and Histopathologic Characterization. J Thorac Oncol [Internet]. 2020 Dec 1;15(12):1823–35. Available from: http://www.ncbi.nlm.nih.gov/pubmed/33011388
18. Sonehara K, Tateishi K, Komatsu M, Yamamoto H, Hanaoka M. Lung immune prognostic index as a prognostic factor in patients with small cell lung cancer. Thorac Cancer [Internet]. 2020 Jun;11(6):1578–86. Available from: http://www.ncbi.nlm.nih.gov/pubmed/32286017
19. Lohinai Z, Bonanno L, Aksarin A, Pavan A, Megyesfalvi Z, Santa B, Hollosi V, Hegedus B, Moldvay J, Conte P, Ter-Ovanesov M, Bilan E, Dome B, Weiss GJ. Neutrophil-lymphocyte ratio is prognostic in early stage resected small-cell lung

cancer. PeerJ [Internet]. 2019;7(7):e7232. Available from: http://www.ncbi.nlm.nih.gov/pubmed/31392087

20. Sugimoto A, Umemura S, Miyoshi T, Nakai T, Kuroe T, Nosaki K, Ikeda T, Udagawa H, Kirita K, Zenke Y, Matsumoto S, Yoh K, Niho S, Tsuboi M, Goto K, Ishii G. High proportion of tumor necrosis predicts poor survival in surgically resected high-grade neuroendocrine carcinoma of the lung. Lung Cancer. 2021 Jul;157:1–8.
21. Liu S V, Reck M, Mansfield AS, Mok T, Scherpereel A, Reinmuth N, Garassino MC, De Castro Carpeno J, Califano R, Nishio M, Orlandi F, Alatorre-Alexander J, Leal T, Cheng Y, Lee JS, Lam S, McCleland M, Deng Y, Phan S, Horn L. Updated Overall Survival and PD-L1 Subgroup Analysis of Patients With Extensive-Stage Small-Cell Lung Cancer Treated With Atezolizumab, Carboplatin, and Etoposide (IMpower133). J Clin Oncol. 2021 Feb 20;39(6):619–30.
22. Marabelle A, Fakih M, Lopez J, Shah M, Shapira-Frommer R, Nakagawa K, Chung HC, Kindler HL, Lopez-Martin JA, Miller WH, Italiano A, Kao S, Piha-Paul SA, Delord JP, McWilliams RR, Fabrizio DA, Aurora-Garg D, Xu L, Jin F, Norwood K, Bang YJ. Association of tumour mutational burden with outcomes in patients with advanced solid tumours treated with pembrolizumab: prospective biomarker analysis of the multicohort, open-label, phase 2 KEYNOTE-158 study. Lancet Oncol. 2020 Oct;21(10):1353–65.
23. Travis WD, Brambilla E, Müller-Hermelink HK, Harris CC, World Health Organization., International Agency for Research on Cancer., International Association for the Study of Lung Cancer., International Academy of Pathology. Pathology and genetics of tumours of the lung, pleura, thymus, and heart. IARC Press; 2004. 344 p.
24. Ganti AKP, Loo BW, Bassetti M, Chiang A, D TA, D CA, Dowlati A, Downey RJ, Edelman M, Gold KA, Goldman JW, Grecula JC, Hann C, Iyengar P, Khalil M, Merritt RE, Mohindra N, Lurie RH, Molina JR, Moran C, Mulvey C, Phan C, Pokharel S, Puri S, Qin A, Rusthoven C, Sands J, Farber D, Santana-Davila R, Shafique M, Waqar SN, Carly Cassara J, Hughes M. NCCN Guidelines Version 3.2023 Small Cell Lung Cancer [Internet]. 2022 [cited 2023 Apr 1]. Available from: https://www.nccn.org/professionals/physician_gls/pdf/sclc.pdf

25. Thomas A, Pattanayak P, Szabo E, Pinsky P. Characteristics and Outcomes of Small Cell Lung Cancer Detected by CT Screening. Chest [Internet]. 2018 Dec 1;154(6):1284–90.
Available from: http://www.ncbi.nlm.nih.gov/pubmed/30080997
26. Lad T, Piantadosi S, Thomas P, Payne D, Ruckdeschel J, Giaccone G. A prospective randomized trial to determine the benefit of surgical resection of residual disease following response of small cell lung cancer to combination chemotherapy. Chest. 1994 Dec;106(6 Suppl):320S-323S.
27. Barnes H, See K, Barnett S, Manser R. Surgery for limited-stage small-cell lung cancer. Cochrane Database Syst Rev. 2017 Apr 21;4(4):CD011917.
28. Evans WK, Osoba D, Feld R, Shepherd FA, Bazos MJ, DeBoer G. Etoposide (VP-16) and cisplatin: an effective treatment for relapse in small-cell lung cancer. J Clin Oncol. 1985 Jan;3(1):65–71.
29. Roberts JJ, Pascoe JM. Cross-linking of complementary strands of DNA in mammalian cells by antitumour platinum compounds. Nature [Internet]. 1972 Feb 4;235(5336):282–4.
Available from: http://www.ncbi.nlm.nih.gov/pubmed/4551181
30. Lokich J, Anderson N. Carboplatin versus cisplatin in solid tumors: an analysis of the literature. Ann Oncol [Internet]. 1998 Jan;9(1):13–21. Available from: http://www.ncbi.nlm.nih.gov/pubmed/9541678
31. Chen GL, Yang L, Rowe TC, Halligan BD, Tewey KM, Liu LF. Nonintercalative antitumor drugs interfere with the breakage-reunion reaction of mammalian DNA topoisomerase II. J Biol Chem. 1984 Nov 10;259(21):13560–6.
32. Ross W, Rowe T, Glisson B, Yalowich J, Liu L. Role of topoisomerase II in mediating epipodophyllotoxin-induced DNA cleavage. Cancer Res. 1984 Dec;44(12 Pt 1):5857–60.
33. Mathieu L, Shah S, Pai-Scherf L, Larkins E, Vallejo J, Li X, Rodriguez L, Mishra-Kalyani P, Goldberg KB, Kluetz PG, Theoret MR, Beaver JA, Pazdur R, Singh H. FDA Approval Summary: Atezolizumab and Durvalumab in Combination with Platinum-Based Chemotherapy in Extensive Stage Small Cell Lung Cancer. Oncologist. 2021 May;26(5):433–8.

34. Verma V, Simone CB, Allen PK, Gajjar SR, Shah C, Zhen W, Harkenrider MM, Hallemeier CL, Jabbour SK, Matthiesen CL, Braunstein SE, Lee P, Dilling TJ, Allen BG, Nichols EM, Attia A, Zeng J, Biswas T, Paximadis P, Wang F, Walker JM, Stahl JM, Daly ME, Decker RH, Hales RK, Willers H, Videtic GMM, Mehta MP, Lin SH. Multi-Institutional Experience of Stereotactic Ablative Radiation Therapy for Stage I Small Cell Lung Cancer. Int J Radiat Oncol Biol Phys. 2017 Feb 1;97(2):362–71.
35. Aupérin A, Arriagada R, Pignon JP, Le Péchoux C, Gregor A, Stephens RJ, Kristjansen PE, Johnson BE, Ueoka H, Wagner H, Aisner J. Prophylactic cranial irradiation for patients with small-cell lung cancer in complete remission. Prophylactic Cranial Irradiation Overview Collaborative Group. N Engl J Med. 1999 Aug 12;341(7):476–84.
36. Takahashi T, Yamanaka T, Seto T, Harada H, Nokihara H, Saka H, Nishio M, Kaneda H, Takayama K, Ishimoto O, Takeda K, Yoshioka H, Tachihara M, Sakai H, Goto K, Yamamoto N. Prophylactic cranial irradiation versus observation in patients with extensive-disease small-cell lung cancer: a multicentre, randomised, open-label, phase 3 trial. Lancet Oncol. 2017 May;18(5):663–71.
37. Dingemans AMC, Früh M, Ardizzoni A, Besse B, Faivre-Finn C, Hendriks LE, Lantuejoul S, Peters S, Reguart N, Rudin CM, De Ruysscher D, Van Schil PE, Vansteenkiste J, Reck M, ESMO Guidelines Committee. Electronic address: clinicalguidelines@esmo.org. Small-cell lung cancer: ESMO Clinical Practice Guidelines for diagnosis, treatment and follow-up☆. Ann Oncol. 2021 Jul;32(7):839–53.
38. Gillet JP, Calcagno AM, Varma S, Marino M, Green LJ, Vora MI, Patel C, Orina JN, Eliseeva TA, Singal V, Padmanabhan R, Davidson B, Ganapathi R, Sood AK, Rueda BR, Ambudkar S V, Gottesman MM. Redefining the relevance of established cancer cell lines to the study of mechanisms of clinical anti-cancer drug resistance. Proc Natl Acad Sci U S A [Internet]. 2011 Nov 15;108(46):18708–13. Available from: http://www.ncbi.nlm.nih.gov/pubmed/22068913
39. Neal JT, Li X, Zhu J, Giangarra V, Grzeskowiak CL, Ju J, Liu IH, Chiou SH, Salahudeen AA, Smith AR, Deutsch BC, Liao L, Zemek AJ, Zhao F, Karlsson K, Schultz LM, Metzner TJ, Nadauld LD, Tseng YY, Alkhairy S, Oh C, Keskula P,

Mendoza-Villanueva D, De La Vega FM, Kunz PL, Liao JC, Leppert JT, Sunwoo JB, Sabatti C, Boehm JS, Hahn WC, Zheng GXY, Davis MM, Kuo CJ. Organoid Modeling of the Tumor Immune Microenvironment. Cell [Internet]. 2018 Dec 13;175(7):1972-1988.e16.
Available from: http://www.ncbi.nlm.nih.gov/pubmed/30550791

40. Gabrilovich DI, Chen HL, Girgis KR, Cunningham HT, Meny GM, Nadaf S, Kavanaugh D, Carbone DP. Production of vascular endothelial growth factor by human tumors inhibits the functional maturation of dendritic cells. Nat Med. 1996 Oct;2(10):1096–103.
41. Menetrier-Caux C, Montmain G, Dieu MC, Bain C, Favrot MC, Caux C, Blay JY. Inhibition of the differentiation of dendritic cells from CD34(+) progenitors by tumor cells: role of interleukin-6 and macrophage colony-stimulating factor. Blood. 1998 Dec 15;92(12):4778–91.
42. Ferrante CJ, Pinhal-Enfield G, Elson G, Cronstein BN, Hasko G, Outram S, Leibovich SJ. The adenosine-dependent angiogenic switch of macrophages to an M2-like phenotype is independent of interleukin-4 receptor alpha (IL-4Rα) signaling.
Inflammation [Internet]. 2013 Aug;36(4):921–31. Available from: http://www.ncbi.nlm.nih.gov/pubmed/23504259
43. Novitskiy S V, Ryzhov S, Zaynagetdinov R, Goldstein AE, Huang Y, Tikhomirov OY, Blackburn MR, Biaggioni I, Carbone DP, Feoktistov I, Dikov MM. Adenosine receptors in regulation of dendritic cell differentiation and function. Blood [Internet]. 2008;112:1822–31. Available from: http://ashpublications.org/blood/article-pdf/112/5/1822/1487721/zh801708001822.pdf
44. Dumitriu IE, Dunbar DR, Howie SE, Sethi T, Gregory CD. Human dendritic cells produce TGF-beta 1 under the influence of lung carcinoma cells and prime the differentiation of CD4+CD25+Foxp3+ regulatory T cells. J Immunol [Internet]. 2009 Mar 1;182(5):2795–807.
Available from: http://www.ncbi.nlm.nih.gov/pubmed/19234174
45. Baban B, Chandler PR, Sharma MD, Pihkala J, Koni PA, Munn DH, Mellor AL. IDO activates regulatory T cells and blocks their conversion into Th17-like T cells.

J Immunol [Internet]. 2009 Aug 15;183(4):2475–83. Available from: http://www.ncbi.nlm.nih.gov/pubmed/19635913

46. Lin EY, Nguyen A V, Russell RG, Pollard JW. Colony-stimulating factor 1 promotes progression of mammary tumors to malignancy.
J Exp Med [Internet]. 2001 Mar 19 [cited 2023 May 23];193(6):727–40. Available from: https://www.ncbi.nlm.nih.gov/pmc/articles/PMC2193412/

47. Liu RY, Zeng Y, Lei Z, Wang L, Yang H, Liu Z, Zhao J, Zhang HT. JAK/STAT3 signaling is required for TGF-β-induced epithelial- mesenchymal transition in lung cancer cells. Int J Oncol. 2014;44(5):1643–51.

48. Ma Y, Adjemian S, Galluzzi L, Zitvogel L, Kroemer G. Chemokines and chemokine receptors required for optimal responses to anticancer chemotherapy. Oncoimmunology [Internet]. 2014 Jan 1;3(1):e27663. Available from: http://www.ncbi.nlm.nih.gov/pubmed/24800170

49. Feldman AL, Friedl J, Lans TE, Libutti SK, Lorang D, Miller MS, Turner EM, Hewitt SM, Alexander HR. Retroviral gene transfer of interferon-inducible protein 10 inhibits growth of human melanoma xenografts. Int J Cancer. 2002 May 1;99(1):149–53.

50. Arenberg DA, Kunkel SL, Polverini PJ, Morris SB, Burdick MD, Glass MC, Taub DT, Iannettoni MD, Whyte RI, Strieter RM. Interferon-gamma-inducible protein 10 (IP-10) is an angiostatic factor that inhibits human non-small cell lung cancer (NSCLC) tumorigenesis and spontaneous metastases. J Exp Med. 1996 Sep 1;184(3):981–92.

51. Zipin-Roitman A, Meshel T, Sagi-Assif O, Shalmon B, Avivi C, Pfeffer RM, Witz IP, Ben-Baruch A. CXCL10 promotes invasion-related properties in human colorectal carcinoma cells. Cancer Res. 2007 Apr 1;67(7):3396–405.

52. Carswell EA, Old LJ, Kassel RL, Green S, Fiore N, Williamson B. An endotoxin-induced serum factor that causes necrosis of tumors. Proc Natl Acad Sci U S A [Internet]. 1975 Sep;72(9):3666–70.
Available from: http://www.ncbi.nlm.nih.gov/pubmed/1103152

53. Elia AR, Grioni M, Basso V, Curnis F, Freschi M, Corti A, Mondino A, Bellone M. Targeting tumor vasculature with TNF leads effector t cells to the tumor and

enhances therapeutic efficacy of immune checkpoint blockers in combination with adoptive cell therapy. Clinical Cancer Research. 2018 May 1;24(9):2171–81.

54. Hartley G, Regan D, Guth A, Dow S. Regulation of PD-L1 expression on murine tumor-associated monocytes and macrophages by locally produced TNF-α. Cancer Immunol Immunother [Internet]. 2017 Apr;66(4):523–35. Available from: http://www.ncbi.nlm.nih.gov/pubmed/28184968

55. Yoshimatsu Y, Wakabayashi I, Kimuro S, Takahashi N, Takahashi K, Kobayashi M, Maishi N, Podyma-Inoue KA, Hida K, Miyazono K, Watabe T. TNF-α enhances TGF-β-induced endothelial-to-mesenchymal transition via TGF-β signal augmentation. Cancer Sci [Internet]. 2020 Jul;111(7):2385–99. Available from: http://www.ncbi.nlm.nih.gov/pubmed/32385953

56. Moore RJ, Owens DM, Stamp G, Arnott C, Burke F, East N, Holdsworth H, Turner L, Rollins B, Pasparakis M, Kollias G, Balkwill F. Mice deficient in tumor necrosis factor-alpha are resistant to skin carcinogenesis. Nat Med. 1999 Jul;5(7):828–31.

57. Emmerich J, Mumm JB, Chan IH, LaFace D, Truong H, McClanahan T, Gorman DM, Oft M. IL-10 directly activates and expands tumor-resident CD8(+) T cells without de novo infiltration from secondary lymphoid organs. Cancer Res. 2012 Jul 15;72(14):3570–81.

58. Ruffell B, Chang-Strachan D, Chan V, Rosenbusch A, Ho CMT, Pryer N, Daniel D, Hwang ES, Rugo HS, Coussens LM. Macrophage IL-10 blocks CD8+ T cell-dependent responses to chemotherapy by suppressing IL-12 expression in intratumoral dendritic cells. Cancer Cell. 2014 Nov 10;26(5):623–37.

59. Propper DJ, Balkwill FR. Harnessing cytokines and chemokines for cancer therapy. Nat Rev Clin Oncol [Internet]. 2022 Apr 1;19(4):237–53. Available from: http://www.ncbi.nlm.nih.gov/pubmed/34997230

60. Galon J, Costes A, Sanchez-Cabo F, Kirilovsky A, Mlecnik B, Lagorce-Pagès C, Tosolini M, Camus M, Berger A, Wind P, Zinzindohoué F, Bruneval P, Cugnenc PH, Trajanoski Z, Fridman WH, Pagès F. Type, density, and location of immune cells within human colorectal tumors predict clinical outcome. Science. 2006 Sep 29;313(5795):1960–4.

61. Binnewies M, Roberts EW, Kersten K, Chan V, Fearon DF, Merad M, Coussens LM, Gabrilovich DI, Ostrand-Rosenberg S, Hedrick CC, Vonderheide RH, Pittet

MJ, Jain RK, Zou W, Howcroft TK, Woodhouse EC, Weinberg RA, Krummel MF. Understanding the tumor immune microenvironment (TIME) for effective therapy. Nat Med. 2018 May 1;24(5):541–50.

62. Wenner CA, Güler ML, Macatonia SE, O'Garra A, Murphy KM. Roles of IFN-gamma and IFN-alpha in IL-12-induced T helper cell-1 development. J Immunol. 1996 Feb 15;156(4):1442–7.
63. Romagnani S. T-cell subsets (Th1 versus Th2). Ann Allergy Asthma Immunol [Internet]. 2000 Jul;85(1):9–18; quiz 18, 21. Available from: http://www.ncbi.nlm.nih.gov/pubmed/10923599
64. Bettelli E, Carrier Y, Gao W, Korn T, Strom TB, Oukka M, Weiner HL, Kuchroo VK. Reciprocal developmental pathways for the generation of pathogenic effector TH17 and regulatory T cells. Nature. 2006 May 11;441(7090):235–8.
65. Infante-Duarte C, Horton HF, Byrne MC, Kamradt T. Microbial Lipopeptides Induce the Production of IL-17 in Th Cells. The Journal of Immunology [Internet]. 2000 Dec 1;165(11):6107–15. Available from: https://journals.aai.org/jimmunol/article/165/11/6107/33705/Microbial-Lipopeptides-Induce-the-Production-of-IL
66. Liang SC, Tan XY, Luxenberg DP, Karim R, Dunussi-Joannopoulos K, Collins M, Fouser LA. Interleukin (IL)-22 and IL-17 are coexpressed by Th17 cells and cooperatively enhance expression of antimicrobial peptides. J Exp Med. 2006 Oct 2;203(10):2271–9.
67. Kawai O, Ishii G, Kubota K, Murata Y, Naito Y, Mizuno T, Aokage K, Saijo N, Nishiwaki Y, Gemma A, Kudoh S, Ochiai A. Predominant infiltration of macrophages and CD8(+) T Cells in cancer nests is a significant predictor of survival in stage IV nonsmall cell lung cancer. Cancer [Internet]. 2008 Sep 15;113(6):1387–95.
Available from: http://www.ncbi.nlm.nih.gov/pubmed/18671239
68. Croft M, Carter L, Swain SL, Dutton RW. Generation of polarized antigen-specific CD8 effector populations: reciprocal action of interleukin (IL)-4 and IL-12 in promoting type 2 versus type 1 cytokine profiles. J Exp Med [Internet]. 1994 Nov 1 [cited 2023 Jun 23];180(5):1715–28.
Available from: http://www.ncbi.nlm.nih.gov/pubmed/7525836

69. Pipkin ME, Sacks JA, Cruz-Guilloty F, Lichtenheld MG, Bevan MJ, Rao A. Interleukin-2 and inflammation induce distinct transcriptional programs that promote the differentiation of effector cytolytic T cells. Immunity. 2010 Jan 29;32(1):79–90.
70. Scheipers P, Reiser H. Role of the CTLA-4 receptor in T cell activation and immunity. Physiologic function of the CTLA-4 receptor. Immunol Res. 1998;18(2):103–15.
71. Tumeh PC, Harview CL, Yearley JH, Shintaku IP, Taylor EJM, Robert L, Chmielowski B, Spasic M, Henry G, Ciobanu V, West AN, Carmona M, Kivork C, Seja E, Cherry G, Gutierrez AJ, Grogan TR, Mateus C, Tomasic G, Glaspy JA, Emerson RO, Robins H, Pierce RH, Elashoff DA, Robert C, Ribas A. PD-1 blockade induces responses by inhibiting adaptive immune resistance. Nature. 2014 Nov 27;515(7528):568–71.
72. Ahn E, Araki K, Hashimoto M, Li W, Riley JL, Cheung J, Sharpe AH, Freeman GJ, Irving BA, Ahmed R. Role of PD-1 during effector CD8 T cell differentiation. Proc Natl Acad Sci U S A. 2018 May 1;115(18):4749–54.
73. St Paul M, Ohashi PS. The Roles of CD8+ T Cell Subsets in Antitumor Immunity. Trends Cell Biol [Internet]. 2020 Sep 1;30(9):695–704. Available from: http://www.ncbi.nlm.nih.gov/pubmed/32624246
74. Rosenberg SA, Sherry RM, Morton KE, Scharfman WJ, Yang JC, Topalian SL, Royal RE, Kammula U, Restifo NP, Hughes MS, Schwartzentruber D, Berman DM, Schwarz SL, Ngo LT, Mavroukakis SA, White DE, Steinberg SM. Tumor progression can occur despite the induction of very high levels of self/tumor antigen-specific CD8+ T cells in patients with melanoma. J Immunol. 2005 Nov 1;175(9):6169–76.
75. Scheper W, Kelderman S, Fanchi LF, Linnemann C, Bendle G, de Rooij MAJ, Hirt C, Mezzadra R, Slagter M, Dijkstra K, Kluin RJC, Snaebjornsson P, Milne K, Nelson BH, Zijlmans H, Kenter G, Voest EE, Haanen JBAG, Schumacher TN. Low and variable tumor reactivity of the intratumoral TCR repertoire in human cancers. Nat Med [Internet]. 2019 Jan 1 [cited 2023 Jun 20];25(1):89–94. Available from: http://www.ncbi.nlm.nih.gov/pubmed/30510250

76. Simoni Y, Becht E, Fehlings M, Loh CY, Koo SL, Teng KWW, Yeong JPS, Nahar R, Zhang T, Kared H, Duan K, Ang N, Poidinger M, Lee YY, Larbi A, Khng AJ, Tan E, Fu C, Mathew R, Teo M, Lim WT, Toh CK, Ong BH, Koh T, Hillmer AM, Takano A, Lim TKH, Tan EH, Zhai W, Tan DSW, Tan IB, Newell EW. Bystander CD8+ T cells are abundant and phenotypically distinct in human tumour infiltrates. Nature [Internet]. 2018 May 24 [cited 2023 Jun 20];557(7706):575–9. Available from: https://pubmed.ncbi.nlm.nih.gov/29769722/

77. Sakaguchi S, Sakaguchi N, Asano M, Itoh M, Toda M. Immunologic self-tolerance maintained by activated T cells expressing IL-2 receptor alpha-chains (CD25). Breakdown of a single mechanism of self-tolerance causes various autoimmune diseases. J Immunol. 1995 Aug 1;155(3):1151–64.

78. Hori S, Nomura T, Sakaguchi S. Control of regulatory T cell development by the transcription factor Foxp3. Science. 2003 Feb 14;299(5609):1057–61.

79. Miyara M, Yoshioka Y, Kitoh A, Shima T, Wing K, Niwa A, Parizot C, Taflin C, Heike T, Valeyre D, Mathian A, Nakahata T, Yamaguchi T, Nomura T, Ono M, Amoura Z, Gorochov G, Sakaguchi S. Functional delineation and differentiation dynamics of human CD4+ T cells expressing the FoxP3 transcription factor. Immunity. 2009 Jun 19;30(6):899–911.

80. Tran DQ, Ramsey H, Shevach EM. Induction of FOXP3 expression in naive human CD4+FOXP3 T cells by T-cell receptor stimulation is transforming growth factor-beta dependent but does not confer a regulatory phenotype. Blood [Internet]. 2007 Oct 15;110(8):2983–90.
Available from: http://www.ncbi.nlm.nih.gov/pubmed/17644734

81. Hsu P, Santner-Nanan B, Hu M, Skarratt K, Lee CH, Stormon M, Wong M, Fuller SJ, Nanan R. IL-10 Potentiates Differentiation of Human Induced Regulatory T Cells via STAT3 and Foxo1. J Immunol. 2015 Oct 15;195(8):3665–74.

82. Liang B, Workman C, Lee J, Chew C, Dale BM, Colonna L, Flores M, Li N, Schweighoffer E, Greenberg S, Tybulewicz V, Vignali D, Clynes R. Regulatory T cells inhibit dendritic cells by lymphocyte activation gene-3 engagement of MHC class II. J Immunol [Internet]. 2008 May 1 [cited 2023 Jun 17];180(9):5916–26. Available from: http://www.ncbi.nlm.nih.gov/pubmed/18424711

83. McNally A, Hill GR, Sparwasser T, Thomas R, Steptoe RJ. CD4+CD25+ regulatory T cells control CD8+ T-cell effector differentiation by modulating IL-2 homeostasis. Proc Natl Acad Sci U S A [Internet]. 2011 May 3;108(18):7529–34. Available from: http://www.ncbi.nlm.nih.gov/pubmed/21502514
84. Grossman WJ, Verbsky JW, Barchet W, Colonna M, Atkinson JP, Ley TJ. Human T regulatory cells can use the perforin pathway to cause autologous target cell death. Immunity. 2004 Oct;21(4):589–601.
85. Read S, Malmström V, Powrie F. Cytotoxic T lymphocyte-associated antigen 4 plays an essential role in the function of CD25(+)CD4(+) regulatory cells that control intestinal inflammation. J Exp Med [Internet]. 2000 Jul 17;192(2):295–302. Available from: http://www.ncbi.nlm.nih.gov/pubmed/10899916
86. Strauss L, Bergmann C, Szczepanski M, Gooding W, Johnson JT, Whiteside TL. A unique subset of CD4+CD25highFoxp3+ T cells secreting interleukin-10 and transforming growth factor-beta1 mediates suppression in the tumor microenvironment. Clin Cancer Res [Internet]. 2007 Aug 1;13(15 Pt 1):4345–54. Available from: http://www.ncbi.nlm.nih.gov/pubmed/17671115
87. Iglesia MD, Parker JS, Hoadley KA, Serody JS, Perou CM, Vincent BG. Genomic Analysis of Immune Cell Infiltrates Across 11 Tumor Types. J Natl Cancer Inst [Internet]. 2016 Nov;108(11).
Available from: http://www.ncbi.nlm.nih.gov/pubmed/27335052
88. Cooley S, Burns LJ, Repka T, Miller JS. Natural killer cell cytotoxicity of breast cancer targets is enhanced by two distinct mechanisms of antibody-dependent cellular cytotoxicity against LFA-3 and HER2/neu. Exp Hematol. 1999 Oct;27(10):1533–41.
89. Park JE, Kim SE, Keam B, Park HR, Kim S, Kim M, Kim TM, Doh J, Kim DW, Heo DS. Anti-tumor effects of NK cells and anti-PD-L1 antibody with antibody-dependent cellular cytotoxicity in PD-L1-positive cancer cell lines. J Immunother Cancer [Internet]. 2020 Aug;8(2):873. Available from: http://www.ncbi.nlm.nih.gov/pubmed/32830112
90. Wang W, Erbe AK, Hank JA, Morris ZS, Sondel PM. NK Cell-Mediated Antibody-Dependent Cellular Cytotoxicity in Cancer Immunotherapy. Front Immunol. 2015;6:368.

91. Weiskopf K, Weissman IL. Macrophages are critical effectors of antibody therapies for cancer. MAbs [Internet]. 2015;7(2):303–10. Available from: http://www.ncbi.nlm.nih.gov/pubmed/25667985
92. Shi JY, Gao Q, Wang ZC, Zhou J, Wang XY, Min ZH, Shi YH, Shi GM, Ding ZB, Ke AW, Dai Z, Qiu SJ, Song K, Fan J. Margin-infiltrating CD20(+) B cells display an atypical memory phenotype and correlate with favorable prognosis in hepatocellular carcinoma. Clin Cancer Res [Internet]. 2013 Nov 1;19(21):5994–6005. Available from: http://www.ncbi.nlm.nih.gov/pubmed/24056784
93. Rossetti RAM, Lorenzi NPC, Yokochi K, Rosa MBS de F, Benevides L, Margarido PFR, Baracat EC, Carvalho JP, Villa LL, Lepique AP. B lymphocytes can be activated to act as antigen presenting cells to promote anti-tumor responses. PLoS One. 2018;13(7):e0199034.
94. Deola S, Panelli MC, Maric D, Selleri S, Dmitrieva NI, Voss CY, Klein H, Stroncek D, Wang E, Marincola FM. Helper B cells promote cytotoxic T cell survival and proliferation independently of antigen presentation through CD27/CD70 interactions. J Immunol. 2008 Feb 1;180(3):1362–72.
95. Olkhanud PB, Damdinsuren B, Bodogai M, Gress RE, Sen R, Wejksza K, Malchinkhuu E, Wersto RP, Biragyn A. Tumor-evoked regulatory B cells promote breast cancer metastasis by converting resting $CD4^+$ T cells to T-regulatory cells. Cancer Res. 2011 May 15;71(10):3505–15.
96. Shao Y, Lo CM, Ling CC, Liu XB, Ng KTP, Chu ACY, Ma YY, Li CX, Fan ST, Man K. Regulatory B cells accelerate hepatocellular carcinoma progression via CD40/CD154 signaling pathway. Cancer Lett. 2014 Dec 28;355(2):264–72.
97. Cheong C, Matos I, Choi JH, Dandamudi DB, Shrestha E, Longhi MP, Jeffrey KL, Anthony RM, Kluger C, Nchinda G, Koh H, Rodriguez A, Idoyaga J, Pack M, Velinzon K, Park CG, Steinman RM. Microbial stimulation fully differentiates monocytes to DC-SIGN/CD209+ dendritic cells for immune T cell areas. Cell [Internet]. 2010 Oct 10 [cited 2023 Jun 23];143(3):416. Available from: /pmc/articles/PMC3150728/
98. Ladányi A, Kiss J, Somlai B, Gilde K, Fejos Z, Mohos A, Gaudi I, Tímár J. Density of DC-LAMP(+) mature dendritic cells in combination with activated T

lymphocytes infiltrating primary cutaneous melanoma is a strong independent prognostic factor. Cancer Immunol Immunother. 2007 Sep;56(9):1459–69.

99. Engelhardt JJ, Boldajipour B, Beemiller P, Pandurangi P, Sorensen C, Werb Z, Egeblad M, Krummel MF. Marginating dendritic cells of the tumor microenvironment cross-present tumor antigens and stably engage tumor-specific T cells. Cancer Cell [Internet]. 2012 Mar 20;21(3):402–17. Available from: http://www.ncbi.nlm.nih.gov/pubmed/22439936

100. Broz ML, Binnewies M, Boldajipour B, Nelson AE, Pollack JL, Erle DJ, Barczak A, Rosenblum MD, Daud A, Barber DL, Amigorena S, Van't Veer LJ, Sperling AI, Wolf DM, Krummel MF. Dissecting the tumor myeloid compartment reveals rare activating antigen-presenting cells critical for T cell immunity. Cancer Cell [Internet]. 2014 Nov 10;26(5):638–52.
Available from: http://www.ncbi.nlm.nih.gov/pubmed/25446897

101. Gabrilovich DI, Nagaraj S. Myeloid-derived suppressor cells as regulators of the immune system. Nat Rev Immunol [Internet]. 2009 Mar [cited 2023 Jun 14];9(3):162–74.
Available from: https://www.ncbi.nlm.nih.gov/pmc/articles/PMC2828349/

102. Diaz-Montero CM, Salem ML, Nishimura MI, Garrett-Mayer E, Cole DJ, Montero AJ. Increased circulating myeloid-derived suppressor cells correlate with clinical cancer stage, metastatic tumor burden, and doxorubicin–cyclophosphamide chemotherapy. Cancer Immunology, Immunotherapy [Internet]. 2009 Jan [cited 2023 Jun 23];58(1):49. Available from: /pmc/articles/PMC3401888/

103. Youn JI, Nagaraj S, Collazo M, Gabrilovich DI. Subsets of myeloid-derived suppressor cells in tumor-bearing mice. J Immunol [Internet]. 2008 Oct 15;181(8):5791–802.
Available from: http://www.ncbi.nlm.nih.gov/pubmed/18832739

104. Movahedi K, Guilliams M, Van den Bossche J, Van den Bergh R, Gysemans C, Beschin A, De Baetselier P, Van Ginderachter JA. Identification of discrete tumor-induced myeloid-derived suppressor cell subpopulations with distinct T cell-suppressive activity. Blood [Internet]. 2008 Apr 15;111(8):4233–44. Available from: http://www.ncbi.nlm.nih.gov/pubmed/18272812

105. Bronte V, Serafini P, De Santo C, Marigo I, Tosello V, Mazzoni A, Segal DM, Staib C, Lowel M, Sutter G, Colombo MP, Zanovello P. IL-4-induced arginase 1 suppresses alloreactive T cells in tumor-bearing mice. J Immunol. 2003 Jan 1;170(1):270–8.
106. Rodriguez PC, Quiceno DG, Zabaleta J, Ortiz B, Zea AH, Piazuelo MB, Delgado A, Correa P, Brayer J, Sotomayor EM, Antonia S, Ochoa JB, Ochoa AC. Arginase I production in the tumor microenvironment by mature myeloid cells inhibits T-cell receptor expression and antigen-specific T-cell responses. Cancer Res. 2004 Aug 15;64(16):5839–49.
107. Ochoa AC, Zea AH, Hernandez C, Rodriguez PC. Arginase, prostaglandins, and myeloid-derived suppressor cells in renal cell carcinoma. Clin Cancer Res. 2007 Jan 15;13(2 Pt 2):721s–6s.
108. Mazzoni A, Bronte V, Visintin A, Spitzer JH, Apolloni E, Serafini P, Zanovello P, Segal DM. Myeloid suppressor lines inhibit T cell responses by an NO-dependent mechanism. J Immunol. 2002 Jan 15;168(2):689–95.
109. Sinha P, Clements VK, Bunt SK, Albelda SM, Ostrand-Rosenberg S. Cross-talk between myeloid-derived suppressor cells and macrophages subverts tumor immunity toward a type 2 response. J Immunol. 2007 Jul 15;179(2):977–83.
110. Yang L, DeBusk LM, Fukuda K, Fingleton B, Green-Jarvis B, Shyr Y, Matrisian LM, Carbone DP, Lin PC. Expansion of myeloid immune suppressor Gr+CD11b+ cells in tumor-bearing host directly promotes tumor angiogenesis. Cancer Cell. 2004 Oct;6(4):409–21.
111. Dora D, Rivard C, Yu H, Bunn P, Suda K, Ren S, Lueke Pickard S, Laszlo V, Harko T, Megyesfalvi Z, Moldvay J, Hirsch FR, Dome B, Lohinai Z. Neuroendocrine subtypes of small cell lung cancer differ in terms of immune microenvironment and checkpoint molecule distribution. Mol Oncol. 2020 Sep;14(9):1947–65.
112. Coley WB. The treatment of malignant tumors by repeated inoculations of erysipelas. With a report of ten original cases. 1893. Clin Orthop Relat Res [Internet]. 1991 Jan;(262):3–11.
Available from: http://www.ncbi.nlm.nih.gov/pubmed/1984929
113. Morales A, Eidinger D, Bruce AW. Intracavitary Bacillus Calmette-Guerin in the treatment of superficial bladder tumors. J Urol. 1976 Aug;116(2):180–3.

114. Nobel Prize Outreach. The 2018 Nobel Prize in Physiology or Medicine - Press release [Internet]. 2018 [cited 2023 May 10]. Available from: https://www.nobelprize.org/prizes/medicine/2018/press-release/
115. Wei SC, Duffy CR, Allison JP. Fundamental Mechanisms of Immune Checkpoint Blockade Therapy. Cancer Discov [Internet]. 2018 Sep 1;8(9):1069–86. Available from: http://www.ncbi.nlm.nih.gov/pubmed/30115704
116. Nishimura H, Nose M, Hiai H, Minato N, Honjo T. Development of lupus-like autoimmune diseases by disruption of the PD-1 gene encoding an ITIM motif-carrying immunoreceptor. Immunity. 1999 Aug;11(2):141–51.
117. Wang J, Yoshida T, Nakaki F, Hiai H, Okazaki T, Honjo T. Establishment of NOD-Pdcd1-/- mice as an efficient animal model of type I diabetes. Proc Natl Acad Sci U S A. 2005 Aug 16;102(33):11823–8.
118. Topalian SL, Hodi FS, Brahmer JR, Gettinger SN, Smith DC, McDermott DF, Powderly JD, Carvajal RD, Sosman JA, Atkins MB, Leming PD, Spigel DR, Antonia SJ, Horn L, Drake CG, Pardoll DM, Chen L, Sharfman WH, Anders RA, Taube JM, McMiller TL, Xu H, Korman AJ, Jure-Kunkel M, Agrawal S, McDonald D, Kollia GD, Gupta A, Wigginton JM, Sznol M. Safety, activity, and immune correlates of anti-PD-1 antibody in cancer. N Engl J Med [Internet]. 2012 Jun 28;366(26):2443–54.
Available from: http://www.ncbi.nlm.nih.gov/pubmed/22658127
119. Forde PM, Spicer J, Lu S, Provencio M, Mitsudomi T, Awad MM, Felip E, Broderick SR, Brahmer JR, Swanson SJ, Kerr K, Wang C, Ciuleanu TE, Saylors GB, Tanaka F, Ito H, Chen KN, Liberman M, Vokes EE, Taube JM, Dorange C, Cai J, Fiore J, Jarkowski A, Balli D, Sausen M, Pandya D, Calvet CY, Girard N, CheckMate 816 Investigators. Neoadjuvant Nivolumab plus Chemotherapy in Resectable Lung Cancer. N Engl J Med. 2022 May 26;386(21):1973–85.
120. Nasser NJ, Gorenberg M, Agbarya A. First line Immunotherapy for Non-Small Cell Lung Cancer. Pharmaceuticals (Basel) [Internet]. 2020 Nov 8 [cited 2023 Sep 6];13(11).
Available from: https://www.ncbi.nlm.nih.gov/pmc/articles/pmid/33171686/
121. Girard N, Bar J, Garrido P, Garassino MC, McDonald F, Mornex F, Filippi AR, Smit HJM, Peters S, Field JK, Christoph DC, Sibille A, Fietkau R, Haakensen VD,

Chouaid C, Markman B, Hiltermann TJN, Taus A, Sawyer W, Allen A, Chander P, Licour M, Solomon B. Treatment Characteristics and Real-World Progression-Free Survival in Patients With Unresectable Stage III NSCLC Who Received Durvalumab After Chemoradiotherapy: Findings From the PACIFIC-R Study. J Thorac Oncol [Internet]. 2023 Feb 1;18(2):181–93. Available from: http://www.ncbi.nlm.nih.gov/pubmed/36307040

122. Chung HC, Piha-Paul SA, Lopez-Martin J, Schellens JHM, Kao S, Miller WH, Delord JP, Gao B, Planchard D, Gottfried M, Zer A, Jalal SI, Penel N, Mehnert JM, Matos I, Bennouna J, Kim DW, Xu L, Krishnan S, Norwood K, Ott PA. Pembrolizumab After Two or More Lines of Previous Therapy in Patients With Recurrent or Metastatic SCLC: Results From the KEYNOTE-028 and KEYNOTE-158 Studies. J Thorac Oncol. 2020 Apr;15(4):618–27.
123. Paz-Ares L, Goldman JW, Garassino MC, Dvorkin M, Trukhin D, Statsenko G, Hotta K, Ji JH, Hochmair MJ, Voitko O, Havel L, Poltoratskiy A, Losonczy G, Reinmuth N, Shrestha Y, Patel N, Mann H, Jiang H, Özgüroğlu M, Chen Y. PD-L1 expression, patterns of progression and patient-reported outcomes (PROs) with durvalumab plus platinum-etoposide in ES-SCLC: Results from CASPIAN. Annals of Oncology. 2019 Oct;30:v928–9.
124. Rudin CM, Awad MM, Navarro A, Gottfried M, Peters S, Tibor ;, Oszi C, Parneet ;, Cheema K, Delvys Rodriguez-Abreu ;, Wollner M, James ;, Yang CH, Mazieres J, Francisco ;, Orlandi J, Luft ; Alexander, Mahmut ;, Kato ; Terufumi, Gregory ;, Kalemkerian P, Luo Y, Ebiana V, Pietanza ; M Catherine, Kim HR. Pembrolizumab or Placebo Plus Etoposide and Platinum as First-Line Therapy for Extensive-Stage Small-Cell Lung Cancer: Randomized, Double-Blind, Phase III KEYNOTE-604 Study [Internet]. Vol. 38, J Clin Oncol. 2020. Available from: https://doi.org/10.
125. Ding XL, Su YG, Yu L, Bai ZL, Bai XH, Chen XZ, Yang X, Zhao R, He JX, Wang YY. Clinical characteristics and patient outcomes of molecular subtypes of small cell lung cancer (SCLC). World J Surg Oncol [Internet]. 2022 Feb 27;20(1):54. Available from: http://www.ncbi.nlm.nih.gov/pubmed/35220975
126. Goldman JW, Dvorkin M, Chen Y, Reinmuth N, Hotta K, Trukhin D, Statsenko G, Hochmair MJ, Özgüroğlu M, Ji JH, Garassino MC, Voitko O, Poltoratskiy A, Ponce S, Verderame F, Havel L, Bondarenko I, Każarnowicz A, Losonczy G, Conev N V,

Armstrong J, Byrne N, Thiyagarajah P, Jiang H, Paz-Ares L, CASPIAN investigators. Durvalumab, with or without tremelimumab, plus platinum-etoposide versus platinum-etoposide alone in first-line treatment of extensive-stage small-cell lung cancer (CASPIAN): updated results from a randomised, controlled, open-label, phase 3 trial. Lancet Oncol. 2021 Jan;22(1):51–65.

127. Merck. Merck Provides Update on KEYTRUDA® (pembrolizumab) Indication in Metastatic Small Cell Lung Cancer in the US - Merck.com [Internet]. 2021 [cited 2023 Apr 3]. Available from: https://www.merck.com/news/merck-provides-update-on-keytruda-pembrolizumab-indication-in-metastatic-small-cell-lung-cancer-in-the-us/
128. Bristol Myers Squibb. Bristol Myers Squibb - Bristol Myers Squibb Statement on Opdivo (nivolumab) Small Cell Lung Cancer U.S. Indication [Internet]. 2020 [cited 2023 Apr 3]. Available from: https://news.bms.com/news/details/2020/Bristol-Myers-Squibb-Statement-on-Opdivo-nivolumab-Small-Cell-Lung-Cancer-US-Indication/
129. Qureshi OS, Zheng Y, Nakamura K, Attridge K, Manzotti C, Schmidt EM, Baker J, Jeffery LE, Kaur S, Briggs Z, Hou TZ, Futter CE, Anderson G, Walker LSK, Sansom DM. Trans-endocytosis of CD80 and CD86: a molecular basis for the cell-extrinsic function of CTLA-4. Science [Internet]. 2011 Apr 29;332(6029):600–3. Available from: http://www.ncbi.nlm.nih.gov/pubmed/21474713
130. Rizvi NA, Cho BC, Reinmuth N, Lee KH, Luft A, Ahn MJ, van den Heuvel MM, Cobo M, Vicente D, Smolin A, Moiseyenko V, Antonia SJ, Le Moulec S, Robinet G, Natale R, Schneider J, Shepherd FA, Geater SL, Garon EB, Kim ES, Goldberg SB, Nakagawa K, Raja R, Higgs BW, Boothman AM, Zhao L, Scheuring U, Stockman PK, Chand VK, Peters S, MYSTIC Investigators. Durvalumab With or Without Tremelimumab vs Standard Chemotherapy in First-line Treatment of Metastatic Non-Small Cell Lung Cancer: The MYSTIC Phase 3 Randomized Clinical Trial. JAMA Oncol [Internet]. 2020 May 1;6(5):661–74. Available from: http://www.ncbi.nlm.nih.gov/pubmed/32271377
131. Paz-Ares LG, Ramalingam SS, Ciuleanu TE, Lee JS, Urban L, Caro RB, Park K, Sakai H, Ohe Y, Nishio M, Audigier-Valette C, Burgers JA, Pluzanski A, Sangha R, Gallardo C, Takeda M, Linardou H, Lupinacci L, Lee KH, Caserta C, Provencio M,

Carcereny E, Otterson GA, Schenker M, Zurawski B, Alexandru A, Vergnenegre A, Raimbourg J, Feeney K, Kim SW, Borghaei H, O'Byrne KJ, Hellmann MD, Memaj A, Nathan FE, Bushong J, Tran P, Brahmer JR, Reck M. First-Line Nivolumab Plus Ipilimumab in Advanced NSCLC: 4-Year Outcomes From the Randomized, Open-Label, Phase 3 CheckMate 227 Part 1 Trial. Journal of Thoracic Oncology. 2022 Feb 1;17(2):289–308.

132. Ready NE, Ott PA, Hellmann MD, Zugazagoitia J, Hann CL, de Braud F, Antonia SJ, Ascierto PA, Moreno V, Atmaca A, Salvagni S, Taylor M, Amin A, Camidge DR, Horn L, Calvo E, Li A, Lin WH, Callahan MK, Spigel DR. Nivolumab Monotherapy and Nivolumab Plus Ipilimumab in Recurrent Small Cell Lung Cancer: Results From the CheckMate 032 Randomized Cohort. J Thorac Oncol. 2020 Mar;15(3):426–35.
133. Reck M, Luft A, Szczesna A, Havel L, Kim SW, Akerley W, Pietanza MC, Wu YL, Zielinski C, Thomas M, Felip E, Gold K, Horn L, Aerts J, Nakagawa K, Lorigan P, Pieters A, Kong Sanchez T, Fairchild J, Spigel D. Phase III Randomized Trial of Ipilimumab Plus Etoposide and Platinum Versus Placebo Plus Etoposide and Platinum in Extensive-Stage Small-Cell Lung Cancer. J Clin Oncol. 2016 Nov 1;34(31):3740–8.
134. Williams MJ. Drosophila hemopoiesis and cellular immunity. J Immunol. 2007 Apr 15;178(8):4711–6.
135. Ginhoux F, Jung S. Monocytes and macrophages: developmental pathways and tissue homeostasis. Nat Rev Immunol. 2014 Jun;14(6):392–404.
136. Gomez Perdiguero E, Klapproth K, Schulz C, Busch K, Azzoni E, Crozet L, Garner H, Trouillet C, de Bruijn MF, Geissmann F, Rodewald HR. Tissue-resident macrophages originate from yolk-sac-derived erythro-myeloid progenitors. Nature. 2015 Feb 26;518(7540):547–51.
137. Epelman S, Lavine KJ, Randolph GJ. Origin and functions of tissue macrophages. Immunity [Internet]. 2014 Jul 17;41(1):21–35. Available from: http://www.ncbi.nlm.nih.gov/pubmed/25035951
138. Hashimoto D, Chow A, Noizat C, Teo P, Beasley MB, Leboeuf M, Becker CD, See P, Price J, Lucas D, Greter M, Mortha A, Boyer SW, Forsberg EC, Tanaka M, van Rooijen N, García-Sastre A, Stanley ER, Ginhoux F, Frenette PS, Merad M. Tissue-

resident macrophages self-maintain locally throughout adult life with minimal contribution from circulating monocytes. Immunity. 2013 Apr 18;38(4):792–804.

139. Gautier EL, Shay T, Miller J, Greter M, Jakubzick C, Ivanov S, Helft J, Chow A, Elpek KG, Gordonov S, Mazloom AR, Ma'ayan A, Chua WJ, Hansen TH, Turley SJ, Merad M, Randolph GJ, Immunological Genome Consortium. Gene-expression profiles and transcriptional regulatory pathways that underlie the identity and diversity of mouse tissue macrophages. Nat Immunol [Internet]. 2012 Nov;13(11):1118–28.
Available from: http://www.ncbi.nlm.nih.gov/pubmed/23023392
140. Schoenberger SP, Toes RE, van der Voort EI, Offringa R, Melief CJ. T-cell help for cytotoxic T lymphocytes is mediated by CD40-CD40L interactions. Nature. 1998 Jun 4;393(6684):480–3.
141. Oishi S, Takano R, Tamura S, Tani S, Iwaizumi M, Hamaya Y, Takagaki K, Nagata T, Seto S, Horii T, Osawa S, Furuta T, Miyajima H, Sugimoto K. M2 polarization of murine peritoneal macrophages induces regulatory cytokine production and suppresses T-cell proliferation. Immunology [Internet]. 2016 Nov;149(3):320–8. Available from: http://www.ncbi.nlm.nih.gov/pubmed/27421990
142. Balic JJ, Albargy H, Luu K, Kirby FJ, Jayasekara WSN, Mansell F, Garama DJ, De Nardo D, Baschuk N, Louis C, Humphries F, Fitzgerald K, Latz E, Gough DJ, Mansell A. STAT3 serine phosphorylation is required for TLR4 metabolic reprogramming and IL-1β expression. Nat Commun [Internet]. 2020 Jul 30;11(1):3816. Available from: http://www.ncbi.nlm.nih.gov/pubmed/32732870
143. Kelly A, Gunaltay S, McEntee CP, Shuttleworth EE, Smedley C, Houston SA, Fenton TM, Levison S, Mann ER, Travis MA. Human monocytes and macrophages regulate immune tolerance via integrin αvβ8-mediated TGFβ activation. J Exp Med [Internet]. 2018 Nov 5;215(11):2725–36. Available from: http://www.ncbi.nlm.nih.gov/pubmed/30355614
144. Madsen DH, Leonard D, Masedunskas A, Moyer A, Jürgensen HJ, Peters DE, Amornphimoltham P, Selvaraj A, Yamada SS, Brenner DA, Burgdorf S, Engelholm LH, Behrendt N, Holmbeck K, Weigert R, Bugge TH. M2-like macrophages are responsible for collagen degradation through a mannose receptor-mediated pathway. J Cell Biol. 2013 Sep 16;202(6):951–66.

145. He XT, Li X, Yin Y, Wu RX, Xu XY, Chen FM. The effects of conditioned media generated by polarized macrophages on the cellular behaviours of bone marrow mesenchymal stem cells. J Cell Mol Med. 2018 Feb;22(2):1302–15.
146. Quiros M, Nishio H, Neumann PA, Siuda D, Brazil JC, Azcutia V, Hilgarth R, O'Leary MN, Garcia-Hernandez V, Leoni G, Feng M, Bernal G, Williams H, Dedhia PH, Gerner-Smidt C, Spence J, Parkos CA, Denning TL, Nusrat A. Macrophage-derived IL-10 mediates mucosal repair by epithelial WISP-1 signaling. J Clin Invest. 2017 Sep 1;127(9):3510–20.
147. Bingle L, Lewis CE, Corke KP, Reed MWR, Brown NJ. Macrophages promote angiogenesis in human breast tumour spheroids in vivo. Br J Cancer. 2006 Jan 16;94(1):101–7.
148. Condeelis J, Segall JE. Intravital imaging of cell movement in tumours. Nat Rev Cancer [Internet]. 2003 Dec;3(12):921–30. Available from: http://www.ncbi.nlm.nih.gov/pubmed/14737122
149. Loke P, Nair MG, Parkinson J, Guiliano D, Blaxter M, Allen JE. IL-4 dependent alternatively-activated macrophages have a distinctive in vivo gene expression phenotype. BMC Immunol [Internet]. 2002 Jul 4;3:7. Available from: http://www.ncbi.nlm.nih.gov/pubmed/12098359
150. Martinez FO, Gordon S, Locati M, Mantovani A. Transcriptional profiling of the human monocyte-to-macrophage differentiation and polarization: new molecules and patterns of gene expression. J Immunol [Internet]. 2006 Nov 15;177(10):7303–11. Available from: http://www.ncbi.nlm.nih.gov/pubmed/17082649
151. te Velde AA, Klomp JP, Yard BA, de Vries JE, Figdor CG. Modulation of phenotypic and functional properties of human peripheral blood monocytes by IL-4. J Immunol. 1988 Mar 1;140(5):1548–54.
152. Stein M, Keshav S, Harris N, Gordon S. Interleukin 4 potently enhances murine macrophage mannose receptor activity: a marker of alternative immunologic macrophage activation. J Exp Med. 1992 Jul 1;176(1):287–92.
153. Mills CD, Kincaid K, Alt JM, Heilman MJ, Hill AM. M-1/M-2 macrophages and the Th1/Th2 paradigm. J Immunol. 2000 Jun 15;164(12):6166–73.

154. Mantovani A, Sica A, Sozzani S, Allavena P, Vecchi A, Locati M. The chemokine system in diverse forms of macrophage activation and polarization. Trends Immunol. 2004 Dec;25(12):677–86.
155. Xue J, Schmidt S V, Sander J, Draffehn A, Krebs W, Quester I, De Nardo D, Gohel TD, Emde M, Schmidleithner L, Ganesan H, Nino-Castro A, Mallmann MR, Labzin L, Theis H, Kraut M, Beyer M, Latz E, Freeman TC, Ulas T, Schultze JL. Transcriptome-based network analysis reveals a spectrum model of human macrophage activation. Immunity [Internet]. 2014 Feb 20;40(2):274–88. Available from: http://www.ncbi.nlm.nih.gov/pubmed/24530056
156. Fridman WH, Zitvogel L, Sautès-Fridman C, Kroemer G. The immune contexture in cancer prognosis and treatment. Nat Rev Clin Oncol. 2017 Dec;14(12):717–34.
157. Stout RD, Jiang C, Matta B, Tietzel I, Watkins SK, Suttles J. Macrophages sequentially change their functional phenotype in response to changes in microenvironmental influences. J Immunol [Internet]. 2005 Jul 1;175(1):342–9. Available from: http://www.ncbi.nlm.nih.gov/pubmed/15972667
158. Liu YC, Zou XB, Chai YF, Yao YM. Macrophage polarization in inflammatory diseases. Int J Biol Sci [Internet]. 2014;10(5):520–9. Available from: http://www.ncbi.nlm.nih.gov/pubmed/24910531
159. Sawa-Wejksza K, Kandefer-Szerszeń M. Tumor-Associated Macrophages as Target for Antitumor Therapy. Arch Immunol Ther Exp (Warsz) [Internet]. 2018 Apr;66(2):97–111.
Available from: http://www.ncbi.nlm.nih.gov/pubmed/28660349
160. Gao J, Liang Y, Wang L. Shaping Polarization Of Tumor-Associated Macrophages In Cancer Immunotherapy. Vol. 13, Frontiers in Immunology. Frontiers Media S.A.; 2022.
161. Hasan MR, Alsaiari AA, Fakhurji BZ, Molla MHR, Asseri AH, Sumon MAA, Park MN, Ahammad F, Kim B. Application of Mathematical Modeling and Computational Tools in the Modern Drug Design and Development Process. Molecules [Internet]. 2022 Jun 29;27(13). Available from: http://www.ncbi.nlm.nih.gov/pubmed/35807415

162. Ferreira LLG, Andricopulo AD. ADMET modeling approaches in drug discovery. Drug Discov Today [Internet]. 2019 May 1;24(5):1157–65. Available from: http://www.ncbi.nlm.nih.gov/pubmed/30890362

163. Simon Z, Peragovics A, Vigh-Smeller M, Csukly G, Tombor L, Yang Z, Zahoránszky-Kohalmi G, Végner L, Jelinek B, Hári P, Hetényi C, Bitter I, Czobor P, Málnási-Csizmadia A. Drug effect prediction by polypharmacology-based interaction profiling. J Chem Inf Model [Internet]. 2012 Jan 23 [cited 2012 Jun 10];52(1):134–45.
Available from: http://www.ncbi.nlm.nih.gov/pubmed/22098080

164. Wishart DS, Feunang YD, Guo AC, Lo EJ, Marcu A, Grant JR, Sajed T, Johnson D, Li C, Sayeeda Z, Assempour N, Iynkkaran I, Liu Y, Maciejewski A, Gale N, Wilson A, Chin L, Cummings R, Le D, Pon A, Knox C, Wilson M. DrugBank 5.0: a major update to the DrugBank database for 2018. Nucleic Acids Res. 2018 Jan 4;46(D1):D1074–82.

165. Kim S, Chen J, Cheng T, Gindulyte A, He J, He S, Li Q, Shoemaker BA, Thiessen PA, Yu B, Zaslavsky L, Zhang J, Bolton EE. PubChem in 2021: new data content and improved web interfaces. Nucleic Acids Res. 2021 Jan 8;49(D1):D1388–95.

166. UniProt Consortium. UniProt: the universal protein knowledgebase in 2021. Nucleic Acids Res. 2021 Jan 8;49(D1):D480–9.

167. Keshava Prasad TS, Goel R, Kandasamy K, Keerthikumar S, Kumar S, Mathivanan S, Telikicherla D, Raju R, Shafreen B, Venugopal A, Balakrishnan L, Marimuthu A, Banerjee S, Somanathan DS, Sebastian A, Rani S, Ray S, Harrys Kishore CJ, Kanth S, Ahmed M, Kashyap MK, Mohmood R, Ramachandra YL, Krishna V, Rahiman BA, Mohan S, Ranganathan P, Ramabadran S, Chaerkady R, Pandey A. Human Protein Reference Database--2009 update. Nucleic Acids Res [Internet]. 2009 Jan;37(Database issue):D767-72. Available from: http://www.ncbi.nlm.nih.gov/pubmed/18988627

168. Ma J, Cai Z, Wei H, Liu X, Zhao Q, Zhang T. The anti-tumor effect of aspirin: What we know and what we expect. Biomed Pharmacother [Internet]. 2017 Nov 1;95:656–61. Available from: http://www.ncbi.nlm.nih.gov/pubmed/28881293

169. Hsieh CC, Wang CH. Aspirin Disrupts the Crosstalk of Angiogenic and Inflammatory Cytokines between 4T1 Breast Cancer Cells and Macrophages.

Mediators Inflamm [Internet]. 2018;2018:6380643. Available from: http://www.ncbi.nlm.nih.gov/pubmed/30034291

170. Lohinai Z, Dome P, Szilagyi Z, Ostoros G, Moldvay J, Hegedus B, Dome B, Weiss GJ. From Bench to Bedside: Attempt to Evaluate Repositioning of Drugs in the Treatment of Metastatic Small Cell Lung Cancer (SCLC). PLoS One [Internet]. 2016 Jan 6;11(1):e0144797.
Available from: http://www.ncbi.nlm.nih.gov/pubmed/26735301
171. Pushpakom S, Iorio F, Eyers PA, Escott KJ, Hopper S, Wells A, Doig A, Guilliams T, Latimer J, McNamee C, Norris A, Sanseau P, Cavalla D, Pirmohamed M. Drug repurposing: progress, challenges and recommendations. Nat Rev Drug Discov [Internet]. 2019 Jan 28;18(1):41–58. Available from: http://www.ncbi.nlm.nih.gov/pubmed/30310233
172. Albert R, Barabási AL. Statistical mechanics of complex networks. Rev Mod Phys. 2002 Jan 30;74(1):47–97.
173. Barabási AL, Oltvai ZN. Network biology: understanding the cell's functional organization. Nat Rev Genet [Internet]. 2004 Feb;5(2):101–13. Available from: http://www.ncbi.nlm.nih.gov/pubmed/14735121
174. Azeloglu EU, Iyengar R. Signaling networks: information flow, computation, and decision making. Cold Spring Harb Perspect Biol [Internet]. 2015 Apr 1;7(4):a005934. Available from: http://www.ncbi.nlm.nih.gov/pubmed/25833842
175. Csermely P, Agoston V, Pongor S. The efficiency of multi-target drugs: the network approach might help drug design. Trends Pharmacol Sci [Internet]. 2005 Apr;26(4):178–82.
Available from: http://www.ncbi.nlm.nih.gov/pubmed/15808341
176. Asghar W, El Assal R, Shafiee H, Pitteri S, Paulmurugan R, Demirci U. Engineering cancer microenvironments for in vitro 3-D tumor models. Mater Today (Kidlington) [Internet]. 2015 Dec;18(10):539–53. Available from: http://www.ncbi.nlm.nih.gov/pubmed/28458612
177. Vogel DYS, Glim JE, Stavenuiter AWD, Breur M, Heijnen P, Amor S, Dijkstra CD, Beelen RHJ. Human macrophage polarization in vitro: maturation and activation methods compared. Immunobiology. 2014 Sep;219(9):695–703.

178. Scotton CJ, Martinez FO, Smelt MJ, Sironi M, Locati M, Mantovani A, Sozzani S. Transcriptional profiling reveals complex regulation of the monocyte IL-1 beta system by IL-13. J Immunol. 2005 Jan 15;174(2):834–45.
179. Lohinai Z, Megyesfalvi Z, Suda K, Harko T, Ren S, Moldvay J, Laszlo V, Rivard C, Dome B, Hirsch FR. Comparative expression analysis in small cell lung carcinoma reveals neuroendocrine pattern change in primary tumor versus lymph node metastases. Transl Lung Cancer Res. 2019 Dec;8(6):938–50.
180. Battifora H. The multitumor (sausage) tissue block: novel method for immunohistochemical antibody testing. Lab Invest. 1986 Aug;55(2):244–8.
181. Rueden CT, Schindelin J, Hiner MC, DeZonia BE, Walter AE, Arena ET, Eliceiri KW. ImageJ2: ImageJ for the next generation of scientific image data. BMC Bioinformatics. 2017 Dec 29;18(1):529.
182. HTG Molecular. HTG EdgeSeq Oncology Biomarker Panel - HTG Molecular [Internet]. [cited 2023 Apr 21].
Available from: https://www.htgmolecular.com/assays/obp
183. Rudin CM, Poirier JT, Byers LA, Dive C, Dowlati A, George J, Heymach J V, Johnson JE, Lehman JM, MacPherson D, Massion PP, Minna JD, Oliver TG, Quaranta V, Sage J, Thomas RK, Vakoc CR, Gazdar AF. Molecular subtypes of small cell lung cancer: a synthesis of human and mouse model data. Nat Rev Cancer. 2019 May;19(5):289–97.
184. Schwab JD, Kühlwein SD, Ikonomi N, Kühl M, Kestler HA. Concepts in Boolean network modeling: What do they all mean? Comput Struct Biotechnol J [Internet]. 2020;18:571–82. Available from: http://www.ncbi.nlm.nih.gov/pubmed/32257043
185. Ambarus CA, Santegoets KCM, van Bon L, Wenink MH, Tak PP, Radstake TRDJ, Baeten DLP. Soluble immune complexes shift the TLR-induced cytokine production of distinct polarized human macrophage subsets towards IL-10. PLoS One. 2012;7(4):e35994.
186. Woolard J, Wang WY, Bevan HS, Qiu Y, Morbidelli L, Pritchard-Jones RO, Cui TG, Sugiono M, Waine E, Perrin R, Foster R, Digby-Bell J, Shields JD, Whittles CE, Mushens RE, Gillatt DA, Ziche M, Harper SJ, Bates DO. VEGF165b, an inhibitory vascular endothelial growth factor splice variant: mechanism of action, in vivo effect on angiogenesis and endogenous protein expression. Cancer Res

[Internet]. 2004 Nov 1;64(21):7822–35. Available from: http://www.ncbi.nlm.nih.gov/pubmed/15520188

187. Kanehisa M, Furumichi M, Sato Y, Ishiguro-Watanabe M, Tanabe M. KEGG: integrating viruses and cellular organisms. Nucleic Acids Res [Internet]. 2021;49(D1):D545–51.
Available from: http://www.ncbi.nlm.nih.gov/pubmed/33125081
188. Su AI, Wiltshire T, Batalov S, Lapp H, Ching KA, Block D, Zhang J, Soden R, Hayakawa M, Kreiman G, Cooke MP, Walker JR, Hogenesch JB. A gene atlas of the mouse and human protein-encoding transcriptomes. Proc Natl Acad Sci U S A [Internet]. 2004 Apr 20;101(16):6062–7. Available from: http://www.ncbi.nlm.nih.gov/pubmed/15075390
189. Szegvari G, Dora D, Lohinai Z. Effective Reversal of Macrophage Polarization by Inhibitory Combinations Predicted by a Boolean Protein-Protein Interaction Model. Biology (Basel) [Internet]. 2023 Feb 27;12(3):376. Available from: http://www.ncbi.nlm.nih.gov/pubmed/36979068
190. Szklarczyk D, Gable AL, Lyon D, Junge A, Wyder S, Huerta-Cepas J, Simonovic M, Doncheva NT, Morris JH, Bork P, Jensen LJ, Mering C von, Von Mering C. STRING v11: protein-protein association networks with increased coverage, supporting functional discovery in genome-wide experimental datasets. Nucleic Acids Res [Internet]. 2019;47(D1):D607–13. Available from: http://www.ncbi.nlm.nih.gov/pubmed/30476243
191. Fazekas D, Koltai M, Türei D, Módos DD, Pálfy M, Dúl Z, Zsákai L, Szalay-Beko M, Lenti K, Farkas IJ, Vellai T, Csermely P, Korcsmáros T, Szalay-Bekő M, Lenti K, Farkas IJ, Vellai T, Csermely P, Korcsmáros T. SignaLink 2 - a signaling pathway resource with multi-layered regulatory networks. BMC Syst Biol [Internet]. 2013 Jan 18;7:7.
Available from: http://www.ncbi.nlm.nih.gov/pubmed/23331499
192. Brent RP. An improved Monte Carlo factorization algorithm. BIT [Internet]. 1980 Jun;20(2):176–84. Available from: http://link.springer.com/10.1007/BF01933190
193. Fumiã HF, Martins ML. Boolean Network Model for Cancer Pathways: Predicting Carcinogenesis and Targeted Therapy Outcomes. PLoS One. 2013;8(7).

194. Dora D, Rivard C, Yu H, Pickard SL, Laszlo V, Harko T, Megyesfalvi Z, Dinya E, Gerdan C, Szegvari G, Hirsch FR, Dome B, Lohinai Z. Characterization of Tumor-Associated Macrophages and the Immune Microenvironment in Limited-Stage Neuroendocrine-High and -Low Small Cell Lung Cancer. Biology (Basel) [Internet]. 2021 Jun 4;10(6).
Available from: http://www.ncbi.nlm.nih.gov/pubmed/34200100

195. Albert R. Scale-free networks in cell biology. J Cell Sci [Internet]. 2005 Nov 1;118(Pt 21):4947–57.
Available from: http://www.ncbi.nlm.nih.gov/pubmed/16254242

196. Ashburner M, Ball CA, Blake JA, Botstein D, Butler H, Cherry JM, Davis AP, Dolinski K, Dwight SS, Eppig JT, Harris MA, Hill DP, Issel-Tarver L, Kasarskis A, Lewis S, Matese JC, Richardson JE, Ringwald M, Rubin GM, Sherlock G. Gene ontology: tool for the unification of biology. The Gene Ontology Consortium. Nat Genet [Internet]. 2000 May [cited 2012 Mar 8];25(1):25–9. Available from: http://www.ncbi.nlm.nih.gov/pubmed/10802651

197. Gene Ontology Consortium, Aleksander SA, Balhoff J, Carbon S, Cherry JM, Drabkin HJ, Ebert D, Feuermann M, Gaudet P, Harris NL, Hill DP, Lee R, Mi H, Moxon S, Mungall CJ, Muruganugan A, Mushayahama T, Sternberg PW, Thomas PD, Van Auken K, Ramsey J, Siegele DA, Chisholm RL, Fey P, Aspromonte MC, Nugnes MV, Quaglia F, Tosatto S, Giglio M, Nadendla S, Antonazzo G, Attrill H, Dos Santos G, Marygold S, Strelets V, Tabone CJ, Thurmond J, Zhou P, Ahmed SH, Asanitthong P, Luna Buitrago D, Erdol MN, Gage MC, Ali Kadhum M, Li KYC, Long M, Michalak A, Pesala A, Pritazahra A, Saverimuttu SCC, Su R, Thurlow KE, Lovering RC, Logie C, Oliferenko S, Blake J, Christie K, Corbani L, Dolan ME, Drabkin HJ, Hill DP, Ni L, Sitnikov D, Smith C, Cuzick A, Seager J, Cooper L, Elser J, Jaiswal P, Gupta P, Jaiswal P, Naithani S, Lera-Ramirez M, Rutherford K, Wood V, De Pons JL, Dwinell MR, Hayman GT, Kaldunski ML, Kwitek AE, Laulederkind SJF, Tutaj MA, Vedi M, Wang SJ, D'Eustachio P, Aimo L, Axelsen K, Bridge A, Hyka-Nouspikel N, Morgat A, Aleksander SA, Cherry JM, Engel SR, Karra K, Miyasato SR, Nash RS, Skrzypek MS, Weng S, Wong ED, Bakker E, Berardini TZ, Reiser L, Auchincloss A, Axelsen K, Argoud-Puy G, Blatter MC, Boutet E, Breuza L, Bridge A, Casals-Casas C, Coudert E, Estreicher

A, Livia Famiglietti M, Feuermann M, Gos A, Gruaz-Gumowski N, Hulo C, Hyka-Nouspikel N, Jungo F, Le Mercier P, Lieberherr D, Masson P, Morgat A, Pedruzzi I, Pourcel L, Poux S, Rivoire C, Sundaram S, Bateman A, Bowler-Barnett E, Bye-A-Jee H, Denny P, Ignatchenko A, Ishtiaq R, Lock A, Lussi Y, Magrane M, Martin MJ, Orchard S, Raposo P, Speretta E, Tyagi N, Warner K, Zaru R, Diehl AD, Lee R, Chan J, Diamantakis S, Raciti D, Zarowiecki M, Fisher M, James-Zorn C, Ponferrada V, Zorn A, Ramachandran S, Ruzicka L, Westerfield M. The Gene Ontology knowledgebase in 2023. Genetics. 2023 May 4;224(1).

198. Brown Lobbins ML, Shivakumar BR, Postlethwaite AE, Hasty KA. Chronic exposure of interleukin-13 suppress the induction of matrix metalloproteinase-1 by tumour necrosis factor α in normal and scleroderma dermal fibroblasts through protein kinase B/Akt. Clin Exp Immunol. 2018 Jan;191(1):84–95.
199. Hornell TMC, Beresford GW, Bushey A, Boss JM, Mellins ED. Regulation of the class II MHC pathway in primary human monocytes by granulocyte-macrophage colony-stimulating factor. J Immunol. 2003 Sep 1;171(5):2374–83.
200. Draijer C, Penke LRK, Peters-Golden M. Distinctive Effects of GM-CSF and M-CSF on Proliferation and Polarization of Two Major Pulmonary Macrophage Populations. J Immunol. 2019 May 1;202(9):2700–9.
201. Maibach F, Sadozai H, Seyed Jafari SM, Hunger RE, Schenk M. Tumor-Infiltrating Lymphocytes and Their Prognostic Value in Cutaneous Melanoma. Front Immunol [Internet]. 2020 Sep 10;11:2105. Available from: http://www.ncbi.nlm.nih.gov/pubmed/33013886
202. Lin A, Schildknecht A, Nguyen LT, Ohashi PS. Dendritic cells integrate signals from the tumor microenvironment to modulate immunity and tumor growth. Immunol Lett. 2010 Jan 4;127(2):77–84.
203. Chen JJW, Lin YC, Yao PL, Yuan A, Chen HY, Shun CT, Tsai MF, Chen CH, Yang PC. Tumor-associated macrophages: The double-edged sword in cancer progression. Journal of Clinical Oncology. 2005;23(5):953–64.
204. Dandekar RC, Kingaonkar A V, Dhabekar GS. Role of macrophages in malignancy. Ann Maxillofac Surg. 2011 Jul;1(2):150–4.
205. Casanova-Acebes M, Dalla E, Leader AM, LeBerichel J, Nikolic J, Morales BM, Brown M, Chang C, Troncoso L, Chen ST, Sastre-Perona A, Park MD,

Tabachnikova A, Dhainaut M, Hamon P, Maier B, Sawai CM, Agulló-Pascual E, Schober M, Brown BD, Reizis B, Marron T, Kenigsberg E, Moussion C, Benaroch P, Aguirre-Ghiso JA, Merad M. Tissue-resident macrophages provide a pro-tumorigenic niche to early NSCLC cells. Nature [Internet]. 2021;595(7868):578–84. Available from: http://www.ncbi.nlm.nih.gov/pubmed/34135508

206. Abbott M, Ustoyev Y. Cancer and the Immune System: The History and Background of Immunotherapy. Semin Oncol Nurs [Internet]. 2019;35(5):150923. Available from: http://www.ncbi.nlm.nih.gov/pubmed/31526550
207. Zhang Y, Zhang Z. The history and advances in cancer immunotherapy: understanding the characteristics of tumor-infiltrating immune cells and their therapeutic implications. Cell Mol Immunol [Internet]. 2020;17(8):807–21. Available from: http://www.ncbi.nlm.nih.gov/pubmed/32612154
208. Hu C, Zhao L, Liu W, Fan S, Liu J, Liu Y, Liu X, Shu L, Liu X, Liu P, Deng C, Qiu Z, Chen C, Jiang Y, Liang Q, Yang L, Shao Y, He Q, Yu D, Zeng Y, Li Y, Pan Y, Zhang S, Shi S, Peng Y, Wu F. Genomic profiles and their associations with TMB, PD-L1 expression, and immune cell infiltration landscapes in synchronous multiple primary lung cancers. J Immunother Cancer [Internet]. 2021 Dec 1;9(12). Available from: http://www.ncbi.nlm.nih.gov/pubmed/34887263
209. Yamauchi Y, Safi S, Blattner C, Rathinasamy A, Umansky L, Juenger S, Warth A, Eichhorn M, Muley T, Herth FJF, Dienemann H, Platten M, Beckhove P, Utikal J, Hoffmann H, Umansky V. Circulating and Tumor Myeloid-derived Suppressor Cells in Resectable Non-Small Cell Lung Cancer. Am J Respir Crit Care Med. 2018 Sep 15;198(6):777–87.
210. Tian Y, Li Q, Yang Z, Zhang S, Xu J, Wang Z, Bai H, Duan J, Zheng B, Li W, Cui Y, Wang X, Wan R, Fei K, Zhong J, Gao S, He J, Gay CM, Zhang J, Wang J, Tang F. Single-cell transcriptomic profiling reveals the tumor heterogeneity of small-cell lung cancer. Signal Transduct Target Ther [Internet]. 2022 Oct 5;7(1):346. Available from: http://www.ncbi.nlm.nih.gov/pubmed/36195615
211. Zhang J, Zhang H, Zhang L, Li D, Qi M, Zhang L, Yu H, Wang D, Jiang G, Wang X, Zhu X, Zhang P. Single-Cell Transcriptome Identifies Drug-Resistance Signature and Immunosuppressive Microenvironment in Metastatic Small Cell Lung Cancer. Advanced Genetics. 2022 Jun;3(2).

212. Chan JM, Quintanal-Villalonga Á, Gao VR, Xie Y, Allaj V, Chaudhary O, Masilionis I, Egger J, Chow A, Walle T, Mattar M, Yarlagadda DVK, Wang JL, Uddin F, Offin M, Ciampricotti M, Qeriqi B, Bahr A, de Stanchina E, Bhanot UK, Lai WV, Bott MJ, Jones DR, Ruiz A, Baine MK, Li Y, Rekhtman N, Poirier JT, Nawy T, Sen T, Mazutis L, Hollmann TJ, Pe'er D, Rudin CM. Signatures of plasticity, metastasis, and immunosuppression in an atlas of human small cell lung cancer. Cancer Cell [Internet]. 2021 Nov 8;39(11):1479-1496.e18. Available from: http://www.ncbi.nlm.nih.gov/pubmed/34653364

213. Belgiovine C, Bello E, Liguori M, Craparotta I, Mannarino L, Paracchini L, Beltrame L, Marchini S, Galmarini CM, Mantovani A, Frapolli R, Allavena P, D'incalci M. Lurbinectedin reduces tumour-associated macrophages and the inflammatory tumour microenvironment in preclinical models. 2017; Available from: www.bjcancer.com

214. Zheng X, Turkowski K, Mora J, Brüne B, Seeger W, Weigert A, Savai R. Redirecting tumor-associated macrophages to become tumoricidal effectors as a novel strategy for cancer therapy. Oncotarget [Internet]. 2017 Jul 18;8(29):48436–52. Available from: http://www.ncbi.nlm.nih.gov/pubmed/28467800

215. Yim S, Yu H, Jang D, Lee D. Annotating activation/inhibition relationships to protein-protein interactions using gene ontology relations. BMC Syst Biol [Internet]. 2018;12(Suppl 1):9.
Available from: http://www.ncbi.nlm.nih.gov/pubmed/29671402

216. Silverbush D, Sharan R. A systematic approach to orient the human protein-protein interaction network. Nat Commun. 2019 Jul 9;10(1):3015.

217. Calzone L, Tournier L, Fourquet S, Thieffry D, Zhivotovsky B, Barillot E, Zinovyev A. Mathematical modelling of cell-fate decision in response to death receptor engagement. PLoS Comput Biol [Internet]. 2010 Mar 5;6(3):e1000702. Available from: http://www.ncbi.nlm.nih.gov/pubmed/20221256

218. Marku M, Verstraete N, Raynal F, Madrid-Mencía M, Domagala M, Fournié JJ, Ysebaert L, Poupot M, Pancaldi V. Insights on TAM Formation from a Boolean Model of Macrophage Polarization Based on In Vitro Studies. Cancers (Basel) [Internet]. 2020 Dec 7;12(12):1–23. Available from: http://www.ncbi.nlm.nih.gov/pubmed/33297362

219. Palma A, Jarrah AS, Tieri P, Cesareni G, Castiglione F. Gene Regulatory Network Modeling of Macrophage Differentiation Corroborates the Continuum Hypothesis of Polarization States. Front Physiol [Internet]. 2018;9(November):1659. Available from: http://www.ncbi.nlm.nih.gov/pubmed/30546316
220. Nilsson A, Peters JM, Meimetis N, Bryson B, Lauffenburger DA. Artificial neural networks enable genome-scale simulations of intracellular signaling. Nat Commun [Internet]. 2022 Jun 2;13(1):3069. Available from: http://www.ncbi.nlm.nih.gov/pubmed/35654811
221. Liu X, Zhang J, Zeigler AC, Nelson AR, Lindsey ML, Saucerman JJ. Network Analysis Reveals a Distinct Axis of Macrophage Activation in Response to Conflicting Inflammatory Cues. J Immunol. 2021 Feb 15;206(4):883–91.
222. Leoni G, Neumann PA, Kamaly N, Quiros M, Nishio H, Jones HR, Sumagin R, Hilgarth RS, Alam A, Fredman G, Argyris I, Rijcken E, Kusters D, Reutelingsperger C, Perretti M, Parkos CA, Farokhzad OC, Neish AS, Nusrat A. Annexin A1-containing extracellular vesicles and polymeric nanoparticles promote epithelial wound repair. J Clin Invest. 2015 Mar 2;125(3):1215–27.
223. Cheng TY, Wu MS, Lin JT, Lin MT, Shun CT, Huang HY, Hua KT, Kuo ML. Annexin A1 is associated with gastric cancer survival and promotes gastric cancer cell invasiveness through the formyl peptide receptor/extracellular signal-regulated kinase/integrin beta-1-binding protein 1 pathway. Cancer. 2012 Dec 1;118(23):5757–67.
224. Lin Y, Lin G, Fang W, Zhu H, Chu K. Increased expression of annexin A1 predicts poor prognosis in human hepatocellular carcinoma and enhances cell malignant phenotype. Med Oncol. 2014 Dec;31(12):327.
225. Boudhraa Z, Rondepierre F, Ouchchane L, Kintossou R, Trzeciakiewicz A, Franck F, Kanitakis J, Labeille B, Joubert-Zakeyh J, Bouchon B, Perrot JL, Mansard S, Papon J, Dechelotte P, Chezal JM, Miot-Noirault E, Bonnet M, D'Incan M, Degoul F. Annexin A1 in primary tumors promotes melanoma dissemination. Clin Exp Metastasis. 2014 Oct;31(7):749–60.
226. Biaoxue R, Xiling J, Shuanying Y, Wei Z, Xiguang C, Jinsui W, Min Z. Upregulation of Hsp90-beta and annexin A1 correlates with poor survival and

lymphatic metastasis in lung cancer patients. J Exp Clin Cancer Res. 2012 Aug 28;31(1):70.

227. De Marchi T, Timmermans AM, Smid M, Look MP, Stingl C, Opdam M, Linn SC, Sweep FCGJ, Span PN, Kliffen M, van Deurzen CHM, Luider TM, Foekens JA, Martens JW, Umar A. Annexin-A1 and caldesmon are associated with resistance to tamoxifen in estrogen receptor positive recurrent breast cancer. Oncotarget. 2016 Jan 19;7(3):3098–110.
228. Sheu MJ, Li CF, Lin CY, Lee SW, Lin LC, Chen TJ, Ma LJ. Overexpression of ANXA1 confers independent negative prognostic impact in rectal cancers receiving concurrent chemoradiotherapy. Tumour Biol. 2014 Aug;35(8):7755–63.
229. de Graauw M, van Miltenburg MH, Schmidt MK, Pont C, Lalai R, Kartopawiro J, Pardali E, Le Dévédec SE, Smit VT, van der Wal A, Van't Veer LJ, Cleton-Jansen AM, ten Dijke P, van de Water B. Annexin A1 regulates TGF-beta signaling and promotes metastasis formation of basal-like breast cancer cells. Proc Natl Acad Sci U S A. 2010 Apr 6;107(14):6340–5.
230. Moraes LA, Kar S, Foo SL, Gu T, Toh YQ, Ampomah PB, Sachaphibulkij K, Yap G, Zharkova O, Lukman HM, Fairhurst AM, Kumar AP, Lim LHK. Annexin-A1 enhances breast cancer growth and migration by promoting alternative macrophage polarization in the tumour microenvironment. Sci Rep. 2017 Dec 20;7(1):17925.
231. Bist P, Leow SC, Phua QH, Shu S, Zhuang Q, Loh WT, Nguyen TH, Zhou JB, Hooi SC, Lim LHK. Annexin-1 interacts with NEMO and RIP1 to constitutively activate IKK complex and NF-κB: implication in breast cancer metastasis. Oncogene. 2011 Jul 14;30(28):3174–85.
232. Ramakrishnan P, Wang W, Wallach D. Receptor-specific signaling for both the alternative and the canonical NF-kappaB activation pathways by NF-kappaB-inducing kinase. Immunity. 2004 Oct;21(4):477–89.
233. Tesselaar K, Xiao Y, Arens R, van Schijndel GMW, Schuurhuis DH, Mebius RE, Borst J, van Lier RAW. Expression of the Murine CD27 Ligand CD70 In Vitro and In Vivo. The Journal of Immunology. 2003 Jan 1;170(1):33–40.
234. Nolte MA, van Olffen RW, van Gisbergen KPJM, van Lier RAW. Timing and tuning of CD27-CD70 interactions: the impact of signal strength in setting the balance between adaptive responses and immunopathology. Immunol Rev

[Internet]. 2009 May;229(1):216–31. Available from: https://onlinelibrary.wiley.com/doi/10.1111/j.1600-065X.2009.00774.x

235. Orengo AM, Cantoni C, Neglia F, Biassoni R, Ferrini S. Reciprocal expression of CD70 and of its receptor, CD27, in human long term-activated T and natural killer (NK) cells: inverse regulation by cytokines and role in induction of cytotoxicity. Clin Exp Immunol. 1997 Mar;107(3):608–13.
236. Seyfrid M, Maich WT, Shaikh VM, Tatari N, Upreti D, Piyasena D, Subapanditha M, Savage N, McKenna D, Mikolajewicz N, Han H, Chokshi C, Kuhlmann L, Khoo A, Salim SK, Archibong-Bassey B, Gwynne W, Brown K, Murtaza N, Bakhshinyan D, Vora P, Venugopal C, Moffat J, Kislinger T, Singh S. CD70 as an actionable immunotherapeutic target in recurrent glioblastoma and its microenvironment. J Immunother Cancer. 2022 Jan;10(1).
237. Yang ZZ, Novak AJ, Ziesmer SC, Witzig TE, Ansell SM. CD70+ non-Hodgkin lymphoma B cells induce Foxp3 expression and regulatory function in intratumoral CD4+CD25 T cells. Blood. 2007 Oct 1;110(7):2537–44.
238. Law CL, Gordon KA, Toki BE, Yamane AK, Hering MA, Cerveny CG, Petroziello JM, Ryan MC, Smith L, Simon R, Sauter G, Oflazoglu E, Doronina SO, Meyer DL, Francisco JA, Carter P, Senter PD, Copland JA, Wood CG, Wahl AF. Lymphocyte activation antigen CD70 expressed by renal cell carcinoma is a potential therapeutic target for anti-CD70 antibody-drug conjugates. Cancer Res. 2006 Feb 15;66(4):2328–37.
239. Jacobs J, Zwaenepoel K, Rolfo C, Van den Bossche J, Deben C, Silence K, Hermans C, Smits E, Van Schil P, Lardon F, Deschoolmeester V, Pauwels P. Unlocking the potential of CD70 as a novel immunotherapeutic target for non-small cell lung cancer. Oncotarget. 2015 May 30;6(15):13462–75.
240. Claus C, Riether C, Schürch C, Matter MS, Hilmenyuk T, Ochsenbein AF. CD27 Signaling Increases the Frequency of Regulatory T Cells and Promotes Tumor Growth. Cancer Res. 2012 Jul 15;72(14):3664–76.
241. Saintigny P, Massarelli E, Lin S, Ahn YH, Chen Y, Goswami S, Erez B, O'Reilly MS, Liu D, Lee JJ, Zhang L, Ping Y, Behrens C, Solis Soto LM, Heymach J V, Kim ES, Herbst RS, Lippman SM, Wistuba II, Hong WK, Kurie JM, Koo JS. CXCR2

expression in tumor cells is a poor prognostic factor and promotes invasion and metastasis in lung adenocarcinoma. Cancer Res. 2013 Jan 15;73(2):571–82.

242. Wei L, Liu Y, Ma Y, Ding C, Zhang H, Lu Z, Gu Z, Zhu C. C-X-C chemokine receptor 2 correlates with unfavorable prognosis and facilitates malignant cell activities via activating JAK2/STAT3 pathway in non-small cell lung cancer. Cell Cycle. 2019 Dec;18(24):3456–71.
243. Liu H, Zhang T, Li X, Huang J, Wu B, Huang X, Zhou Y, Zhu J, Hou J. Predictive value of MMP-7 expression for response to chemotherapy and survival in patients with non-small cell lung cancer. Cancer Sci. 2008 Nov;99(11):2185–92.
244. Thomas GJ, Lewis MP, Hart IR, Marshall JF, Speight PM. AlphaVbeta6 integrin promotes invasion of squamous carcinoma cells through up-regulation of matrix metalloproteinase-9. Int J Cancer. 2001 Jun 1;92(5):641–50.
245. Munger JS, Huang X, Kawakatsu H, Griffiths MJ, Dalton SL, Wu J, Pittet JF, Kaminski N, Garat C, Matthay MA, Rifkin DB, Sheppard D. The integrin alpha v beta 6 binds and activates latent TGF beta 1: a mechanism for regulating pulmonary inflammation and fibrosis. Cell [Internet]. 1999 Feb 5;96(3):319–28. Available from: http://www.ncbi.nlm.nih.gov/pubmed/10025398
246. Massion PP, Taflan PM, Jamshedur Rahman SM, Yildiz P, Shyr Y, Edgerton ME, Westfall MD, Roberts JR, Pietenpol JA, Carbone DP, Gonzalez AL. Significance of p63 amplification and overexpression in lung cancer development and prognosis. Cancer Res. 2003 Nov 1;63(21):7113–21.
247. Coles LS, Diamond P, Occhiodoro F, Vadas MA, Shannon MF. Cold shock domain proteins repress transcription from the GM-CSF promoter. Nucleic Acids Res. 1996 Jun 15;24(12):2311–7.
248. van der Poel CE, Spaapen RM, van de Winkel JGJ, Leusen JHW. Functional characteristics of the high affinity IgG receptor, FcγRI. J Immunol [Internet]. 2011 Mar 1;186(5):2699–704.
Available from: http://www.ncbi.nlm.nih.gov/pubmed/21325219
249. Yao Z, Zhang J, Zhang B, Liang G, Chen X, Yao F, Xu X, Wu H, He Q, Ding L, Yang B. Imatinib prevents lung cancer metastasis by inhibiting M2-like polarization of macrophages. Pharmacol Res [Internet]. 2018;133:121–31. Available from: http://www.ncbi.nlm.nih.gov/pubmed/29730267

250. Tariq M, Zhang JQ, Liang GK, He QJ, Ding L, Yang B. Gefitinib inhibits M2-like polarization of tumor-associated macrophages in Lewis lung cancer by targeting the STAT6 signaling pathway. Acta Pharmacol Sin [Internet]. 2017 Nov;38(11):1501–11. Available from: http://www.ncbi.nlm.nih.gov/pubmed/29022575

251. Xiao H, Guo Y, Li B, Li X, Wang Y, Han S, Cheng D, Shuai X. M2-Like Tumor-Associated Macrophage-Targeted Codelivery of STAT6 Inhibitor and IKKβ siRNA Induces M2-to-M1 Repolarization for Cancer Immunotherapy with Low Immune Side Effects. ACS Cent Sci [Internet]. 2020 Jul 22;6(7):1208–22. Available from: http://www.ncbi.nlm.nih.gov/pubmed/32724855

252. Ghoreschi K, Jesson MI, Li X, Lee JL, Ghosh S, Alsup JW, Warner JD, Tanaka M, Steward-Tharp SM, Gadina M, Thomas CJ, Minnerly JC, Storer CE, LaBranche TP, Radi ZA, Dowty ME, Head RD, Meyer DM, Kishore N, O'Shea JJ. Modulation of innate and adaptive immune responses by tofacitinib (CP-690,550). J Immunol [Internet]. 2011 Apr 1;186(7):4234–43. Available from: http://www.ncbi.nlm.nih.gov/pubmed/21383241

253. De Vries LCS, Duarte JM, De Krijger M, Welting O, Van Hamersveld PHP, Van Leeuwen-Hilbers FWM, Moerland PD, Jongejan A, D'Haens GR, De Jonge WJ, Wildenberg ME. A JAK1 Selective Kinase Inhibitor and Tofacitinib Affect Macrophage Activation and Function. Inflamm Bowel Dis [Internet]. 2019;25(4):647–60.
Available from: http://www.ncbi.nlm.nih.gov/pubmed/30668755

254. Liu Y, Peng J, Xiong X, Cheng L, Cheng X. Tofacitinib enhances IGF1 via inhibiting STAT6 transcriptionally activated-miR-425-5p to ameliorate inflammation in RA-FLS. Mol Cell Biochem [Internet]. 2022 May 10; Available from: http://www.ncbi.nlm.nih.gov/pubmed/35536531

255. Di Benedetto P, Ruscitti P, Berardicurti O, Panzera N, Grazia N, Di Vito Nolfi M, Di Francesco B, Navarini L, Maurizi A, Rucci N, Teti AM, Zazzeroni F, Guggino G, Ciccia F, Dolo V, Alesse E, Cipriani P, Giacomelli R. Blocking Jak/STAT signalling using tofacitinib inhibits angiogenesis in experimental arthritis. Arthritis Res Ther [Internet]. 2021;23(1):213. Available from: http://www.ncbi.nlm.nih.gov/pubmed/34391476

256. Weng L, Wu Z, Zheng W, Meng H, Han L, Wang S, Yuan Z, Xu Y. Malibatol A enhances alternative activation of microglia by inhibiting phosphorylation of Mammalian Ste20-like kinase1 in OGD-BV-2 cells. Neurol Res [Internet]. 2016 Apr;38(4):342–8. Available from: http://www.ncbi.nlm.nih.gov/pubmed/27098434
257. Yadav P, Bhatt B, Balaji KN. Selective Activation of MST1/2 Kinases by Retinoid Agonist Adapalene Abrogates AURKA-Regulated Septic Arthritis. J Immunol [Internet]. 2021;206(12):2888–99. Available from: http://www.ncbi.nlm.nih.gov/pubmed/34031150
258. Tornin J, Martinez-Cruzado L, Santos L, Rodriguez A, Núñez LE, Oro P, Hermosilla MA, Allonca E, Fernández-García MT, Astudillo A, Suarez C, Morís F, Rodriguez R. Inhibition of SP1 by the mithramycin analog EC-8042 efficiently targets tumor initiating cells in sarcoma. Oncotarget [Internet]. 2016 May 24;7(21):30935–50.
Available from: http://www.ncbi.nlm.nih.gov/pubmed/27105533
259. Yuan P, Wang L, Wei D, Zhang J, Jia Z, Li Q, Le X, Wang H, Yao J, Xie K. Therapeutic inhibition of Sp1 expression in growing tumors by mithramycin a correlates directly with potent antiangiogenic effects on human pancreatic cancer. Cancer [Internet]. 2007 Dec 15;110(12):2682–90. Available from: http://www.ncbi.nlm.nih.gov/pubmed/17973266
260. Zhao Y, Zhang W, Guo Z, Ma F, Wu Y, Bai Y, Gong W, Chen Y, Cheng T, Zhi F, Zhang Y, Wang J, Jiang B. Inhibition of the transcription factor Sp1 suppresses colon cancer stem cell growth and induces apoptosis in vitro and in nude mouse xenografts. Oncol Rep [Internet]. 2013 Oct;30(4):1782–92. Available from: http://www.ncbi.nlm.nih.gov/pubmed/23877322
261. Ni SH, Sun SN, Zhou Z, Li Y, Huang YS, Li H, Wang JJ, Xiao W, Xian SX, Yang ZQ, Wang LJ, Lu L. Arctigenin alleviates myocardial infarction injury through inhibition of the NFAT5-related inflammatory phenotype of cardiac macrophages/monocytes in mice. Lab Invest [Internet]. 2020;100(4):527–41. Available from: http://www.ncbi.nlm.nih.gov/pubmed/31792391
262. IMPC. IMPC: Mouse Phenotype [Internet]. [cited 2023 Apr 15]. Available from: https://www.ebi.ac.uk/mi/impc/essential-genes-search/

263. Cacheiro P, Muñoz-Fuentes V, Murray SA, Dickinson ME, Bucan M, Nutter LMJ, Peterson KA, Haselimashhadi H, Flenniken AM, Morgan H, Westerberg H, Konopka T, Hsu CW, Christiansen A, Lanza DG, Beaudet AL, Heaney JD, Fuchs H, Gailus-Durner V, Sorg T, Prochazka J, Novosadova V, Lelliott CJ, Wardle-Jones H, Wells S, Teboul L, Cater H, Stewart M, Hough T, Wurst W, Sedlacek R, Adams DJ, Seavitt JR, Tocchini-Valentini G, Mammano F, Braun RE, McKerlie C, Herault Y, de Angelis MH, Mallon AM, Lloyd KCK, Brown SDM, Parkinson H, Meehan TF, Smedley D, Genomics England Research Consortium, International Mouse Phenotyping Consortium. Human and mouse essentiality screens as a resource for disease gene discovery. Nat Commun [Internet]. 2020;11(1):655. Available from: http://www.ncbi.nlm.nih.gov/pubmed/32005800

264. Munitic I, Kuka M, Allam A, Scoville JP, Ashwell JD. CD70 deficiency impairs effector CD8 T cell generation and viral clearance but is dispensable for the recall response to lymphocytic choriomeningitis virus. J Immunol. 2013 Feb 1;190(3):1169–79.

265. Fowler KD, Kuchroo VK, Chakraborty AK. A model for how signal duration can determine distinct outcomes of gene transcription programs. PLoS One [Internet]. 2012;7(3):e33018.
Available from: http://www.ncbi.nlm.nih.gov/pubmed/22427931

266. Palmieri EM, Gonzalez-Cotto M, Baseler WA, Davies LC, Ghesquière B, Maio N, Rice CM, Rouault TA, Cassel T, Higashi RM, Lane AN, Fan TWM, Wink DA, McVicar DW. Nitric oxide orchestrates metabolic rewiring in M1 macrophages by targeting aconitase 2 and pyruvate dehydrogenase. Nat Commun. 2020 Feb 4;11(1):698.

267. Basudhar D, Bharadwaj G, Somasundaram V, Cheng RYS, Ridnour LA, Fujita M, Lockett SJ, Anderson SK, McVicar DW, Wink DA. Understanding the tumour micro-environment communication network from an NOS2/COX2 perspective. Br J Pharmacol. 2019 Jan;176(2):155–76.

268. Ding L, Liang G, Yao Z, Zhang J, Liu R, Chen H, Zhou Y, Wu H, Yang B, He Q. Metformin prevents cancer metastasis by inhibiting M2-like polarization of tumor associated macrophages. Oncotarget [Internet]. 2015 Nov 3;6(34):36441–55. Available from: http://www.ncbi.nlm.nih.gov/pubmed/26497364

269. Helikar T, Konvalina J, Heidel J, Rogers JA. Emergent decision-making in biological signal transduction networks. Proc Natl Acad Sci U S A [Internet]. 2008 Feb 12;105(6):1913–8.
Available from: http://www.ncbi.nlm.nih.gov/pubmed/18250321

9. Bibliography of the candidate's publications

9.1. Related to the Thesis

- **Szegvari G**, Dora D, Lohinai Z. Effective Reversal of Macrophage Polarization by Inhibitory Combinations Predicted by a Boolean Protein-Protein Interaction Model. Biology (Basel) [Internet]. 2023 Feb 27;12(3):376. Available from: http://www.ncbi.nlm.nih.gov/pubmed/36979068
- Dora D, Rivard C, Yu H, Pickard SL, Laszlo V, Harko T, Megyesfalvi Z, Dinya E, Gerdan C, **Szegvari G**, Hirsch FR, Dome B, Lohinai Z. Characterization of Tumor-Associated Macrophages and the Immune Microenvironment in Limited-Stage Neuroendocrine-High and -Low Small Cell Lung Cancer. Biology (Basel) [Internet]. 2021 Jun 4;10(6). Available from: http://www.ncbi.nlm.nih.gov/pubmed/34200100
- Dora D, Dora T, **Szegvari G**, Gerdán C, Lohinai Z. EZCancerTarget: an open-access drug repurposing and data-collection tool to enhance target validation and optimize international research efforts against highly progressive cancers. BioData Min. 2022 Oct 1;15(1):25.

9.2. Other Publications

- Bátora D, Zsigmond Á, Lőrincz IZ, **Szegvári G**, Varga M, Málnási-Csizmadia A. Subcellular Dissection of a Simple Neural Circuit: Functional Domains of the Mauthner-Cell During Habituation. Front Neural Circuits. 2021;15:648487.
- Horváth ÁI, Gyimesi M, Várkuti BH, Képiró M, **Szegvári G**, Lőrincz I, Hegyi G, Kovács M, Málnási-Csizmadia A. Effect of allosteric inhibition of non-muscle myosin 2 on its intracellular diffusion. Sci Rep. 2020 Aug 7;10(1):13341.

10. Acknowledgments

We would like to express our thanks to the patients and clinical teams that made the *in vitro* studies possible.

The candidate would also like to thank Dr. Dávid Dóra and Dr. Zoltán Lohinai for their collaboration and guidance, and prof. Zoltán Benyó for his support during the writing of this thesis.